

2017-12-19

A Simulation Study on Enhanced Gas Recovery from Unconventional Resources (Coal Bed Methane)

Alenthwar, Vasavi Nandini

<http://hdl.handle.net/1880/106217>

Downloaded from PRISM Repository, University of Calgary

UNIVERSITY OF CALGARY

A Simulation Study on Enhanced Gas Recovery from Unconventional Resources (Coal Bed Methane)

by

Vasavi Nandini Alenthwar

A THESIS

SUBMITTED TO THE FACULTY OF GRADUATE STUDIES

IN PARTIAL FULFILMENT OF THE REQUIREMENTS FOR THE

DEGREE OF MASTER OF SCIENCE

GRADUATE PROGRAM IN CHEMICAL AND PETROLEUM ENGINEERING

CALGARY, ALBERTA

DECEMBER, 2017

© Vasavi Nandini Alenthwar 2017

ACKNOWLEDGEMENT

I want to thank my supervisor Dr. Hemanta Sarma for providing me his valuable guidance and time during my research work. He showed immense patience while I was developing my knowledge curve and gave me liberty to make mistakes so that I can express my thoughts more freely and with more confidence. Thanks go to my co-supervisor, Dr. Anil Kumar Mehrotra for his valuable suggestions and comments. I would like to express sincere gratitude to my committee members Dr. Sudarshan R. Mehta and Dr. Hossein Hejazi for taking out time from their busy schedule to review my thesis work. I also want to thank CMG's supporting service team for making me understand the workflow of software by clearing off the doubts that I came across my research.

I express my thanks and appreciation to my parents and my fiancé, Abdul Akbar Khan, for their understanding, motivation and patience during the many hours I dedicated to achieving this milestone in my life and career, without their support walking on this path would have been difficult. I want to thank two special friends, Abdullah Al-Gawfi and Parvaneh Heidari for their meticulous consultation and support throughout my research. Lastly, I am thankful to all colleagues and administrative staff of University of Calgary who made my stay a memorable and valuable experience.

ABSTRACT

During the past 20 years of research on CBM reserves, it has been found that CBM resources as unconventional are highly potential for natural gas production and used as geological sinks for CO₂ storage where ECBMR by CO₂ injection evolved as a new strategy of development. It has been proven that affinity of CO₂, CH₄, and N₂ coal is in the ratio of 4:2:1. The main drawback of enhanced coal bed methane recovery by CO₂ injection found to be the reduction of coal permeability due to matrix swelling effects and it has been found that, N₂ gas has the capacity to reduce the partial pressure of CH₄ which helps in quick desorption of CH₄ and early production.

Apart from this, the production of pure CO₂ gas in surface facilities for sequestration is a costly process. The different behavior of CO₂ and N₂ towards coal making it as a separation medium which cuts the surface separation cost. The produced gas is a mixture of CH₄ and N₂ and separation units are required to increase the quality of CH₄ gas to pipeline specification and recent economic studies says that this cost is less than the cost of CO₂ generation. But the question is what exact compositions of flue gas are reliable to obtain the benefit of enhancing gas recovery? Therefore, the focus of this thesis is to develop an approach to evaluate the potential of CBM resources as a sink for CO₂, and to assess how effective is the recovery of the CH₄ gas trapped in coal beds using flue gas (CO₂ and N₂) injection.

In finding so, first, sensitivity analysis, uncertainty assessment studies have been conducted on 11 hypothetical coal bed simulation models that are developed based on different well completion methods and in each model (M-5 to M-11) flue gas (with normalized compositions CO₂ – 0.99, N₂- 0.01) is injected. The results derived from the study will help the design of a reliable operating strategy in implementing the CO₂ sequestration and enhanced CBM recovery using flue gas injection in deep coal zones in Western Canadian Sedimentary Basin, Canada and elsewhere.

Table of Contents

ACKNOWLEDGEMENT	ii
ABSTRACT	iii
LIST OF FIGURES	vi
LIST OF TABLES	ix
LIST OF ABBREVIATIONS	x
NOMENCLATURE	xi
Chapter 1 : Introduction	1
1.1. Introduction:	1
1.2. Objective of the study:	5
1.3. Organization of Thesis:	5
1.4. Coal Bed Methane Reserves:	6
1.4.1. World Potential:	6
1.4.2. Canada’s Potential:	10
Chapter 2 : Coal Reservoir Properties	18
2.1. Porosity:.....	19
2.2. Permeability:	21
2.3. Adsorption/ Desorption:	24
2.4. Coal Shrinkage/Swelling:	29
2.4.1. Mathematical models for calculating change in porosity and permeability:	33
2.5. Simulation studies on ECBMR:	40
Chapter 3 : Simulation Model Inputs and Construction.....	41
3.1. Dual Porosity Modelling:	43
3.2. Adsorption Modelling:.....	45
3.3. Matrix Shrinkage and Swelling effects:	47
3.4. Simulation Data:	51
3.4.1. Grid System:	51
3.4.2. Relative permeability (using quick CBM set up):	55
3.4.3. Hydraulic fracturing:	56
3.4.4. Input parameters for sensitivity analysis:	58
Chapter 4 : Results and Analysis.....	59
4.1. Matrix Shrinkage and swelling effects in the model:	67

4.2. CO ₂ Breakthrough:.....	76
4.3. Sensitivity Analysis and Optimization:.....	88
4.4. Uncertainty Assessment:.....	95
Chapter 5 : Conclusions and Recommendations.....	102
REFERENCES	106

LIST OF FIGURES

Figure 1.1. Major Coal basins in the world (Thakur P., 2017)	7
Figure 1.2. Distribution of major coal bearing formations with CBM potential, Alberta (AGS, ES report, 2003)	12
Figure 1.3. Areas with potentially favorable CBM exploration potential, Alberta Plains (AGS, ES report, 2003)	13
Figure 1.4. Coal rank trends across Alberta (AGS, ES report, 2003)	14
Figure 1.5. Stratigraphy of coal bearing strata, Alberta (AGS, ES report, 2003)	15
Figure 2.1. Dual porosity system of coal (Saulsberry et al., 1996)	21
Figure 2.2. Schematic representation of transportation of CH ₄ gas in coal seams (Harpalani et al., 1990)	22
Figure 2.3. Cleat system in CBM reservoir (plan view) (Shi et al., 2005)	23
Figure 2.4. IUPAC Classification of physical adsorption (Sing et al., 1985)	25
Figure 2.5. Adsorption isotherms of CH ₄ , CO ₂ and N ₂ gases on Fruitland coal sample at 115 ^o F (Yee et al., 1993)	29
Figure 2.6. Volumetric strain of coal matrix with decreasing gas pressure (St. George et al., 2001) ..	30
Figure 2.7. Variation in 'K' with decreasing in pr. at 4 hydrostatic stress levels (Harpalani et al., 1989)	32
Figure 2.8. Variation in absorbed gas volume and 'K' of coal to CH ₄ with gas pr. (Harpalani et al., 1990)	32
Figure 2.9. A bundled matchstick geometry representation of the coal seam (Seidle et al., 1992)	35
Figure 2.10. Effect of CO ₂ and Differential Swelling on Coal Permeability (Pekot et al., 2002)	39
Figure 3.1. Comparison of different shape factors (Lai et. al., 2013)	45
Figure 3.2. Pure Langmuir Isotherm curves developed in the model	46
Figure 3.3. Fracture Permeability changes w.r.t. pressure	48
Figure 3.4. Top view of the simulation model	53
Figure 3.5. 3D view of the simulation model	53
Figure 3.6. Relative permeability curves in the model	56
Figure 3.7. Planar and complex Hydraulic fracture modelling in CMG software	57
Figure 4.1. Top view of Model 1 – O.V.P.W. (vertical production well)	61
Figure 4.2. Top view of Model 2 – O.V.P.W.HF. (Vertical production well with Hydraulic fracturing) ..	62

Figure 4.3. Top view of Model 3 – O.H.P.W. (Horizontal production well).....	62
Figure 4.4. Top view of Model 4 – O.H.P.W.HF. (Horizontal production well with Hydraulic fracturing)	63
Figure 4.5. Top view of Model 5 – O.V.P.W-O.V.I.W. (Vertical production and injection well).....	63
Figure 4.6. Top view of Model 6 – O.V.P.W.HF – O.V.I.W. (Vertical production well with hydraulic fracturing and vertical injection well).....	64
Figure 4.7. Top view of Model 7 – O.V.P.W. – O.V.I.W.HF. (Vertical production well and vertical injection well with hydraulic fracturing).....	64
Figure 4.8. Top view of Model 8 – O.V.P.W.HF. – O.V.I.W.HF. (Vertical production and injection well both with hydraulic fracturing).....	65
Figure 4.9. Top view of Model 9 – O.H.P.W. – O.V.I.W. (Horizontal production and injection well)...	65
Figure 4.10. Top view of Model 10 – O.H.P.W.HF – O.V.I.W. (Horizontal production well with hydraulic fracturing and vertical injection well).....	66
Figure 4.11. Top view of Model 11 – O.V.P.W. – O.H.I.W. (Vertical production well and horizontal injection well).....	66
Figure 4.12. Change in Permeability w.r.t. fracture pressure	69
Figure 4.13. Comparison of gas recovery with and without P and M parameters in Model 1	71
Figure 4.14. Comparison of gas recovery with and without P and M parameters in Model 2	71
Figure 4.15. Comparison of gas recovery with and without P and M parameters in Model 3	72
Figure 4.16. Comparison of gas recovery with and without P and M parameters in Model 4	72
Figure 4.17. Comparison of gas recovery with and without P and M parameters in Model 5	73
Figure 4.18. Comparison of gas recovery with and without P and M parameters in Model 6	73
Figure 4.19. Comparison of gas recovery with and without P and M parameters in Model 7	74
Figure 4.20. Comparison of gas recovery with and without P and M parameters in Model 8	74
Figure 4.21. Comparison of gas recovery with and without P and M parameters in Model 9	75
Figure 4.22. Comparison of gas recovery with and without P and M parameters in Model 10	75
Figure 4.23. Comparison of gas recovery with and without P and M parameters in Model 11	76
Figure 4.24. CO ₂ fraction in produced gas of model 5 to model 11	77
Figure 4.25. Breakthrough time of model 5 to model 11 determined at 5% of CO ₂ in produced gas .	78
Figure 4.26. Forecast of gas rates for models from 5 to 11	80
Figure 4.27. CO ₂ adsorption in Model 5 in 20, 40 and 60 years of flue gas injection	81
Figure 4.28. CO ₂ adsorption in Model 6 in 20, 40 and 60 years of flue gas injection	82

Figure 4.29. CO ₂ adsorption in Model 7 in 20, 40 and 60 years of flue gas injection	83
Figure 4.30. CO ₂ adsorption in Model 8 in 20, 40 and 60 years of flue gas injection	84
Figure 4.31. CO ₂ adsorption in Model 9 in 20, 40 and 60 years of flue gas injection	85
Figure 4.32. CO ₂ adsorption in Model 10 in 20, 40 and 60 years of flue gas injection	86
Figure 4.33. CO ₂ adsorption in Model 11 in 20, 40 and 60 years of flue gas injection	87
Figure 4.34. Cumulative Gas Recovery of models from 1 to 11	88
Figure 4.35. Amount of CO ₂ gas adsorption in models from 5 to 11	89
Figure 4.36. Sensitivity of parameters towards Cumulative gas recovery by Tornado plot	92
Figure 4.37. Sensitivity of parameters towards CO ₂ gas adsorption by Tornado plot	93
Figure 4.38. Sobol Result Analysis for Cumulative Gas Recovery	94
Figure 4.39. Sobol Result Analysis for CO ₂ Gas Adsorption.....	94
Figure 4.40. Probability distribution of Cumulative Gas Recovery.....	98
Figure 4.41. Probability distribution of CO ₂ gas adsorption.....	98
Figure 4.42. Cumulative gas recovery vs CO ₂ gas composition in flue gas.....	100
Figure 4.43. CO ₂ gas adsorption vs CO ₂ gas composition in flue gas	101

LIST OF TABLES

Table 1.1. Coal Bed Methane Resources by Country/Region (Godec M. et. al, 2014).....	7
Table 1.2. CO ₂ storage and methane production potential of the world’s coal basins (Godec M. et. al, 2014)	9
Table 1.3. Characteristics of different coal zones in Alberta Plains (AGS, ES report, 2003)	16
Table 1.4. Coal Bed Methane potential of Alberta Plains (AGS, ES report, 2003).....	17
Table 3.1. Coalbed characteristics (Gentzis <i>et al.</i> , 2008; Deisman <i>et al.</i> , 2008)	52
Table 3.2. Langmuir isotherm parameters (Goodarzi <i>et al.</i> , 2008; Deisman <i>et al.</i> , 2008)	52
Table 3.3. Rock mechanics properties of coalbed (Gentzis T., 2009; Gu F., 2009)	54
Table 3.4. Operational parameters in the model.....	54
Table 3.5. Relative permeability data developed in the simulator	55
Table 3.6. Hydraulic fracturing designing parameter in the model	57
Table 3.7. Rock Mechanical parameters	58
Table 3.8. Hydraulic Fracturing parameters	58
Table 3.9. Operating parameters	58
Table 4.1. Well drilling combinations used to develop 11 base simulation models	60
Table 4.2. Rock compaction data used in matrix shrinkage and swelling modelling for primary depletion	67
Table 4.3. Changes in porosity and permeability calculated by P and M model	68
Table 4.4. Breakthrough times and adsorbed CO ₂ amount of model 5 to model 11.....	80
Table 4.5. Individual parameters to obtain objective function values at P50.....	97

LIST OF ABBREVIATIONS

BHP – Bottom Hole Pressure

CBM – Coal Bed Methane

CH₄ – Methane

CMG – Computer Modelling Group

CO₂ – Carbon Dioxide

Dmmf – Dry Mineral Matter free

ECBMR – Enhanced Coal Bed Methane Recovery

EGR – Enhanced Gas Recovery

EOR – Enhanced Oil Recovery

HC- Hydrocarbon

M-1-O.V.P. W. – Model 1- One Vertical Production Well

M-2-O.V.P.W. HF. – Model 2 – One Vertical Production Well with Hydraulic Fracturing

M-3-O.H.P. W. – Model 3 – One Horizontal Production Well

M-4- O.H.P.W. HF. – Model 4 – One Horizontal Production Well with Hydraulic Fracturing

M-5- O.V.P.W. -O.V.I. W. – Model 5 – One Vertical Production Well and One Vertical Injection Well

M-6- O.V.P.W. HF. -O.V.I. W. – Model 6 – One Vertical Production Well with Hydraulic Fracturing and One Vertical Injection Well

M-7- O.V.P. W. - O.V.I.W. HF. – Model 7 – One Vertical Production Well and One Vertical Injection Well with Hydraulic Fracturing

M-8- O.V.P.W. HF. - O.V.I.W. HF. – Model 8 – One Vertical Production Well with Hydraulic Fracturing and One Vertical Injection Well with Hydraulic Fracturing

M-9- O.H.P.W. - O.V.I. W. – Model 9 – One Horizontal Production Well and One Vertical Injection Well

M-10- O.H.P.W. HF-O.V.I. W. – Model 10 – One Horizontal Production Well with Hydraulic Fracturing and One Vertical Injection Well

M-11- O.V.P.W. - O.H.I.W. – Model 11- One Vertical Production Well and One Horizontal Injection Well

TCF – Trillion Cubic Feet

TCM – Trillion Cubic Meters

NOMENCLATURE

<u>Symbol</u>	<u>SI Unit</u>	<u>Definition</u>
b	kPa ⁻¹	Langmuir pressure constant
b _j	kPa ⁻¹	Langmuir pressure constant for j component
C (k, gas, i)	gmole/m ³	Concentration of the component 'k' in the gas phase of the v\block I
C (k, gas, j)	gmole/m ³	Concentration of the component 'k' in the gas phase of the v\block J
C	-	Constant related to heat of adsorption
C	gmole/m ³	Reservoir gas concentration
C _f	kPa ⁻¹	Cleat volume compressibility
C _k	-	Differential swelling coefficient
C _m	kPa ⁻¹	Matrix shrinkage compressibility
C ₀	gmole/m ³	Initial reservoir gas concentration
C _p	kPa ⁻¹	Pore volume compressibility
C _t	gmole/m ³	Total reservoir gas concentration
D	-	Dubinin's constant
E	J	Characteristic heat of adsorption
E	kPa	Young's modulus of coal bed
K	mD	Absolute permeability
K	kPa	Bulk modulus
K _{eff}	mD	Effective permeability of the hydraulic fracture
K _f	mD	Intrinsic permeability of hydraulic fracture
K _g	Fraction	Relative permeability of gas
K ₀	mD	Virgin permeability/ initial cleat permeability
K _w	Fraction	Relative permeability of water
L _e	m	Fracture effective length
L _x	m	Fracture length in x

L_y	m	Fracture length in y
L_z	m	Fracture length in z
M	kPa	Axial modulus
n	-	Number of fractures
n	gmole	Moles of gas adsorbed
n_0	m^3	Pore volume of adsorbent
P	kPa	Reservoir pore pressure
P_c	kPa	Critical sorption pressure
P_f	kPa	Fracture pressure
P_j	kPa	Partial free-gas pressure
P_L	kPa	Langmuir pressure
P_{Li}	kPa	Langmuir pressure of component 'i'
P_{Lj}	kPa	Langmuir pressure for component j
P_{Lk}	kPa	Langmuir pressure for component k
P_m	kPa	Matrix pressure
P_0	kPa	Initial reservoir pore pressure
P_0	kPa	Saturation pressure of the adsorbate
P_{ref}	kPa	Reference state pressure
ΔP_s	kPa	Change in sorption pressure
P_ϵ	-	Langmuir type matrix shrinkage constant
q	m^3/s	Matrix-fracture transfer rate
R	-	Gas constant
S_g	Fraction	Gas saturation in the simulation grid block
S_w	Fraction	Saturation of water
ΔS	kg	Change in adsorbate mass
T	K or $^{\circ}C$	Temperature

V	m^3/t	Gas adsorption capacity
V_j	m^3	Adsorbed volume for gas component j at current reservoir condition
V_{j0}	m^3	Adsorbed volume for gas component j at initial reservoir condition
V_L	m^3	Langmuir volume
V_{Lj}	m^3	Langmuir volume for gas component j
V_0	m^3/kg	Monolayer adsorption capacity
V_p	m^3	Pore volume
W_{eff}	m	Effective width of hydraulic fracture
W_f	m	Width of hydraulic fracture
Y_{ig}	Fraction	Mole fraction of adsorbed gas component 'i' in the gas phase
Y_j	Fraction	Mole fraction of component j in a gas mixture
Y_k	Fraction	Mole fraction of component k in a gas mixture
$Y_{ref,j}$	Fraction	Mole fraction of component j at reference condition
$Y_{ref,k}$	Fraction	Mole fraction of component k at reference condition
β	-	Affinity coefficient
ϕ	Fraction	Porosity
ϕ	Fraction	Fracture system porosity
Φ_0	Fraction	Initial fracture system porosity
ϕ_{ref}	Fraction	Reference state natural fracture porosity
ρ_{Hg}	kg/m^3	Density of mercury
ρ_{He}	kg/m^3	Density of helium
ϵ_l	-	Langmuir type matrix shrinkage constant/ Maximum matrix shrinkage strain at $V=V_L$
ϵ_L	-	Strain at infinite pressure
ϵ_{Lj}	-	Strain at infinite pressure for component j
ϵ_{Lk}	-	Strain at infinite pressure for component k
ϵ_s	-	Volumetric matrix shrinkage for n -component gas mixture

$\Delta\varepsilon_s$	-	Strain
ω_i	gmole/Kg	Moles of adsorbed gas component per unit mass of rock
$\omega_{i, \max}$	gmole/kg	Maximum moles of adsorbed gas component per unit mass of rock
γ	kPa ⁻¹	Grain compressibility
σ	kPa	Effective horizontal stress
σ	-	Shape factor
σ_c	kPa	Critical effective horizontal stress
σ_0	kPa	In-situ effective horizontal stress
ϑ	Fraction	Poisson's ratio
α	-	Volumetric swelling coefficient
α	-	P and M exponent
α_{sj}	-	Shrinkage/swelling coefficient
μ	Kg/m-s	Viscosity

Chapter 1 : Introduction

1.1. Introduction:

According to the recent research on the topic “Climate change”, a clear evidence of rise in earth’s temperature by rise in CO₂ concentration in the atmosphere is noticed, and the fossil fuel is perceived as the major contributor towards increase of levels of CO₂ in the atmosphere (BP’s world energy report, 2017). To reduce the anthropogenic effects on climate, critical research is going on to capture and store the Carbon Dioxide from the atmosphere into deep oceans and geological sinks for significant time periods (Dai *et al.*, 2016). Even though the oceans are the largest sinks for CO₂ storage, geological storage systems are gaining a lot of attention mainly due to the benefits in recovering hydrocarbons while sequestering the Carbon Dioxide into them. Depleted Oil and Gas reservoirs, Salt caverns, Deep Aquifers and Unconventional reserves are mainly considered as the geological sinks for CO₂ storage. The depleting of proven conventional oil and gas resources and the significant gap between energy demand and supply, increasing the exploration and development activities for the unconventional resources such as shale and tight oil/gas, unminable coal bed methane resources.

The coal seams which are unminable are considered as the coal bed methane resources (Saulsberry *et al.*, 1996). The main constituent in these reservoirs is methane gas which is mostly (>95%) present in the adsorbed state on the coal surface which makes it different

from the conventional gas resources and considered as an unconventional resource. The coal seam consists of a matrix and fracture system. The porosity and permeability of the matrix system is different from the fracture system. The fractures present in the coal seam are natural and generally known as cleats and are classified as face and butt cleats.

The methane is produced from the coal seams by two mechanisms. Initially, the desorption of methane occurs as the pressure is reduced and the desorbed methane diffuses through the matrix pore system into the butt cleats and to the face cleats. The flow of gas from the face cleats to the production well is explained by Darcy flow principles. Coal seams generally contain water in the cleats system. To reduce the pressure in the coal seams, water needs to be produced out of the seams. Thus, it is crucial to consider the relative permeability of gas and water.

The recovery of methane by primary production mechanism is low, about 60% and enhancing gas recovery by CO₂ sequestration shows promising results in increasing the recovery about 90-100% depending on the reservoir and fluid properties. The injected CO₂ is adsorbed onto the coal surface by replacing the methane molecule. It is experimentally confirmed that the replacement ratio of methane by CO₂ varies from 1:2 to 1:10 (Harpalani *et al.*, 2006; Mastalerz *et al.*, 2004; Busch *et al.*, 2003; Bustin, 2002). It states that a methane molecule is replaced by 2 to 10 CO₂ molecules and shows that there is a high possibility of CO₂ gas storage for significant geological time. The physical adsorption of gases on coal seams depends on pressure, temperature, coal's rank, moisture content, organic and mineral content etc. Apart from successful storage of CO₂ into coal seams, it is

also important to optimize the methane gas production from the coal seams which mainly depends on the relative permeability to gases in multicomponent system.

Coal seams are highly compressible compared to sandstone and siltstone and fluctuations in pressure shows major impact on the permeability of cleat system. During the desorption of methane from matrix system due to the pressure reduction, the matrix shrinkage takes place which increases the distance between two adjacent blocks, and this distance consequently increases the cleat permeability and at the same time the over burden pressure compresses the coal seam shows quite the opposite phenomenon and decreases the cleat permeability. The relative presence of both phenomena decides the cleat permeability. Therefore, it is very important to know the coal properties and characteristics before applying the enhanced gas recovery methods.

Nowadays, it became easier to understand the behavior of unminable coal seams using the simulation and modelling technology. Coal seams are acts as natural separators of CO₂ from the flue gas. N₂ and CO₂ are the main components of flue gas. The cost of separating or purifying flue gas is very high. Injection of flue gas into the coal seams is also done to check its impact on the methane recovery. Studies have shown that coal seams have high adsorptive capacity towards CO₂ than N₂ in 4:1 ratio (Curt *et al.*, 2005). When flue gas is injected, breakthrough of N₂ occurs very quickly and CO₂ break through occurs after a long duration of time which evident the natural separation characteristics of the coal seams.

Apart from this adsorption characteristic, N₂ gas also reduces the partial pressure of the CH₄ gas to get desorbed into the cleat system to the production well. Even though the enhanced coal bed methane recovery by pure CO₂ and pure N₂ injection are showing the promising results on the technical front, it is also important to see the economic components like cost of pure CO₂ and N₂ generation and the current gas prices and whether the percentage increase in the production of methane is compensating the percentage of pure CO₂ and N₂ generation in terms of cost.

The production of pure CO₂ gas in surface facilities for sequestration is a costly process. The different behavior of CO₂ and N₂ towards the coal makes it as a separation medium which cuts the surface separation cost. The produced gas is a mixture of CH₄ and N₂ and separation units are required to increase the quality of CH₄ gas to pipeline specification and it is reported that the separation factors of the binary mixtures follow a trend of CO₂/N₂ (14.6) > CO₂/CH₄ (4.37) > CH₄/N₂ (3.33) at 298 K and 100 kPa (Yi *et al.*, 2012). Canada's deep unminable coal-bed methane (CBM) reserves are present in Western Canada Sedimentary basin in Alberta's plains and foothill areas. With the aid of recent developments in well stimulation methods and by understanding the interaction between the coal and fluids, this research identifies the most economical and effective approach to producing the methane gas while sequestering the CO₂ in coal beds.

Having known the above mentioned benefits of distinct behavior of coal towards injecting flue gas (CO₂ and N₂), research studies on ECBMR by flue gas injection could have been served its 3 profits at a time to oil and gas industry by saving the surface separation unit

cost, enhancing the gas production to shrink the energy gap by sequestering greenhouse gas in unminable CBM reserves and there was not much study has been conducted on what range of flue gas (CO₂ and N₂) compositions will results in ECBMR? Therefore, this new CBM developmental strategy is taken as research topic in this thesis and multi-component modelling simulator is used to address the final results.

1.2. Objective of the study:

The objective of this study is to do qualitative and quantitative analysis of flue gas (CO₂ and N₂) composition in the injecting gas to

1. Evaluate the potential of CBM resources as a sink for greenhouse gases (mainly CO₂)
2. Assessment of how effective is the recovery of the methane gas trapped in coal beds using flue gas (CO₂ and N₂) injection.

1.3. Organization of Thesis:

The research work carried out to fulfill the objective of the thesis is arranged in five chapters. The detail of each chapter is briefly mentioned below:

Chapter 1 introduces the topic of the research, its significance and the objectives to achieve in the research. The rest of the chapter details the CBM potential over the world and in Canada to support this research work. Chapter 2 is completely a literature review which details the interpretation of past research on coal properties and the analytical model equations that mainly describes the interaction between coal and the gas components and how these interpretations are useful in simulation study of CBM reserves. Chapter 3 gives

the details of input parameters and the modelling equations used to develop a hypothetical CBM reservoir using multi-component modelling simulator (CMG). In chapter 4, the simulation work flow is described step-by-step to get the results and analysis has been conducted to obtain reliable flue gas compositions to achieve effective and economical gas recoveries and CO₂ sequestration. The conclusions and recommendations for future work from this research work are given in chapter 5.

1.4. Coal Bed Methane Reserves:

Coal is one of the fossil fuels which are the most abundantly occurring resource. For past 200 years, the mineable coal is used as energy source which has contributed 26% towards global energy demand and generated 41% of the world's electricity (Thakur P., 2017). Apart from the mineable coal resources, the deep unminable coals are classified as another source of energy which are famously known as CBM resources and contain natural gas as the main component.

1.4.1. World Potential:

The presence of natural gas in deep unminable coals and extraction of this gas for reducing the gap between supply and demand are the general considerations for exploring the resources. Apart from this, the prominent outcomes from the research on ECBMR by CO₂ injection evident as one of the upcoming developments to store CO₂ which is one of the main greenhouse gas to mitigate or reduce their impact on global warming. **Table 1.1** gives the details of CBM resources in the world, shows that North America is having the highest Gas-in-place and recoverable resources, **Table 1.2** gives the details of worldwide CO₂

storage and methane production potentials and **Figure 1.1** shows the major coal basins of the world.



- | | | |
|--------------------------|------------------|----------------------------------|
| 1. Western Canada | 7. Upper Silesia | 13. China |
| 2. Western United States | 8. Donetsk | 14. Raniganj/Jharia |
| 3. Illinois | 9. Perchora | 15. Kilimantan |
| 4. Appalachian | 10. Ekibastuz | 16. Bowen |
| 5. East Pennine | 11. Karaganda | 17. Sydney |
| 6. Ruhr | 12. Kuznetsk | 18. Karoo |
| | | 19. Northern Columbia/ Venezuela |

Figure 1.1. Major Coal basins in the world (Thakur P., 2017)

Table 1.1. Coal Bed Methane Resources by Country/Region (Godec M. et. al, 2014)

Country	Coal Reserves Million Tonnes	CBM Gas-in-place		CBM Recoverable	
		TCF	TCM	TCF	TCM
United States	237,295	1,746	49	170	4.82
Canada	6,582	550	15.6	184	5.21
Mexico	1,211	9	0.3	1	0.04
North America	245,088	2,305	65.3	355	10.06
Brazil	4,559	36	1	5	0.15
Colombia	6,746	23	0.7	3	0.1
Venezuela	479	17	0.5	3	0.07
Others and Cen. America	724		0	0	0

South and Central America	12,508	76	2.2	11	0.32
Bulgaria	2,366				
Czech Republic	1,100	13	0.4	2	0.06
Germany	40,699	106	3	16	0.45
Greece	3,020		0	0	0
Hungary	1,660	4	0.1	1	0.02
Kazakhstan	33,600	50	1.4	10	0.28
Poland	5,709	50	1.4	5	0.14
Romania	291				
Russian Federation	157,010	1,682	47.6	200	5.66
Spain	530				
Turkey	2,343	51	1.4	10	0.28
Ukraine	33,873	170	4.8	25	0.71
United Kingdom	228	102	2.9	15	0.43
Other Europe and Eurasia	22,175				
Europe and Eurasia	304,604	2,228	63.1	284	8.04
Botswana		105	3	16	0.45
Mozambique		88	2.5	13	0.37
Namibia		104	2.9	16	0.44
South Africa	30,156	60	1.7	9	0.25
Zimbabwe	502	60	1.7	9	0.25
Other Africa	1,034				
Middle East	1,203				
Middle East and Africa	32,895	417	11.8	63	1.77
Australia	76,400	153	6.4	34	0.95
China	114,500	1,299	36.8	195	5.52
India	60,600	80	2.3	20	0.57
Indonesia	5,529	453	12.8	68	1.93
Japan	350				
New Zealand	571				
North Korea	600				
Pakistan	2,070				
South Korea	126				
Thailand	1,239				
Vietnam	150				
Other Asia Pacific	3,707				
Asia Pacific	265,842	1,985	58.2	316	8.96
Total World	860,938	7,011	201	1,030	29.15

Table 1.2. CO₂ storage and methane production potential of the world's coal basins (Godec M. et. al, 2014)

Country	Estimated Methane Recovery (TCM)			CO ₂ Storage	
	Primary	ECBM	TOTAL	TCF	Gt
United States	5	7.54	12.4	52.82	86.16
Canada	5.21	4.35	9.6	17.85	29.11
Mexico	0.04	0.09	0.1	0.34	0.55
North America	10.06	11.99	22.1	71	116
Brazil	0.15	0	0.2	0.57	0.93
Colombia	0.1	0.22	0.3	1.29	2.11
Venezuela	0.07	0.3	0.4	3.57	5.83
South and Central America	0.32	0.52	0.85	5.44	8.87
Czech Republic	0.06	0	0.1	0	0
Germany	0.45	0	0.5	0.62	1.01
Hungary	0.02	0.04	0.1	0.1	0.17
Kazakhstan	0.28	0	0.3	0.5	0.82
Poland	0.14	0.94	1.1	4.07	6.63
Russian Federation	5.66	12.61	18.3	35.2	57.41
Turkey	0.28	0	0.3	0.58	0.94
Ukraine	0.71	1.72	2.4	4.54	7.41
United Kingdom	0.43	1.03	1.5	2.73	4.46
Europe and Eurasia	8.04	16.35	24.39	48.34	78.84
Botswana	0.45	1.06	1.5	9.18	14.97
Mozambique	0.37	0.89	1.3	1.84	3.01
Namibia	0.44	1.05	1.5	2.18	3.56
South Africa	0.25	0.61	0.9	1.26	2.05
Zimbabwe	0.25	0.61	0.9	3.44	5.62
Middle East and Africa	1.77	4.22	5.99	17.9	29.2
Australia	0.95	0.67	1.62	9.01	14.7
China	6	7.13	12.64	47.83	78.01
India	0.57	0.63	1.2	4.04	6.6
Indonesia	1.93	8.05	9.97	95.4	155.6
Asia Pacific	8.96	16.47	25.43	156.28	254.91
Total World	29.15	49.55	78.7	298.97	487.64

1.4.2. Canada's Potential:

Canada has a world class natural gas base, with estimated 33 TCF and 9 TCF of remaining established conventional natural gas resources in Alberta and British Columbia provinces respectively. Most of these resources are present in Western Canadian Sedimentary Basin. It is estimated that, Canada is having higher unconventional resources compared to the conventional gas resources, but the resources are yet to be proven. About 80% of the natural gas production in Canada comes from Alberta, making it as one of the world's largest suppliers of natural gas (Albertacanada Statistics).

Alberta's CBM Potential:

Alberta Geological survey estimates that there may be up to 500 TCF natural gas in Alberta's coals but it is not yet confirmed what portion of these resources may be recoverable. The Alberta Energy Regulator (AER) estimates that the remaining established reserves of CBM to be approximately 2 TCF in areas of Alberta where commercial production is occurring. Coal resources of Alberta distributed throughout the southern Plains, Foothills and Mountains. The plant debris originally deposited in the flat-laying peat swamps and the organic matter was buried by sediments derived from uplift in the west and gradually changed into coal with increasing heat and pressure burial. Overtime the coals were in turn uplifted and partially eroded, resulting in the present distribution of coal across the plains as shown in Figure 1.2 (AGS Earth Science report, 2003).

Most of the coal seams occur within distinctive horizons of the Scollard, Horseshoe Canyon, Belly River and Mannville strata in the Alberta Plains, and within the Wapiti, Luscar and Kootenay strata of the Foothills as shown in **Figure 1.2** These coal zones are laterally

continuous with interbedded coals and inorganic partings and the individual coal seams are separated by 30-50 meters of rock. In plains, most of the shallow coal seams (<1000m) are within the rank range of sub-bituminous to high-volatile bituminous C-B. Foothill coals are more mature, with rank ranging from high-volatile bituminous B to low-volatile bituminous and the most potential CBM resources in plains for exploration are shown in **Figure 1.3** **Figure 1.4** shows the distribution of coal zones according to their rank and **Figure 1.5** shows the stratigraphic relationships of the coal zones in Alberta plains and Foothills. Some of the basic characteristics of the CBM produced from these coal zones are as follows:

1. The natural gas found in coals is “sweet gas”; i.e., it does not contain hydrogen sulphide in it.
2. The gas is generally near-pipeline quality when produced and requires minimum processing.
3. The gas is produced at low pressures than conventional natural gas.

Most common characteristics of the coal seams in different formations of Alberta’s plains and foothills are observed from the Alberta Geological Survey report on Alberta’s CBM potential and tabulated in **Table 1.3** and **Table 1.4**.

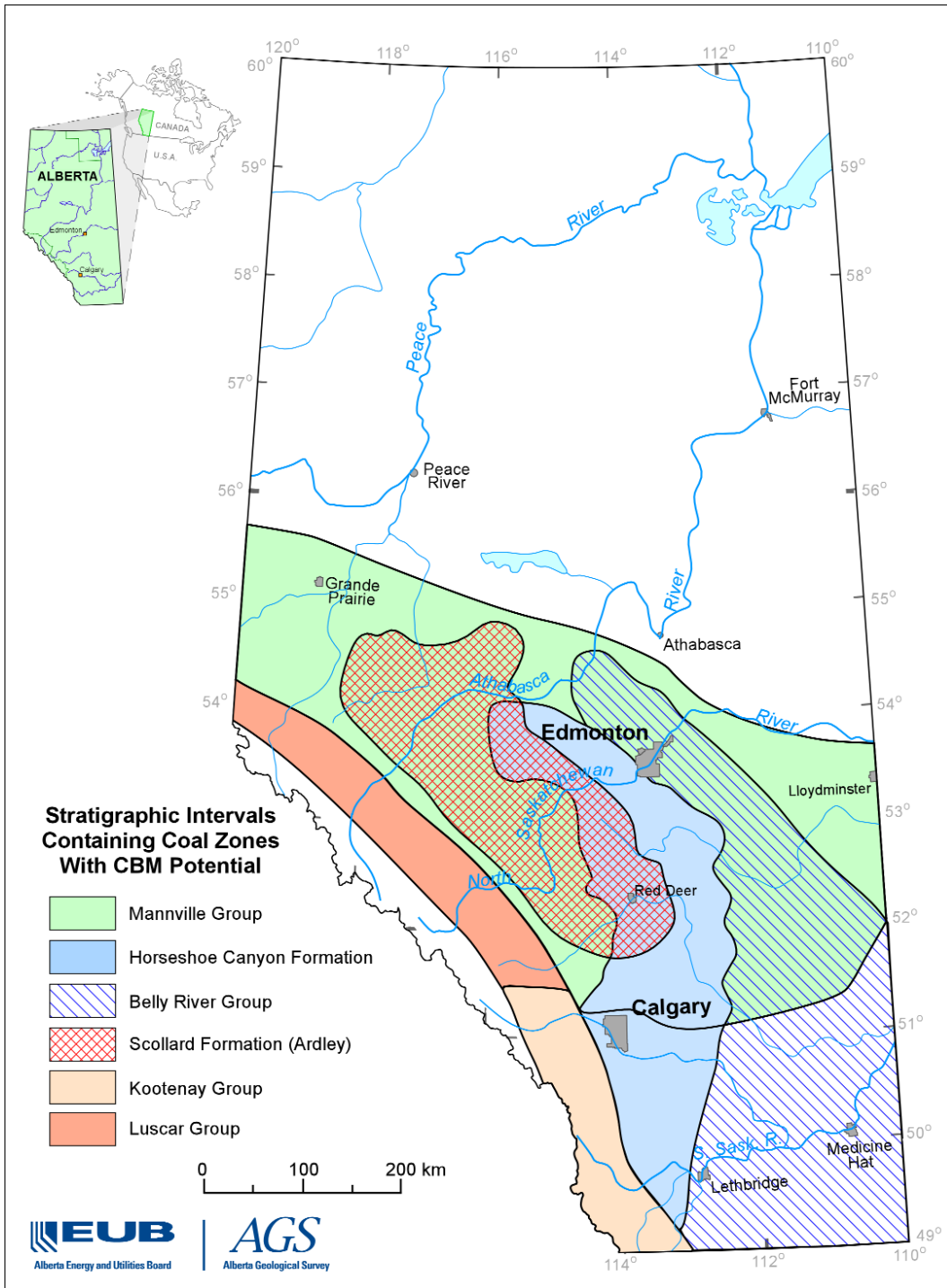


Figure 1.2. Distribution of major coal bearing formations with CBM potential, Alberta (AGS, ES report, 2003)

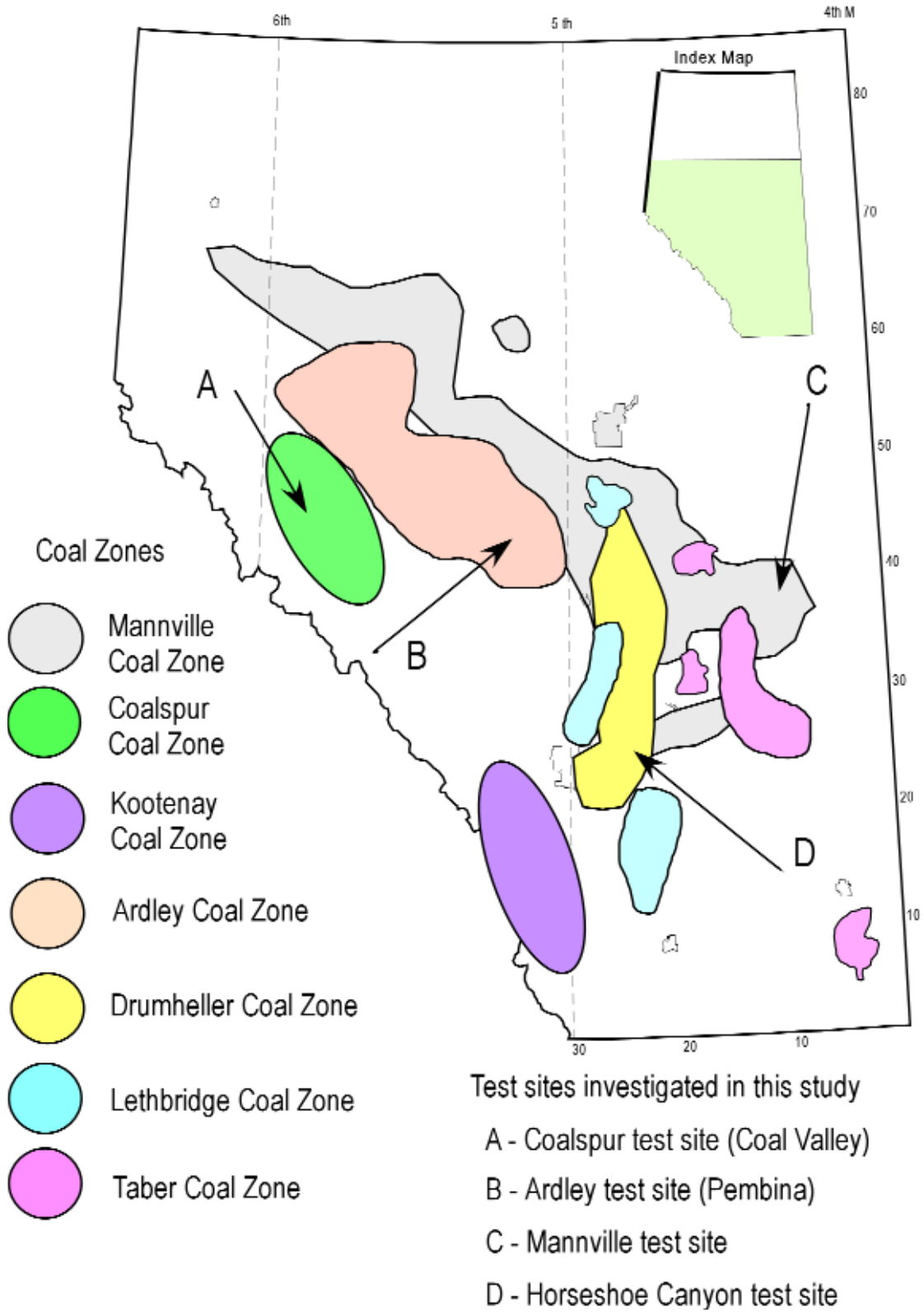


Figure 1.3. Areas with potentially favorable CBM exploration potential, Alberta Plains (AGS, ES report, 2003)

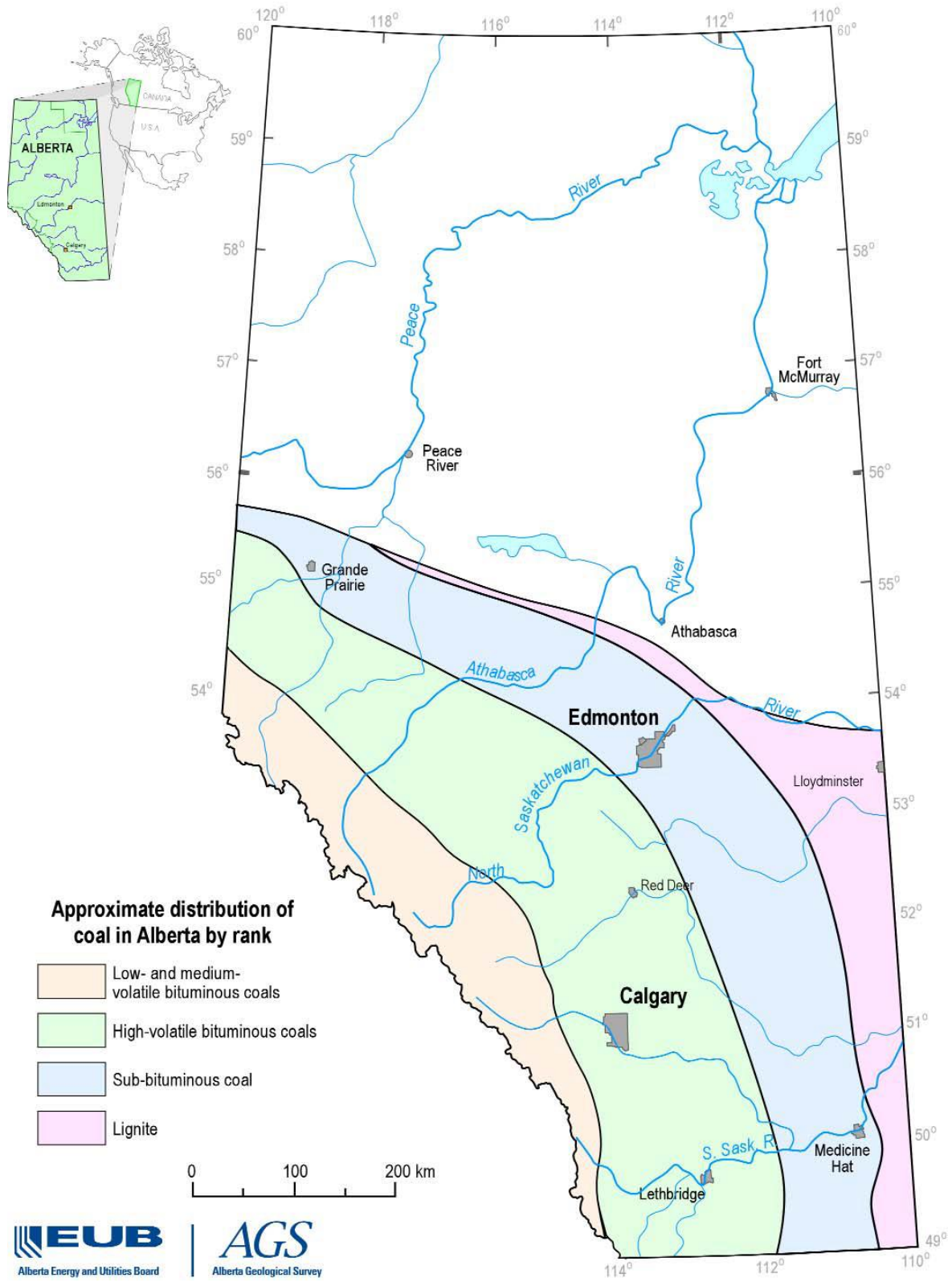


Figure 1.4. Coal rank trends across Alberta (AGS, ES report, 2003)

	Foothills/Mountains	Plains	Major Coal Zones	
Tertiary	Paskapoo Fm	Paskapoo Fm	Obed	
	Coalspur Fm	Scollard Fm	Ardley/Coalspur	
Upper Cretaceous	Entrance Cgl			
	Saunders Gp	Battle/Whitemud Fm	Carbon/Thompson	
		Brazeau Fm	Wapiti Fm	Drumheller
	Belly River Gp		Horseshoe Canyon Fm	Lethbridge
			Bearpaw Fm	
	Oldman Fm	Taber		
	Foremost Fm	McKay		
	Alberta Gp	Lea Park Fm		
		Colorado Gp		
	Lower Cretaceous	Luscar Gp	Mannville Gp	Luscar
Mannville				
Jurassic	Kootenay Gp / Nikanassin		Kootenay	

Figure 1.5. Stratigraphy of coal bearing strata, Alberta (AGS, ES report, 2003)

Table 1.3. Characteristics of different coal zones in Alberta Plains (AGS, ES report, 2003)

Formation	Major Coal Zones	Common Characteristics	
Scollard or Paskopoo	<ul style="list-style-type: none"> • Ardley Sub coal zones: • Val D’Or • Silkstone • Mynheer 	<ul style="list-style-type: none"> • Rank: Sub-bituminous to High volatile bituminous B • Reflectance: 0.5 – 0.65 % 	<ul style="list-style-type: none"> • Laterally continuous • Thick in west and thin in east of Alberta’s plains • Net thickness ~ > 20 m • Methane concentration in favorable CBM potential areas ~ > 4 bcf/Section
Horseshoe Canyon	Drumheller	<ul style="list-style-type: none"> • Rank: Sub- bituminous to Highly volatile • Reflectance: 0.5 – 0.65 % 	<ul style="list-style-type: none"> • Utmost 10 potential economic coal seams and a target for exploitation • Gas concentration ~ 2-3 bcf/Section • High permeable ~ 4.9 mD • Average thickness of coal seam: <18m • Discontinuous and Net thickness > 4 m • Under pressured coal seams
	Daly-weaver		<ul style="list-style-type: none"> • Thin and Discontinuous • Not a target for exploitation
	Carbon-Thompson		<ul style="list-style-type: none"> • Discontinuous and thin coal seams • Laterally persistent but not a target for exploitation • Net thickness ~ 2-3 m • Gas concentration ~ < 1 bcf/ Section
Belly River	McKay	<ul style="list-style-type: none"> • Rank: Highly volatile bituminous B to C • Reflectance: 0.55 – 0.70 % • Shallow in depth • Gas concentration: 0.75-1 bcf/Section 	<ul style="list-style-type: none"> • Discontinuous and Thickness ~ 30-50 m • Net average thickness ~ 1-3 m
	Taber		<ul style="list-style-type: none"> • Discontinuous and Avg. Thickness ~ 25 m • Net thickness ~ 3-4 m
	Lethbridge		<ul style="list-style-type: none"> • Laterally continuous • Average Thickness ~ 10-15 m • Net thickness ~ 3-4 m
Mannville	Mannville coal zone	<ul style="list-style-type: none"> • Rank: Sub- bituminous to Highly volatile bituminous • enhanced permeable shallow depth (< 1500 m) 	<ul style="list-style-type: none"> • Continuous coal seams • Thick coals in Red Deer area ~ 6-12 m • Thin coals in Fort McMurry which are shallow and Net thickness ~ < 1 – 11 m • High gas content ~ > 5 bcf/Section • Low permeable ~ 0.1 – 2 mD • Target potential: structurally

Table 1.4. Coal Bed Methane potential of Alberta Plains (AGS, ES report, 2003)

Coal Zone	CBM Potential	
	m³	TCF
Ardley	1.50 x 10 ¹²	53
Carbon Thompson	3.97x 10 ¹¹	14
Daly-Weaver	3.97x 10 ¹¹	14
Drum Heller	1.08x 10 ¹²	38
Lethbridge	5.10x 10 ¹¹	18
Taber	5.67x 10 ¹¹	20
McKay	7.93x 10 ¹¹	28
Mannville	1.13x 10 ¹³	400

Chapter 2 : Coal Reservoir Properties

Generally, under tropical or semitropical conditions the plant material accumulates and deposits in swamps undergoes compaction forms coal beneath the younger sediments. The buried plant material undergoes decomposition due to the action of pressure and temperature and gas is generated during the maturation of organic matter into coal by microbial activities that occur. In the initial stages of burial of plant material peat is formed which is characterized as dark brown residuum produced by the partial decomposition and disintegration of plants that grow in marshes and swamps. By driving off water and volatiles, peat undergoes coalification and transforms into coal.

Coal is classified into peat, lignite, bituminous, sub-bituminous and anthracite depending on the amount of carbon content it contains which increases as the degree of maturation increases. This property is defined as rank of the coal which is defined as “the degree of coalification that takes place during the transformation from peat to anthracite”. Therefore, peat is known as the low rank coal and anthracite as high rank coal.

Unlike the conventional resources, mostly the gas generated is present in the adsorbed state onto the coal surface rather than in the pore spaces. The amount of gas formed is rank dependent. Methane is the predominant gas present in the coal seams with small amount of ethane, carbon dioxide, nitrogen, helium and hydrogen (Gunter *et al.*, 1997). Water is also produced during the maturation process. In reservoir terms, coal seams are the low porosity, low permeability, naturally fractured, water saturated gas reservoirs.

Before understanding the interaction of coal with the fluids in place and driving mechanisms to produce methane gas from coal beds, it is essential to understand the properties and their relative variations under change in pressure and temperature.

2.1. Porosity:

Size of the coal pores varies in a range from micrometer to angstrom dimensions. Coal pores are classified into four groups depending on the pore sizes (IUPAC, 1972)

- I. Macro pores (>500) Å⁰
- II. Mesopores (20-500) Å⁰
- III. Micro pores (8-20) Å⁰
- IV. Submicropores (<8) Å⁰

Measuring the porosity of the coal is essential to understand the storage system of gases like methane and CO₂ in the coal seams. The total open pore volume measured using gas and liquid adsorption method is given by the following equation:

$$V_p = \frac{1}{\rho_{Hg}} - \frac{1}{\rho_{He}} \quad (2.1)$$

Where, ρ_{Hg} and ρ_{He} are the densities of mercury and helium respectively.

According to Curt *et al.*, 2005; the above densities are measured on a dry mineral-matter-free (dmmf) basis. That means, the original density measurements are corrected for mineral matter and moisture content assuming an average mineral density. Coal density is related

to the chemical composition and the density measured on dmmf basis is correlated to the rank and carbon content of coal.

Coal porosity is defined as the percentage of the volume of the coal accessible to helium molecule and is calculate by the following equation:

$$\phi = 100 \rho_{\text{Hg}} \left(\frac{1}{\rho_{\text{Hg}}} - \frac{1}{\rho_{\text{He}}} \right) \quad (2.2)$$

It is difficult to classify the coal's complex porous structure with complex material. Micro porosity of the coal is the dominant factor in the gas adsorption process (explained ahead in the literature) regardless of the mechanism by which gases are transported through the organic matrix of the coal. Canadian Mannville coals are deep and water content in the cleat system is low i.e., mostly dry coals and the moisture content reduces as the depth increases. From above review, it can be understood that the original density measurement of coal doesn't require much correction.

Generally, most coals are characterized by dual porosity system: Primary porosity and secondary porosity. Primary porosity system consists of micropores and mesopores. The secondary porosity system constitutes macropores and natural fractures. In 1968, Warren and Root represented the coal beds using dual porosity model as shown in the **Figure 2.1**. (Warren *et al.*, 1968).

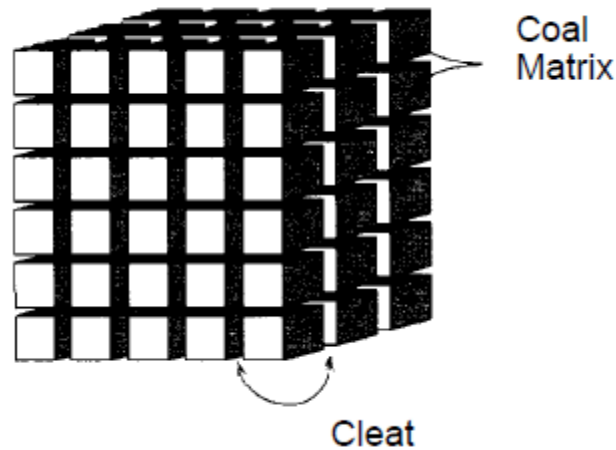


Figure 2.1. Dual porosity system of coal (Saulsberry et al., 1996)

They represented the coal beds as a set of building blocks where these blocks are defined as the matrix blocks and space between them as fractures or cleats. Primary porosity is defined by the pore space between the coal matrix grain particles and is formed during deposition and lithification process in geological time scale. Most of the methane gas is adsorbed to the coal surface in these micropores. The secondary porosity (macro porosity) of the coal is controlled by fractures, fissures, and jointing.

2.2. Permeability:

Unlike the conventional hydrocarbon resources, when it comes to Coal Bed Methane Resources, permeability is explained in two senses. In one sense, it describes the flow of gas in the matrix pores after it's desorption from coal surface. In second sense, it is the term used for describing the transportation of the gas through the cleat system. The gas desorption from coal surface into matrix pores and diffusion through the matrix block is explained by Fick's law with concentration gradient as the primary driving force and gas transportation in cleat system by Darcy's law which is shown in the **Figure 2.2** schematically.

The relative rate of occurrence of both mechanisms decides the model that is used to describe the gas flow mechanism. It means that when the rates of gas desorption (i.e. diffusion) from the coal surface is higher than the flow rate in the cleats, then gas production is flow limited which means Darcy's law is applicable to model flow of gas in the cleat system. However, if the desorption rate is slower than the flow rate in the cleats, gas production is diffusion limited and modelled using Fick's law.

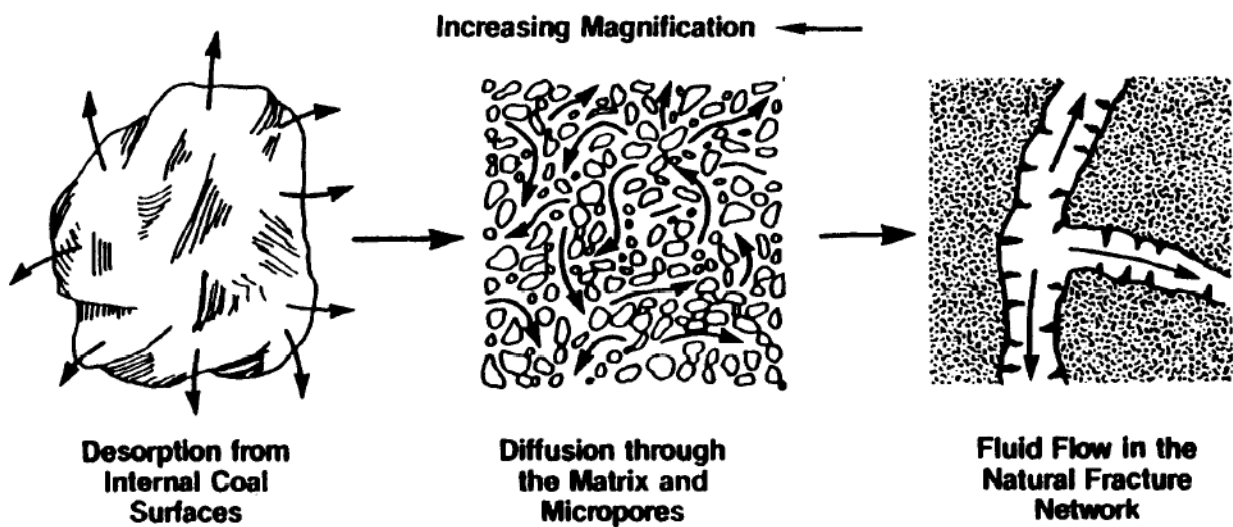


Figure 2.2. Schematic representation of transportation of CH_4 gas in coal seams (Harpalani et al., 1990)

The coal bed consists of wide network of cleats or fractures. These cleats or fractures are said to be formed during the compaction of the organic matter due to coalification and during tectonic activities. Cleats are referred to as face cleats and butt cleats as shown in the **Figure 2.3**. Face cleats are very prominent compared to butt cleats.

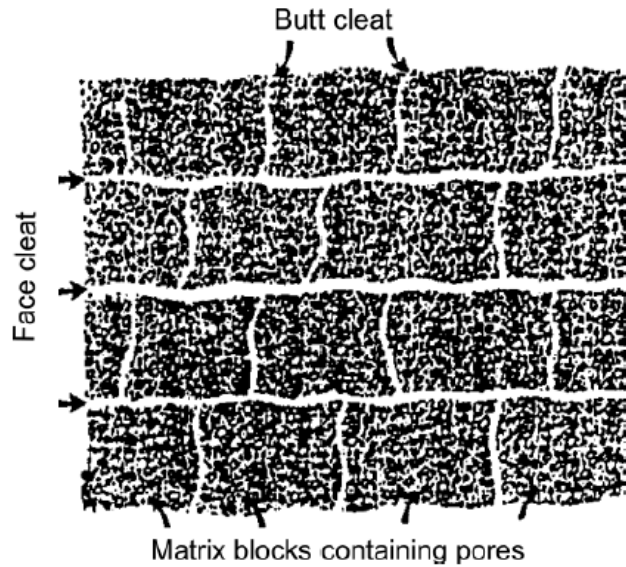


Figure 2.3. Cleat system in CBM reservoir (plan view) (Shi et al., 2005)

The spacing between the face cleats can range from one tenth of an inch to several inches. Face cleats are relatively planar and continuous those are like systematic joints and butt cleats are orthogonal to the face cleats. However, these cleats are tending to be discontinuous and non-planar cross joints (Cervik, 1969). In CBM reservoirs, Cleats are very permeable towards gas and water compare to matrix system which are mostly impermeable (Harpalani *et al.*, 1995). Most commonly, the permeability range between 1 and 10 mD and it may range up to 100 mD and it is the direction and connectivity of these cleats which decides the productivity of the gas from the coal seam. When the exposure to the natural fractures is high, high gas production can be expected. This is only possible by having horizontal wells which are drilled perpendicular to the face cleats rather than parallel to them because perpendicular position has high exposure to the natural face cleats.

2.3. Adsorption/ Desorption:

Methane gas is the predominant gas component in CBM reservoirs which is mostly present in the adsorption form on coal surface by van der Waals forces of attraction the amount of gas adsorbed can be evaluated by direct methods which include measurement of volume of gas released from a coal sample into a sealed desorption canister and indirect methods which includes sorption isotherms obtained in laboratories (Curt *et al.*, 2005). An adsorption isotherm test is conducted to determine the maximum gas holding capacity of a sample coal because the gas storage capacity of coal is dependent on pressure of the system (Moore, 2012).

According to the IUPAC classification, all type of physical adsorption mechanisms are classified into six isotherms as shown in **Figure 2.4**. These isotherms are classified based on different pore sizes, number layers of adsorbate adsorbed onto the solid surface and gives amount of adsorbate adsorbed with respect to change in pressure at constant temperature. From the past research work, it is known that adsorption of CH₄ and CO₂ gases onto coal surface is characterized by Type I isotherm which represents the monolayer adsorption of gas molecule on to the non-porous solid or microporous solid. The double curves in Type IV and V isotherms represent the occurrence of hysteresis due to capillary condensation (Sing *et al.*, 1985).

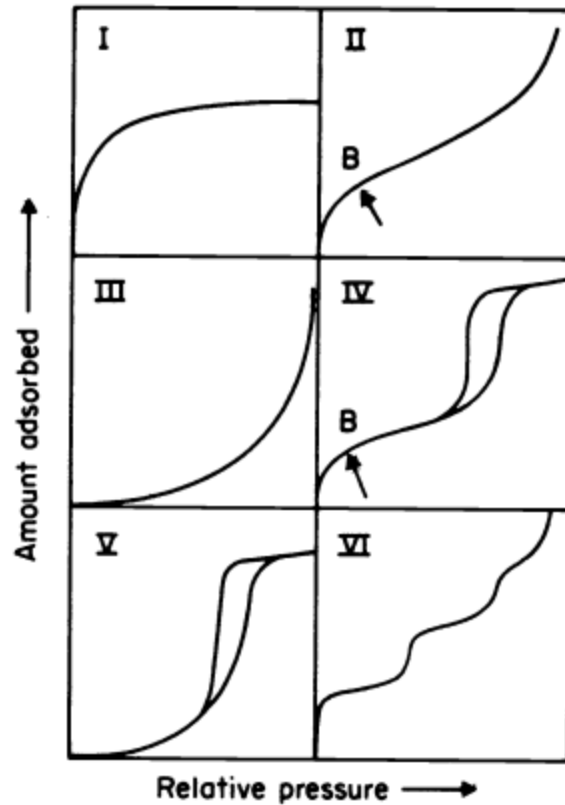


Figure 2.4. IUPAC Classification of physical adsorption (Sing et al., 1985)

There exist the following mathematical models to describe the adsorption isotherms. Among them, Langmuir isotherm model is the initial and simplest model which describes the adsorption phenomenon of gases on coal internal surface. Langmuir assumed that any solid surface consists of fixed number of well-defined localized sites, each site can able to hold only one adsorbate molecule, all the sites are equally energized and there exists no interaction between the adsorbate molecules (Langmuir, 1918). The above assumptions depict that this model is valid for monolayer adsorption of gas molecules and the mathematical equation is given as (Moore, 2012);

$$V = \frac{V_L * P}{P_L + P} \quad (2.3)$$

Where,

V = maximum gas adsorption capacity at any Pressure (m^3/kg)

V_L = Langmuir volume (m^3)

P_L = Langmuir pressure (kPa)

P = pressure (kPa)

In 1938, Brunauer, Emmett and Teller made a slight modification to the original Langmuir model to account for multilayer adsorption phenomenon which assumes that the adsorbate molecules in the first layer act as sites for second layer adsorption and so on and involve heat of adsorption. This model is popularly known as extended Langmuir equation or BET equation given as (Brunauer *et al.*, 1938);

$$V = \frac{V_0 C P}{(P_0 - P)[1 + (C - 1)(P/P_0)]} \quad (2.4)$$

$$V = \frac{V_0 C P / P_0}{[1 + C(P/P_0)]}; \text{ When } P \ll P_0 \quad (2.5)$$

Where,

V_0 = Maximum volume of gas adsorbed (monolayer adsorption capacity)

C = Constant related to heat of adsorption

P= Pressure (kPa)

P_0 = Saturation pressure of the adsorbate at adsorption temperature (kPa)

Langmuir and BET model equations are applicable for the surfaces with large pores and not properly describe the adsorption phenomenon on the surface with micropores. Dubinin's pore filling theory describes the adsorption of gases in micropores and the model equation is given as (Curt *et al.*, 2005);

$$n = n_0 e^{-[D \ln(P_0/P)]} \quad (2.6)$$

Where,

n = moles of gas adsorbed gmole)

n_0 = Pore volume of the adsorbent

D = Dubinin's constant; $D = RT/\beta E$; R = Gas constant, T = Temperature, β = Affinity coefficient, and E = Characteristic heat of adsorption

In the past, most of the CO₂ adsorption experiments were performed at low pressures and temperatures and extrapolating this data to in-situ high temperature and pressure lead to large errors in interpreting the coal seam properties. ECBM recovery involves the simultaneous adsorption of CO₂ and desorption of CH₄ from coal surface and composition of each component changes during depressurization (Scott, 1993). It is very important to properly understand the sorption properties of the both gas molecules to correctly estimate the total amount of CO₂ storage and CH₄ recovery. The presence of multi-components in the gas affects the volume of single component adsorbed in the coal system. The above

mentioned mathematical models are used individually or in combination to describe the sorption behavior of the binary or multicomponent gas on coal surface.

As the pressure increases at a constant temperature, the attraction of adsorbate molecule towards coal surface increases rapidly and it is also proven that CO₂ has higher affinity than CH₄ and N₂ has less affinity than CH₄ towards coal at any pressure (**Figure 2.5**). The adsorption ratio of CO₂ to CH₄ of 2:1 is widely reported in the literature (Gentzis, 2000; Gunter *et al.*, 1997; Greaves *et al.*, 1993; Yee *et al.*, 1993; Arri *et al.*, 1992). The dimensions of sorbate molecules and the pore structure are the major factors affecting the selective gas sorption and diffusion (Stefanska *et al.*, 2008). Apart from this general acceptance, some studies on different coal samples gave the ratios ranging from 10:1 to less than 2:1 (Harpalani *et al.*, 2006; Mastalerz *et al.*, 2004; Busch *et al.*, 2003; Bustin, 2002). Hence, the amount of gas adsorbed on to the coal surface is reservoir specific and depends on many factors like coal rank, maceral content, mineral matter, moisture content, type of adsorbate, pressure and temperature. Langmuir equation perfectly describes the sorption characteristic of CH₄ at lower pressures. Larger V_L and smaller P_L values results in higher CH₄ adsorption capacity (Liu *et al.*, 2016). Moisture content in the coal reduces the pore size due to swelling of coal which eventually reduces the adsorption capacity (Harpalani *et al.*, 2006).

The critical point to take from this observation is that when there exist multi components in the coal system, each component doesn't adsorb independently; rather they compete each other to get adsorbed. Therefore, the interaction of the components among them and with coal is a complex and dynamic process which needs to be understood by rigorous lab work.

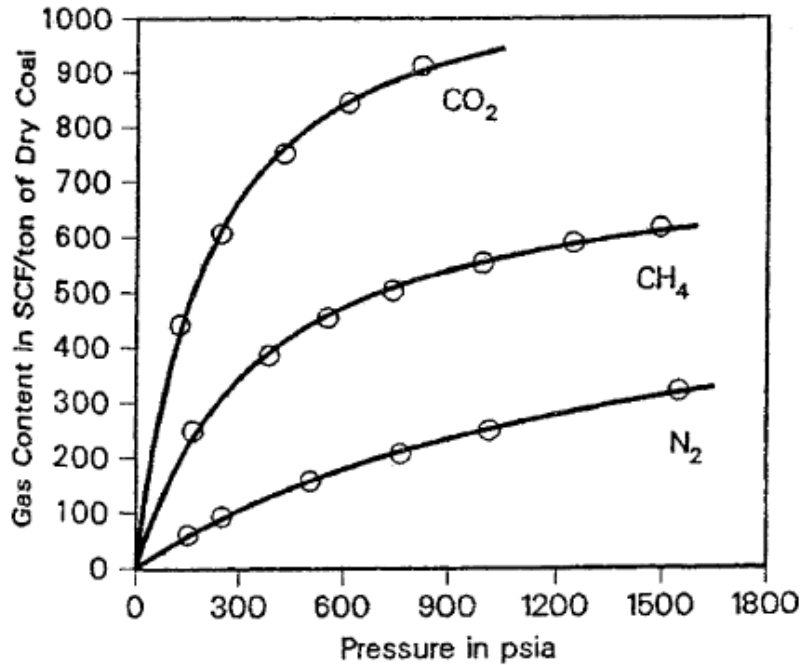


Figure 2.5. Adsorption isotherms of CH₄, CO₂ and N₂ gases on Fruitland coal sample at 115°F (Yee et al., 1993)

2.4. Coal Shrinkage/Swelling:

Unlike the conventional hydrocarbon reservoir rocks, coal is not a rigid solid. It is like a polymer network which is always affected by the fluids that are in contact which consequently result in changes in permeability and porosity of the coal system (Curt *et al.*, 2005). Production of water and gas makes coal seams to shrink, adsorption of gases makes coal to swell, and sorption of gases is related to the pressure in the coal seams which fundamentally shows the influence of mechanical and elastic properties of coal (Duruca *et al.*, 2009). Generally, matrix shrinkage increases the distance between two adjacent matrix blocks and there by increases the cleat permeability. Contrast to the shrinkage, matrix swelling decreases the distance between two adjacent matrix blocks and consequently

reduces the cleat permeability. By their nature both phenomena show opposite impact on coal seam. During ECBM operation simultaneous shrinkage and swelling occur due to operating conditions which result change in porosity and permeability of the coal seams.

In 1995, Seidel and Huitt conducted experiments to measure shrinkage under in-situ coal temperatures and pressures. They concluded from their experiments that “the pressure had to fall below a certain crucial pressure before shrinkage occurred. Below this crucial pressure, desorption led to matrix shrinkage and permeability increases”. It is also concluded that the change in permeability is dependent on the composition of the gas and is larger for CO₂ than CH₄ (Seidle *et al.*, 1995).

In 2001, from studies by St. George and Barakat, it is observed that methane desorption increases stress by a factor of 2.5 times more than what was expected from the incremental relief of gas pressure within the coal seams.

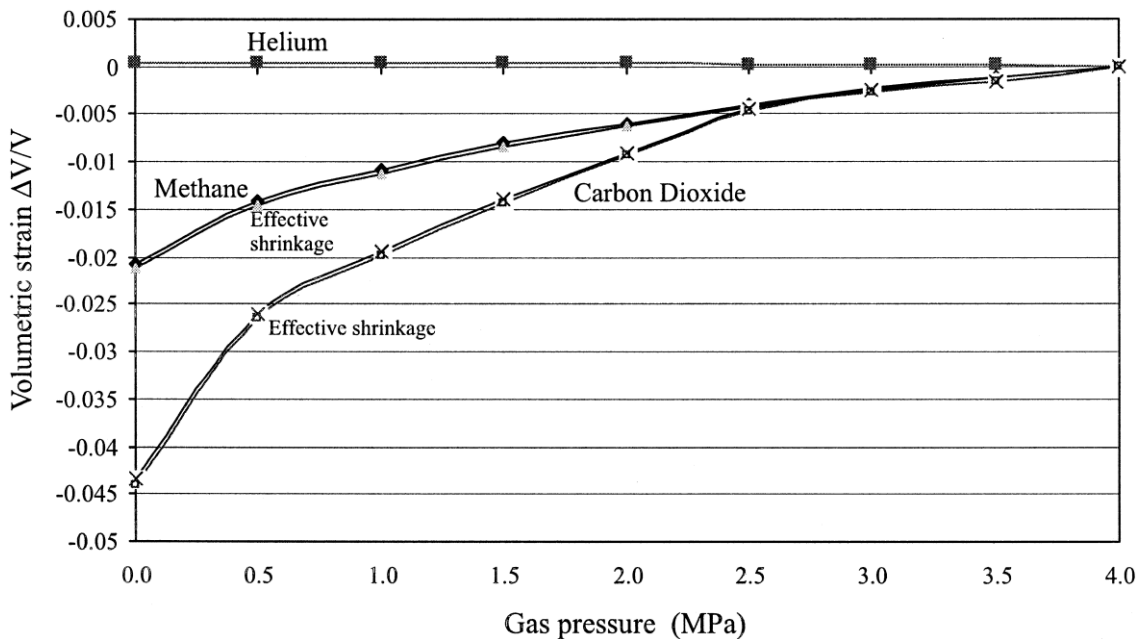


Figure 2.6. Volumetric strain of coal matrix with decreasing gas pressure (St. George et al., 2001)

Figure 2.6 shows the volumetric strain of coal matrix with decreasing in gas pressure and it is observed that the effective shrinkage of coal is much higher for CO₂ than CH₄ when gas pressure reduces.

According to Kuuskaraa, from his studies on coal permeability, in under saturated coals, the reduction in coal permeability due to depletion in pressure (i.e., compressibility) of coal is much less and the increase in coal permeability due to desorption of gas counteracts the decrease in permeability due to compressibility of rock in initial production life (Curt *et al.*, 2005).

In 1989, Harpalani and Zhao conducted experiments to investigate the coal permeability in respect to CH₄ desorption from coal seams. From their experimental work it is observed that, upon reduction of pressure to certain crucial point without desorption of CH₄ gas, coal permeability reduces and then further reduction of pressure below that crucial point makes the CH₄ gas to desorb from the coal surface and permeability increases dramatically (Harpalani *et al.*, 1989). They concluded that the increase in permeability is mainly due to the matrix shrinkage by which the fracture width is increased (Harpalani *et al.*, 1990). **Figure 2.7 and 2.8** shows the variation in coal permeability with decrease in pressure and variation in adsorbed gas volume and permeability of coal to CH₄, relative to increase in gas pressure.

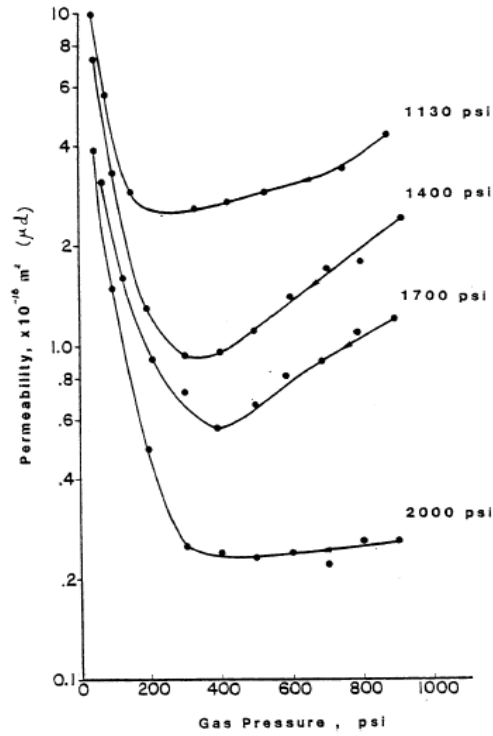


Figure 2.7. Variation in 'K' with decreasing in pr. at 4 hydrostatic stress levels (Harpalani et al., 1989)

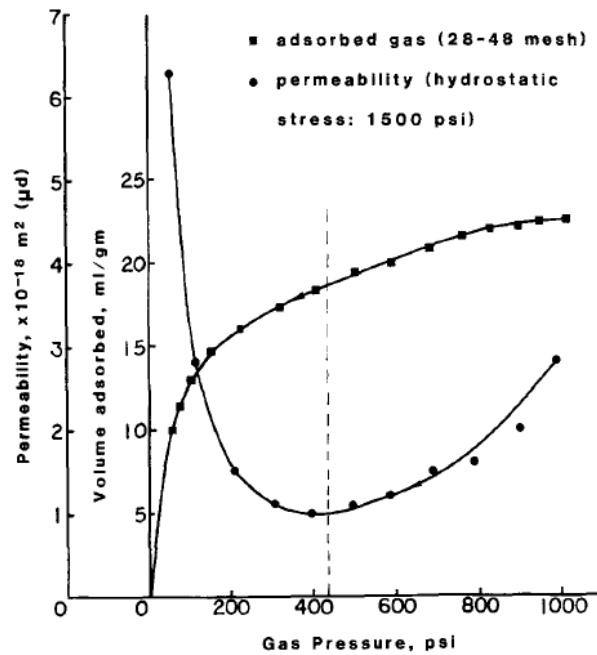


Figure 2.8. Variation in absorbed gas volume and 'K' of coal to CH₄ with gas pr. (Harpalani et al., 1990)

During primary production only CH₄ desorption takes place in CBM system hence, high matrix shrinkage occurs which results in permeability increase and during ECBM operation, the high affinity of CO₂ towards coal reduces the matrix shrinkage by imposing swelling effects on coal which decreases the rate of permeability increase and this impact can be observed in gas recoveries.

2.4.1. Mathematical models for calculating change in porosity and permeability:

The above-mentioned findings clearly indicate that the coal swells, shrinks and undergoes stress in all directions anisotropically all of which change coal's porosity and permeability during gas production and it seems there exists a relationship between porosity and permeability. In past 25 years, several studies were conducted to come up with a mathematical model to describe the changes in porosity and permeability and relationship between them. The following are the brief explanation to the most popular models:

In 1990, a mathematical model was developed by Sawyer, Paul, and Schraufnagel to calculate the changes in porosity. The mathematical model equation is a linear relationship between strain and total adsorbed amount and it is written as (Sawyer *et al.*, 1990):

$$\varphi = \varphi_0 * [1 + C_P \cdot (P - P_0)] - C_m * (1 - \varphi_0) * \left(\frac{\Delta P_0}{\Delta C_0}\right) * (C - C_0) \quad (2.7)$$

Where,

φ = Fracture system porosity, fraction

φ_0 = Initial fracture system porosity, fraction

C_m = Matrix shrinkage compressibility, kPa^{-1}

C_p = Pore volume compressibility, kPa^{-1}

P = Reservoir pore pressure, kPa

P_0 = Initial reservoir pore pressure, kPa

C = Reservoir gas concentration, dimensionless

C_0 = Initial reservoir gas concentration, dimensionless

In 1995, Seidle and Huitt also developed a linear model equation to calculate the change in porosity due to matrix shrinkage effect and is given by (Seidle *et al.*, 1995):

$$\frac{\varphi}{\varphi_0} = 1 + \left(1 + \frac{2}{\varphi_0}\right) * C_m * V_m * \left(\frac{bP_0}{bP_0 + 1} - \frac{bP}{bP + 1}\right) \quad (2.8)$$

Where,

C_m = Matrix shrinkage coefficient, micro-kg/m^3

V_m = Langmuir volume constant, m^3/kg

P = Reservoir pore pressure, kPa

P_0 = Initial reservoir pore pressure, kPa

b = Langmuir Pressure constant, kPa^{-1}

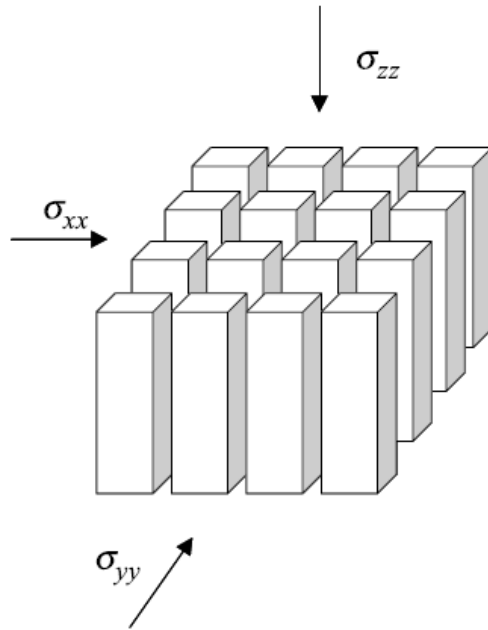


Figure 2.9. A bundled matchstick geometry representation of the coal seam (Seidle et al., 1992)

Considering the changes in porosity in a bundled matchstick geometry shown in **Figure 2.9**, the change in permeability is obtained by (Seidel *et al.*, 1992):

$$\frac{K}{K_0} = \left(\frac{\varphi}{\varphi_0} \right)^3 \quad (2.9)$$

Where,

φ = Natural fracture porosity, fraction

φ_0 = Porosity at virgin reservoir pressure, fraction

K = Permeability, mD

K_0 = Virgin permeability, mD

Palmer and Mansoori developed a new mathematical model in 1998 to express the changes in porosity by considering the uniaxial strains in the coal seams. The single mathematical equation given below includes both stress and matrix shrinkage effects in it. The matrix shrinkage is incorporated as a function of the reservoir pressure instead of considering the average value during the drawdown phase. This equation is valid for the porosity changes less than a factor of 2 and permeability changes less than a factor of 1 (Palmer *et al.*, 1998).

$$\frac{\varphi}{\varphi_0} = 1 + \frac{C_m}{\varphi_0} * (P - P_0) + \frac{\varepsilon_1}{\varphi_0} * \left(\frac{K}{M} - 1\right) * \left(\frac{\beta P}{1+\beta P} - \frac{\beta P_0}{1+\beta P_0}\right) \quad (2.10)$$

$$C_m = \frac{1}{M} - \left(\frac{K}{M} + f - 1\right) * \gamma \quad (2.11)$$

Assuming that permeability varies with porosity by $\frac{K}{K_0} = \left(\frac{\varphi}{\varphi_0}\right)^3$

Where,

φ = Natural fracture porosity, fraction

φ_0 = Porosity at virgin reservoir pressure, fraction

M = Constrained axial modulus, kPa

K = Bulk modulus, kPa

f = Fraction 0 to 1

P = Reservoir pressure, kPa

P_0 = Virgin reservoir pressure, kPa

ε_1 , β = Parameters of Langmuir curve match to volumetric strain change because of matrix shrinkage (ε_1 dimensionless, β psi⁻¹), usually $\beta = 1/P_L$

γ = Grain compressibility, kPa⁻¹

In 2004, Shi and Durucan developed a model which is like Gray's model (1987) to show the relationship between horizontal stress and change in permeability assuming that "adsorbed gas is in equilibrium with the free gas in the pore spaces and the coal seams are saturated with adsorbed gas at initial reservoir pressure P_0 " (Shi *et al.*, 2004). The mathematical equation is given as:

$$\sigma - \sigma_0 = - \frac{\nu}{1-\nu} (P - P_0) + \frac{E\varepsilon_1}{3(1-\nu)} \left(\frac{P}{P+P_\varepsilon} - \frac{P_0}{P_0+P_\varepsilon} \right) \quad (2.12)$$

Where, σ = Effective horizontal stress, kPa

σ_0 = In-situ effective horizontal stress, kPa

ν = Poisson's ratio of coalbed, fraction

ε_1 , P_ε = Langmuir-type matrix shrinkage constants

E = Young's modulus of coalbed, kPa

P_0 = Initial reservoir pressure, kPa

If the coal under-saturated, i.e. there is delay in gas desorption as the pressure is reduced, the following equation is applicable:

$$\sigma - \sigma_0 = - \frac{\nu}{1-\nu} (P - P_0), \quad P_c < P \leq P_0 \quad (2.13)$$

$$\sigma - \sigma_c = -\frac{v}{1-v}(P - P_c) + \frac{E\varepsilon_1}{3(1-v)}\left(\frac{P}{P+P_\varepsilon} - \frac{P_0}{P_0+P_\varepsilon}\right), \quad 0 < P \leq P_c \quad (2.14)$$

Where,

P_c = Langmuir pressure or critical sorption pressure, kPa and

$$\sigma_c - \sigma_0 = -\frac{v}{1-v}(P_c - P_0) \quad (2.15)$$

The first term on the right-hand side of the equations **2.12** and **2.14** represents the cleat compression and second term as the matrix shrinkage. The relative occurrence of the both opposing phenomenon decides the effective stress in the coal seams. The relationship between cleat permeability and horizontal stress for a bundled matchstick geometry is given by (Seidle *et al.*, 1992):

$$K = K_0 * e^{-3(\sigma-\sigma_0)C_f} \quad (2.16)$$

Where,

C_f = Cleat volume compressibility with respect to changes in the effective horizontal stress normal to the cleat, K_0 = Initial cleat permeability

The permeability models get complicated when the Enhanced coal bed methane recovery and CO₂ sequestration is considered because it involves the adsorption of CO₂ along with desorption of CH₄. The permeability reduction due to matrix swelling during CO₂ adsorption

counteracts the increase in permeability due to matrix shrinkage during CH₄ desorption. Previous studies on adsorption behavior of CO₂ and CH₄ confirmed that the CO₂ has high affinity towards coal than CH₄ in the ratio 2:1 and in some specific cases of low rank coals it even reached to 10:1 (Harpalani *et al.*, 2006). In 1996, Levine from his model study expressed that the matrix swelling is adsorbate specific and increases with increase of gas affinity to coal seam but the rank, petrographic composition, mineral matter content and sorbate composition are important factors controlling the magnitude of the effect (Levine, 1996).

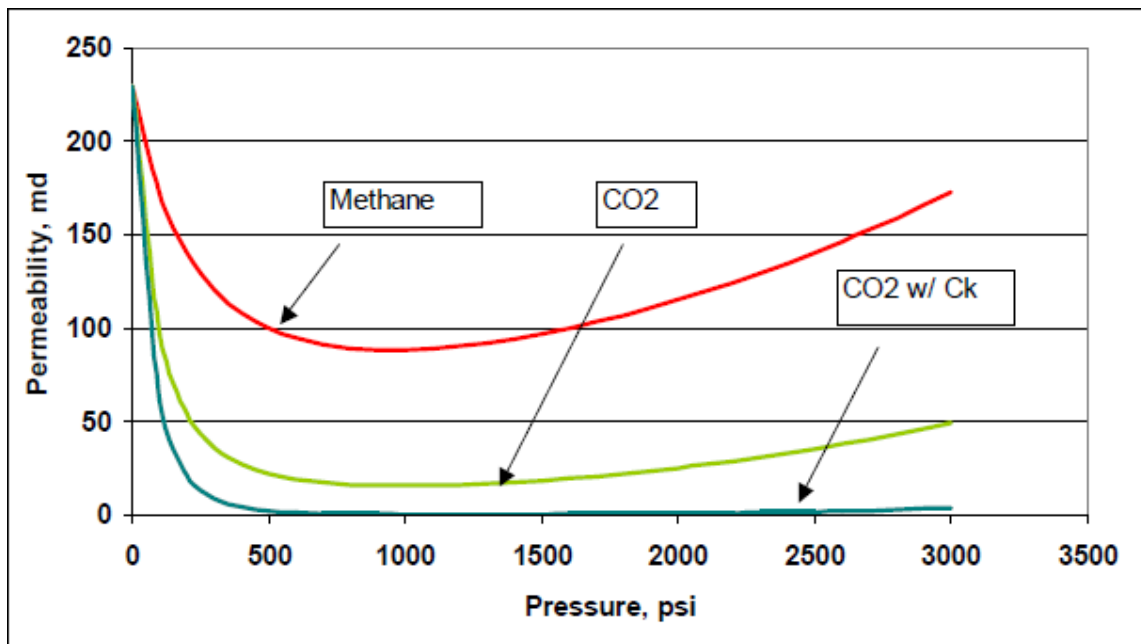


Figure 2.10. Effect of CO₂ and Differential Swelling on Coal Permeability (Pekot *et al.*, 2002)

Pekot and Reeves from their studies in 2002, 2003 found that the swelling strain is different for different gas species even if the adsorbed gas amount is same and named this phenomenon as differential swelling and agreed that the development of differential

swelling due to high adsorptive behavior of CO₂ than CH₄ has high impact on coal cleat permeability, porosity as shown in **Figure 2.10**.

2.5. Simulation studies on ECBMR:

Primary production from CBM resources involves depletion of pressure in the system so that the adsorbed CH₄ is pulled towards production well but it has been reported that production by this process recovers < 50% of original gas in place because the reservoir loses its energy and due to imposed restrictions on drawdown pressures (Puri et al., 1990 and Hall et al., 1994). Therefore, like in conventional resource development, new methods are required to enhance the gas production from CBM resources where ECBMR comes in to light. In finding so, vast research has been conducted to understand the flow mechanism and interaction of fluids (House *et al.*, 2003, Jikich *et al.*, 2003, Oldenburg *et al.*, 2002, Sams *et al.*, 2002 and Smith *et al.*, 2003) in coal system using reservoir simulation. Wo *et al.*, 2004 from his work on CO₂/N₂ ECBM recovery confirmed that there is a linkage between production and operational strategies. It has been reported in Rahul et al., 2006 thesis work that apart from the permeability anisotropy and other coal properties, optimizing the operational parameters like injection pressure, gas rates will enhance the gas recoveries by CO₂ sequestration.

Chapter 3 : Simulation Model Inputs and Construction

In this thesis work, simulation modelling studies are conducted to understand the characteristics of the reservoir and its interaction with the fluids in it. In doing so, a hypothetical CBM reservoir whose characteristic properties are observed from literature review. In this chapter, assumptions, theories, model equations and parameters that applied to develop the model are given in detail.

For long time, it has been known and believed that hydrocarbon formation takes place in rock known as “source rock” and during geological period oil and gas migrates and accumulates in anticlinal rock structures known as “reservoir rock” which is covered by proper seal known as “cap rock”. Later, with recent development in geological studies, it is also observed that hydrocarbons generated and accumulated in the same rock without migration. A hydrocarbon resource is considered as unconventional based on the HC migration system and the production or extraction methods that applied other than the conventional methods (Law *et al.*, 2002). Shale, coal bed methane and Tight Oil resources are considered as unconventional resources based on the fluid migration system that involved as explained above. The gas storage mechanism and rock characteristics of CBM resources are completely different from conventional resources. These differences are taken into consideration by having the following parameters and assumptions in the geological model.

1. Coal is a dual porous medium. The porosity of matrix (Primary porosity) is higher in relative to fracture or cleat porosity (Secondary porosity) but the porosity values of coal seams are much lower (Microporous 8-20 A⁰) compared to conventional porosity.
2. Methane is the main HC gas component present.
3. In initial condition, matrix contains 0% water, 100 % methane gas adsorbed on coal surface, and cleats contains 0% CH₄, 100% water.
4. The reservoir system is in under-saturated condition, i.e., when drawdown is created, only water is produced, and gas produces when desorption pressure is reached.
5. During pressure depletion, the gas molecules diffuse through the coal matrix system and desorb from coal surface into cleats.
6. In injecting flue gas, only CO₂ and N₂ gas components are considered.
7. CO₂ has a higher affinity than CH₄ and N₂ has a lower affinity than CH₄ towards coal surface.
8. Matrix shrinkage and swelling are significant in coal during CH₄ desorption and flue gas adsorption which shows ultimate impact on porosity and permeability of fractures and on CH₄ production.

Having the above-mentioned assumptions and concepts, a multi-gas component modelling simulator (CMG's GEM) is chosen as simulation software. It is one of the well-known software written and distributed by Computer Modelling Group (CMG). It provides relatively mature models to handle coal bed methane and its interaction with other gas components. The advantage of using reservoir simulation approach is that it helps to visualize different

operational scenarios and it also increases the level of confidence in decision making. It is to agree that in any computer simulation, the output results completely depend on the quality of input data. A reservoir simulation model will produce reliable results, if and only if, the major inputs to the model are correct. Hence, it is more important to choose the proper input parameters to construct a hypothetical simulation model that could correctly represent the subsurface characteristics of the Canada's Mannville formation CBM reservoirs.

3.1. Dual Porosity Modelling:

In the simulator, dual porosity-single permeability system is controlled by keyword DUALPOR and Since the CBM reservoirs consist of natural fracture system, shape factor is taken into consideration to define the interaction or the transfer of the fluid between matrix blocks and cleats. GEM is designed with Warren and Root (1963) and Gilman and Kazemi (1973) shape factors. The shape factor decides how rapidly the communication occurring between matrix blocks and fractures.

The interaction or the matrix-fracture transfer mass rate per unit bulk volume was given by Warren and Root (1963) as (Lim *et al.*, 1994):

$$q = \sigma \frac{k\rho}{\mu} (P_m - P_f) \quad (3.1)$$

Where,

q = Matrix-fracture transfer rate, kg/m³-s

k = Absolute permeability, mD

ρ = Density of coal, kg/m³

σ = Shape factor, 1/m²

μ = Viscosity, kg/ m-s

P_m = Matrix pressure, kPa

P_f = Fracture pressure, kPa

Warren and Root (1963) defined rectangular shape factor as:

$$\sigma = \frac{4n(n + 2)}{L_e^2} \quad (3.2)$$

Where,

n = Number of fractures

L_e = fracture effective length, m

In 1973, Gilman and Kazemi developed another shape factor for rectangular geometry using finite difference method given as:

$$\sigma = 4 \left(1/L_x^2 + 1/L_y^2 + 1/L_z^2 \right) \quad (3.3)$$

where, L_x, L_y, L_z are fracture lengths along X, Y, Z axis respectively.

In 2013, Lai *et. al.* assessed different shape factors in dual porosity medium and concluded that Warren and Root, Gilman and Kazemi shape factors are both extremes and there exist other shape factor models in between them. It is also being said that initially the transfer rate of fluid from matrix to fractures is so high and reduces rapidly within 5 years of production if Warren and Root model is considered. In case of Gilman and Kazemi, initially

the transfer rates are low, but it maintains a steady rate for long time and have higher rates compared to Warren and Root in later years of production as shown in **Figure 3.1**.

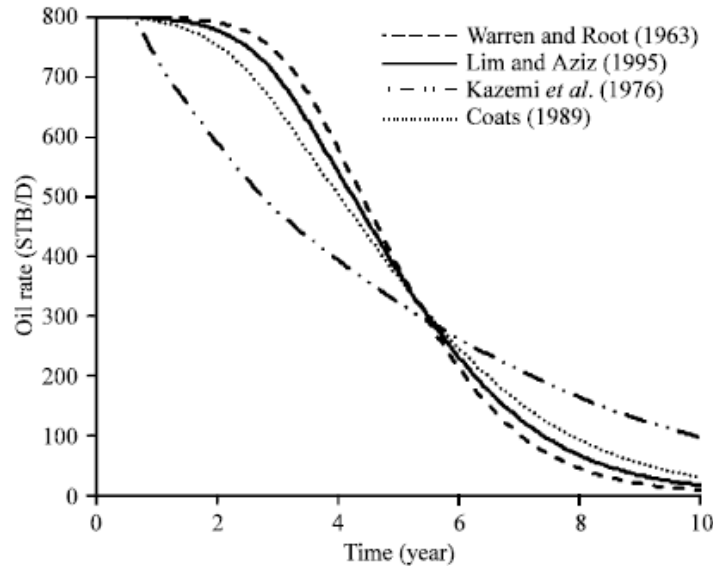


Figure 3.1. Comparison of different shape factors (Lai et. al., 2013)

Because of above described reason, Gilman and Kazemi (1976) shape factor is considered in developing the model. Having taken dual porosity system, each grid block consists of two simulation cells which represents coal matrix and fracture system. The properties of the matrix and fracture are defined independently. The system will choose top half of the layers as coal matrix and the bottom layers as fractures for calculating the water- gas contact and to establish fluid distribution using gravity equilibrium.

3.2. Adsorption Modelling:

One of the assumptions in constructing the model is there is no interaction between the gas components in the system and the fractures having less water. From the literature review given in chapter 2, it has been observed that under these assumptions, extended Langmuir

curves fit with less error compared to other isotherms. 'ADSORBTMAX' is the keyword which activates the adsorption modelling in GEM. The simulator automatically builds the Langmuir isotherm curves for pure CH₄, CO₂ and N₂ components by providing information like Langmuir pressure, maximum gas content of each gas component as shown in the **Figure 3.2.**

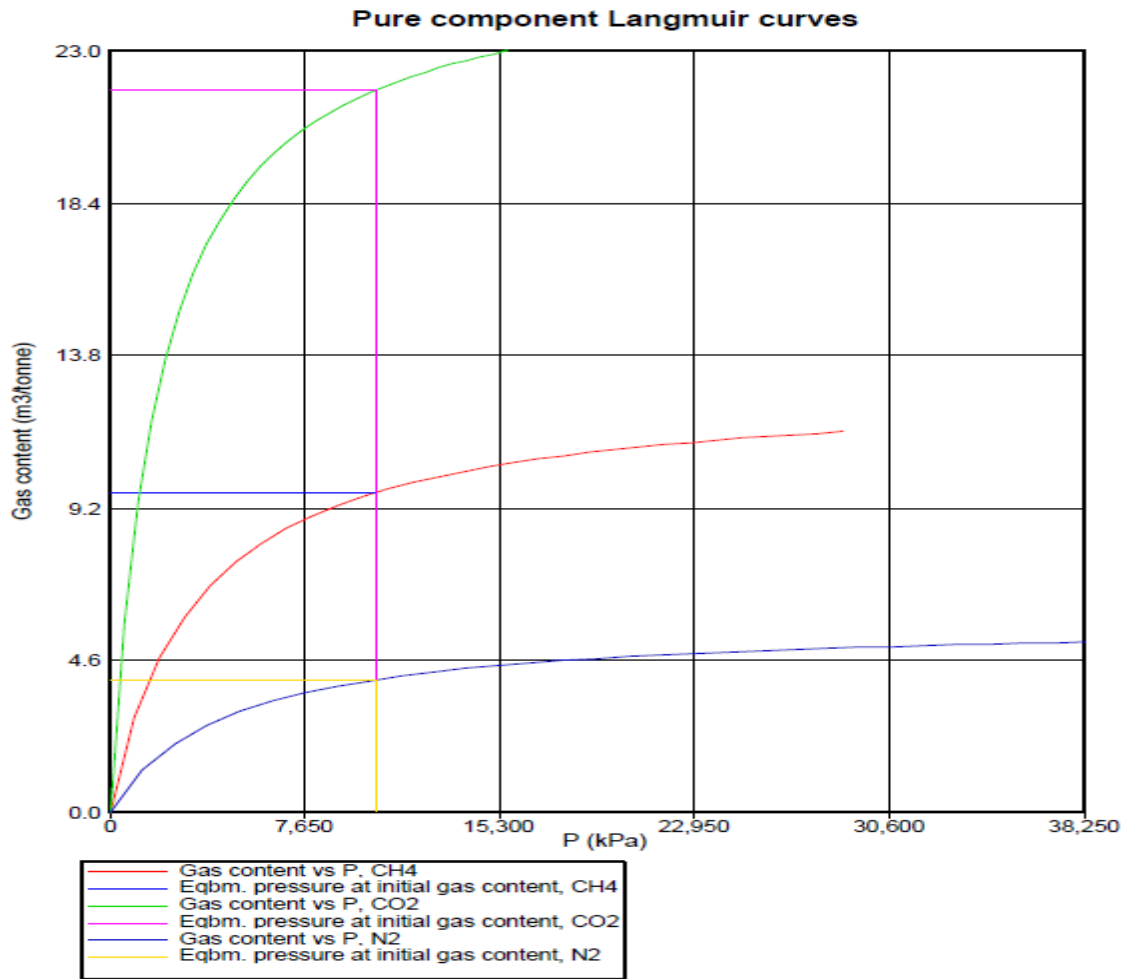


Figure 3.2. Pure Langmuir Isotherm curves developed in the model

Multi-component adsorption (Extended Langmuir) model equation used in the model simulator is given as;

$$\omega_i = \omega_{i,max} \left(\frac{(y_{ig}P/P_{Li})}{1 + \sum_j (y_{jg}P/P_{Lj})} \right) \quad (3.4)$$

Where,

ω_i = moles of adsorbed gas component per unit mass of rock

$\omega_{i,max}$ = Maximum moles of adsorbed gas component per unit mass of rock

P = Pressure, kPa

P_{Li} = Langmuir pressure of component 'i'

Y_{ig} = mole fraction of adsorbed gas component 'i' in the gas phase

3.3. Matrix Shrinkage and Swelling effects:

Permeability changes due to matrix shrinkage and swelling are very significant in CBM reservoirs during pressure depletions in CBM wells. The changes are even high in case of ECBMR due to flue gas injection and its ability to adsorb on coal surface. There exist many analytical models which explain this behavior better and provide reasonable results. CMG's GEM module has capacity for shrinkage and swelling modelling. "CROCKTYPE" is the keyword used to activate these effects and the input parameters are entered through "Compaction/Dilation" section in the model builder.

The **Figure 3.3** explains the change in absolute permeability with pressure depletion. Initially the CBM reservoir is in under-saturated condition denoted by point 'A' i.e., the

pressures in fractures is high compared to the matrix pressure. As the pressure gets depleted during primary production, the water produces from fractures and get compressed due to overburden pressure which results in reduction in absolute permeability.

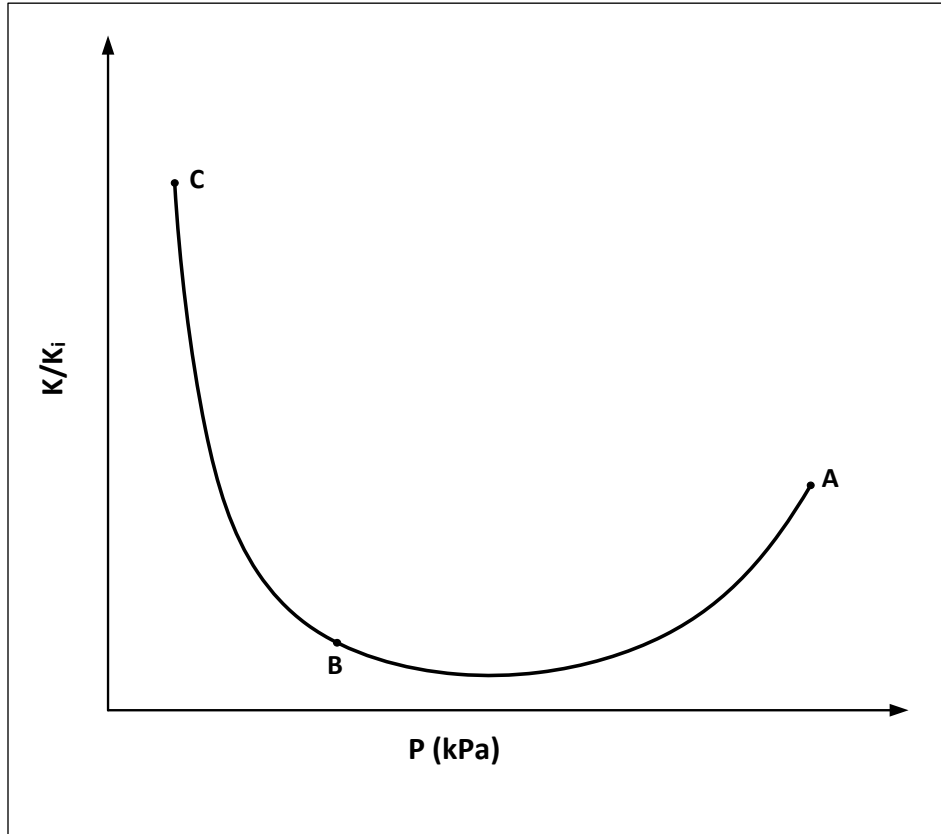


Figure 3.3. Fracture Permeability changes w.r.t. pressure

This trend will continue till reaching point 'B' known as the desorption pressure at which gas starts desorbing from coal surface into fractures and starts flow towards producing well. When gas desorbs from coal surface, the matrix shrinks towards inside resulting in enhancing the absolute permeability of fractures which will continue till point 'C'. During the ECBMR, the injected CO_2 gas adsorbs on the coal surface which swells the matrix

outwardly shows reduction in absolute permeability of fractures. In this manner, both effects counter attacks each other.

GEM is designed with Palmer and Mansoori (1996) (Eq. 3.5) and ARC or multi component extension of P and M (2004) (Eq. 3.9) analytical models for primary depletion and ECBM. The original P and M model equation used by GEM module for primary depletion is given as;

$$\frac{\phi}{\phi_i} = \exp[C_f (P - P_i)] + \frac{\epsilon_L}{\phi_i} \left(1 - \frac{K}{M}\right) \left(\frac{P_i}{P_i + P_L} - \frac{P}{P + P_L}\right) \quad (3.5)$$

Where,

ϕ_i = Initial natural fracture porosity (fraction)

ϕ = Fracture porosity at pressure p (fraction)

C_f = Fracture pore volume compressibility (1/ kPa)

P_i = Initial Pressure (kPa)

P = Pressure (kPa)

ϵ_L = Strain at infinite pressure

K = Bulk modulus (kPa)

M = Axial modulus (kPa), P_L = Langmuir pressure (kPa)

The pressures in the first term (pore compressibility) of the R.H.S. of the equation are the fracture pressures and that in the second term (matrix shrinkage/swelling) are the matrix pressures for a given grid block. And, Bulk modulus (K) and axial modulus (M) are related to each other and depends on Young's modulus (E) and Poisson's ration (γ) as follows;

$$\frac{K}{M} = \frac{1}{3} \left(\frac{1 + \gamma}{1 - \gamma} \right) \quad (3.6)$$

$$M = E \frac{(1 - \gamma)}{(1 + \gamma)(1 - 2\gamma)} \quad (3.7)$$

P and M theory relates the absolute permeability ration to the porosity ratio in the following manner,

$$\frac{K}{K_i} = \left(\frac{\phi}{\phi_i} \right)^\alpha \quad (3.8)$$

Where,

α = P and M exponent typically between 2 to 3

In case of multi-component adsorption, the original P and M model equation is modified by introducing the generalized multi component Langmuir concept as follows;

$$\frac{\phi}{\phi_{ref}} = \exp[C_f(P - P_{ref})] + \frac{1}{\phi_{ref}} \left(1 - \frac{K}{M} \right) \left(\sum_{j=1}^{j=n} \frac{\epsilon_{Lj} y_{ref,j} P_{ref}/P_{Lj}}{1 + P_{ref} \sum_{k=1}^{k=n} y_{ref,k}/P_{Lk}} - \sum_{j=1}^{j=n} \frac{\epsilon_{Lj} y_j P/P_{Lj}}{1 + P \sum_{k=1}^{k=n} y_k/P_{Lk}} \right) \quad (3.9)$$

Where,

Φ_{ref} = Reference state natural fracture porosity

P_{ref} = Reference state pressure (kPa)

$\epsilon_{Lj}, \epsilon_{Lk}$ = strain at infinite pressure, component j, k

P_{Lj}, P_{Lk} = Langmuir pressure (kPa), component j, k

n = Number of adsorbing components

$y_{ref,j}, y_{ref,k}$ = Composition at reference conditions, component j, k

y_j, y_k = Composition of gas mixture, component j, k

3.4. Simulation Data:

Including the assumption mentioned in the beginning of the chapter, a model of coal bed methane reservoir is established using the following data. Since the model is homogenous, the parameter values are chosen based on the range of values provided in most of the published papers. The properties of base model for coal bed are listed as follows:

3.4.1. Grid System:

Rectangular (X-Y-Z) grid system: 55 x 55 x 6

Total blocks = 18150, Null blocks = 0

Area = 650 acre

X and Y direction = 55 x 30 (m)

Z direction = 6 x 1 (m)

Table 3.1. Coalbed characteristics (Gentzis *et al.*, 2008; Deisman *et al.*, 2008)

Property		Value
Matrix	Porosity (fraction)	0.01
	Permeability (I, J, K), mD	0.01
	Rock compressibility, 1/ kPa	2e ⁻⁵
	Initial pressure, kPa	10500
Fracture	Porosity (fraction)	0.005
	Permeability I, mD	0.8
	Permeability J, mD	4
	Permeability K, mD	0.4
	Fracture spacing (I, J, K), m	0.2
	Rock compressibility, 1/ kPa	2e ⁻⁵
	Initial pressure, kPa	12000
Rock Density, kg/m ³		1435
Temperature, °C		40
Water viscosity, cP		0.7
Water density, kg/m ³		1000

Table 3.2. Langmuir isotherm parameters (Goodarzi *et al.*, 2008; Deisman *et al.*, 2008)

Property	Units	CH ₄	CO ₂	N ₂
Max. gas content/Langmuir volume constant	m ³ /ton	12.92	25.8399	5.76
Initial gas content	m ³ /ton	9.68991	21.8806	4.03198
Langmuir pressure, P _L	kPa	4826	3537	5200

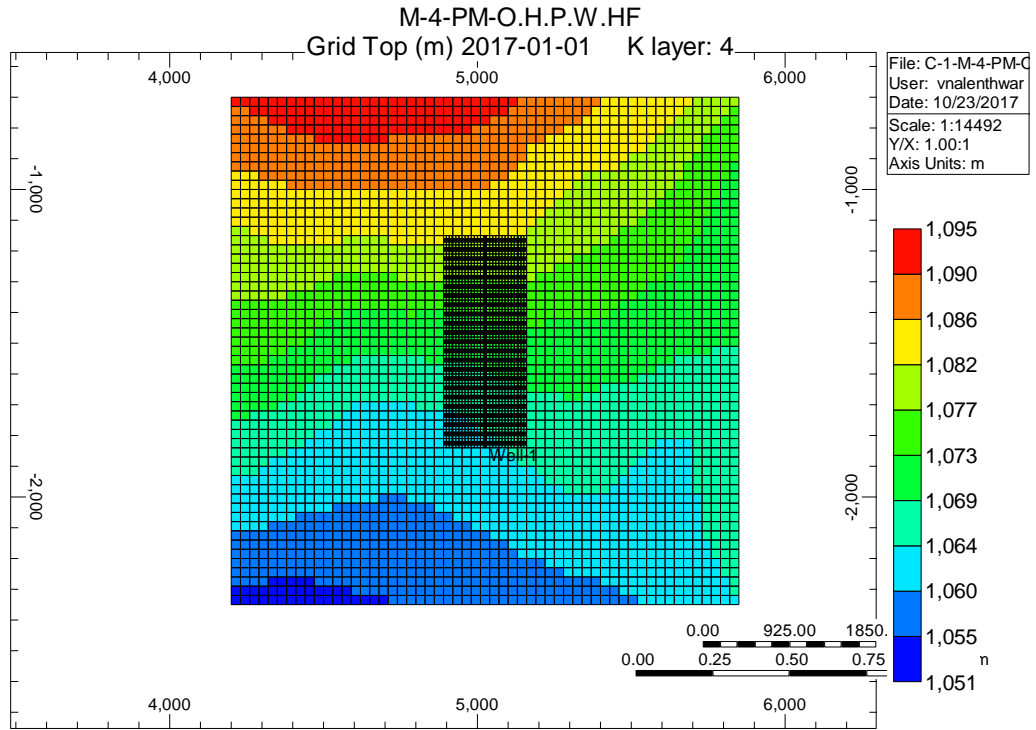


Figure 3.4. Top view of the simulation model

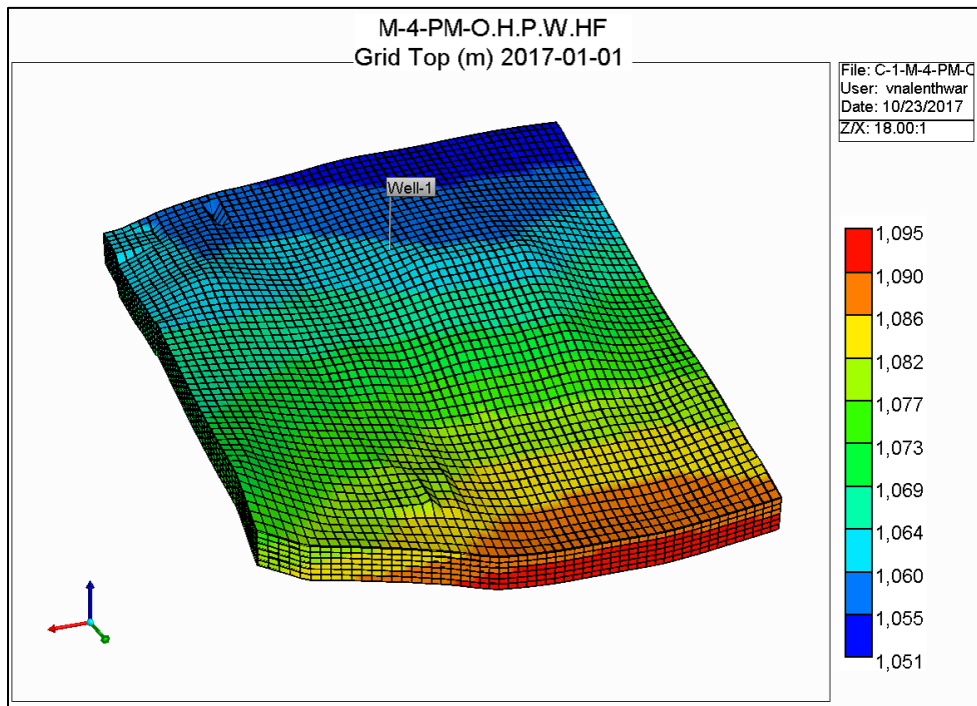


Figure 3.5. 3D view of the simulation model

Table 3.3. Rock mechanics properties of coalbed (Gentzis T., 2009; Gu F., 2009)

Property		Value
Matrix	Pressure dependence of formation porosity/ rock compressibility (CCPOR MATRIX), 1/kPa	2e ⁻⁵
	Ref. pressure for calculating the effect of rock compressibility (CPRPOR MATRIX), kPa	12000
Fracture	Pressure dependence of formation porosity/ rock compressibility (CCPOR FRACTURE), 1/ kPa	2e ⁻⁵
	Ref. pressure for calculating the effect of rock compressibility (CPRPOR FRACTURE), kPa	12000
Poisson ratio (POISSR)		0.25
Young's modulus (YOUNGM), kPa		9.997E ⁶
Palmer and Mansoori exponent (EXPPM)		2

Table 3.4. Operational parameters in the model

Parameter		Production well	Injection well
Well activation date (D/M/Y)		01/01/2017	01/01/2019
BHP (kPa)		200 (MIN)	14000 (MAX)
Surface water rate (m ³ /day)		200 (MAX)	-
Flue gas injection rate (m ³ /day)		-	14000 (MAX)
Injection Fluid		-	CO ₂ and N ₂
Inj. Fluid Composition (Normalized)	CO ₂	-	0.99
	N ₂	-	0.01
Vertical well location (I, J, K)		28 28 1:6	3 3 1:6
Horizontal well location (I, J, K)		13:28 28 4	1:16 2 4
Horizontal well length (m)		436	436
Well diameter (m)		0.15	0.15

3.4.2. Relative permeability (using quick CBM set up):

The Darcy's law is only applicable in fracture system. Therefore, relative permeability curves valid only in fractures. As stated in the beginning of the chapter, it is assumed that at initial condition, fractures contain full of water, matrix contain 100% gas and the system is in under-saturated condition. When the pressure in the fracture reduces below the matrix pressure, gas starts desorbs into the fractures and flows towards production well. By considering the above assumption, the relative permeability data has been developed as shown in **Table 3.5 and Figure 3.6** by using Corey's correlation that are applicable for gas and water flow in the fractures.

Table 3.5. Relative permeability data developed in the simulator

S_w	K_w	K_g	S_w	K_w	K_g
0	0	1	0.55	0.116	0.18
0.05	0.0006	0.835	0.6	0.154	0.147
0.1	0.0013	0.72	0.65	0.2	0.118
0.15	0.002	0.627	0.7	0.251	0.09
0.2	0.007	0.537	0.75	0.312	0.07
0.25	0.015	0.466	0.8	0.392	0.051
0.3	0.024	0.401	0.85	0.49	0.033
0.35	0.035	0.342	0.9	0.601	0.018
0.4	0.049	0.295	0.95	0.731	0.007
0.45	0.067	0.253	0.975	0.814	0.0035
0.5	0.088	0.216	1	1	0

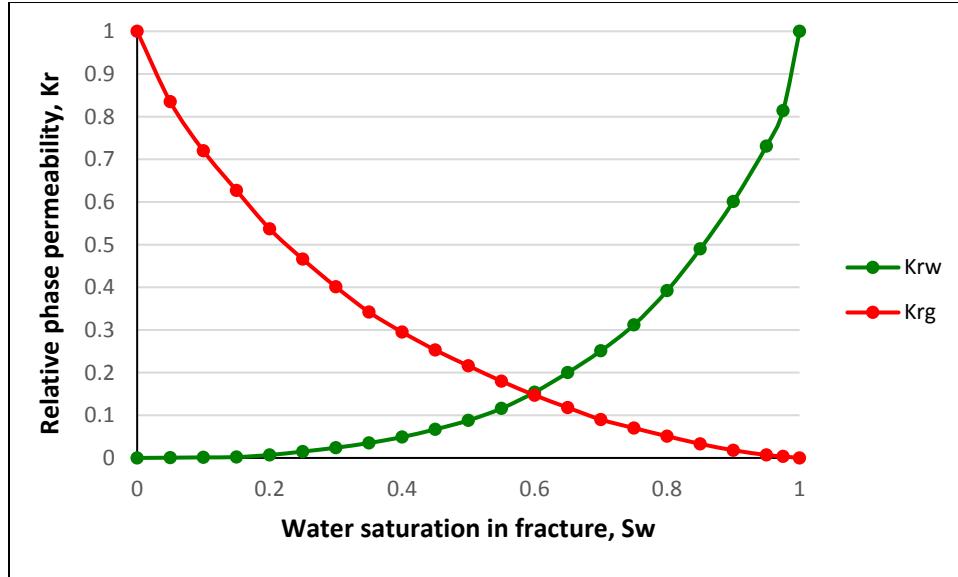


Figure 3.6. Relative permeability curves in the model

3.4.3. Hydraulic fracturing:

There is a separate wizard available for entering ‘Hydraulic fracturing’ properties in BUILDER section. There is provision for developing ‘Planar’ and ‘Complex’ hydraulic fracture network or can be introduced by importing micro-seismic data around a well. For showing the clear impact of hydraulic fractures on Enhanced gas recovery, planar hydraulic fractures are taken in the simulation model. Since the model having ‘DUALPOR’ system, the permeability enhancement occurs only in the fracture system. The effective hydraulic fracture permeability is calculated using the following model equation;

$$Q_{\text{original}} = Q_{\text{new}} \quad (3.10)$$

$$K_f W_f h_f / \mu * (dP/dX) = K_{\text{eff}} W_{\text{eff}} h_f / \mu * (dP/dX) \quad (3.11)$$

$$K_f W_f = K_{\text{eff}} W_{\text{eff}} \quad (3.12)$$

$$K_{eff} = K_f W_f / W_{eff} \quad (3.13)$$

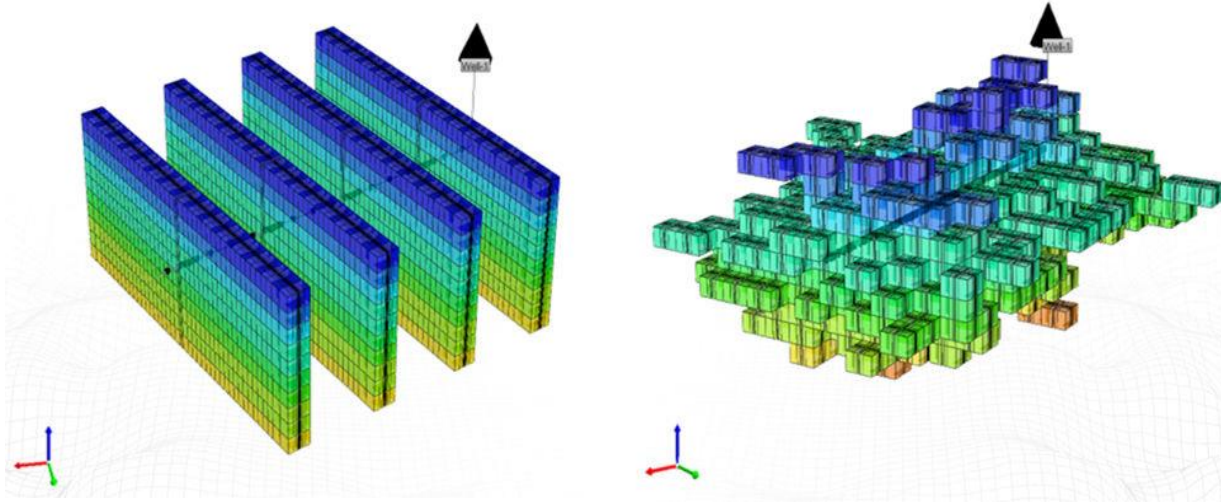


Figure 3.7. Planar and complex Hydraulic fracture modelling in CMG software

The resultant value of permeability ‘ K_{eff} ’ is added to the original natural fracture permeability around the well. The ‘Hydraulic fracture’ parameters are given in **Table 3.6**.

Table 3.6. Hydraulic fracturing designing parameter in the model

Property	Value
H. Fracture width (W_f), m	0.001
Intrinsic permeability (K_f), mD	10000
Effective permeability (K_{eff}), mD	16.4042
Tip permeability, mD	5000
H. Fracture orientation	J - Direction
Half length, m	106.68
H. Fracture Effective width (W_{eff}), m	0.6096

3.4.4. Input parameters for sensitivity analysis:

Even though the simulator is giving reliable results, it is not sure that the same results could be obtained in the real field operations. Therefore, it is very important to do sensitivity analysis, optimization and uncertainty assessment to achieve effective and reliable results. The objective in this thesis to do quantitative and qualitative analysis of flue gas composition which gives reliable gas recovery and CO₂ sequestration in production life of a well. In doing so, 12 parameters with their ranges as shown in **Tables from 3.7 to 3.9.** are considered for proceeding the analysis.

Table 3.7. Rock Mechanical parameters

	Parameter	Units	Base case	Lower Limit	Upper Limit
1	Rock compressibility	kPa	2E ⁻⁵	1E ⁻⁵	1E ⁻⁴
2	Poisson Ration	fraction	0.25	0.2	0.45
3	Young's Modulus	kPa	9.99E ⁶	5E ⁶	5E ⁷
4	P and M Exponent	-	2	1.5	3

Table 3.8. Hydraulic Fracturing parameters

	Parameter	Units	Base case	Lower Limit	Upper Limit
1	Half length	m	106.7	80	250
2	Width	m	0.001	0.0005	0.005
3	Intrinsic Permeability	mD	10000	7500	15000

Table 3.9. Operating parameters

	Parameter	Units	Base case	Lower Limit	Upper Limit
1	CO ₂ _Composition	(Normalized)	0.99	0.01	0.99
2	N ₂ _Composition	(Normalized)	0.01	0.01	0.99
3	Injection Bottom Hole Pressure	kPa	14000	13000	15000
4	Injection gas rate	m ³ /day	15000	14000	16000
5	Production Bottom Hole Pressure	kPa	200	150	300

Chapter 4 : Results and Analysis

This chapter focuses on the work flow of simulation models; discuss the obtained analyzed results to achieve the objectives of this research work. Having the input reservoir properties same for all base models, different well drilling and completion strategies that include vertical, horizontal wells and hydraulic fracturing stimulations are considered in combination to develop 11 base simulation models as shown in **Figures from 4.1 to 4.11** and run in CMG's GEM model simulator to compare the enhanced gas recoveries and CO₂ gas adsorptions and select the best base models for further results and analysis. For all models, 5-spot drilling pattern is considered, and simulation is run on quarter portion of the whole area. Throughout the work, screening is done at several stages and details of it are discussed in the following pages. The simulation names and well completion details of all base models are detailed in **Table 4.1**.

As discussed in previous chapters, matrix shrinkage and swelling effects are noticeable in coal and show impact on gas recoveries by changing the cleat permeability. To check these effects and their contribution, each base model is subdivided into two models. One with Palmer and Mansoori rock mechanical properties and another without these parameters. Five years is the production period considered for the initial screening to compare the cumulative gas recoveries and CO₂ adsorption on coal surface.

Table 4.1. Well drilling combinations used to develop 11 base simulation models

Model No.	Model Name	Well Type	Vertical Well	Horizontal Well	Hydraulic Fracturing
Primary Recovery			✓		
1	M-1-O.V.P.W	Production	✓	-	-
2	M-2-O.V.P.W.HF		✓	-	✓
3	M-3-O.H.P.W		-	✓	-
4	M-4-O.H.P.W.HF		-	✓	✓
Enhanced Recovery (ECBMR)					
5	M-5-O.V.P.W-O.V.I.W	Production	✓	-	-
		Injection	✓	-	
6	M-6-O.V.P.W.HF-O.V.I.W	Production	✓	-	✓
		Injection	✓	-	-
7	M-7-O.V.P.W-O.V.I.W.HF	Production	✓	-	-
		Injection	✓	-	✓
8	M-8-O.V.P.W.HF-O.V.I.W.HF	Production	✓	-	✓
		Injection	✓	-	✓
9	M-9-O.H.P.W-O.V.I.W	Production	-	✓	-
		Injection	✓	-	-
10	M-10-O.H.P.W.HF-O.V.I.W	Production	-	✓	✓
		Injection	✓	-	-
11	M-11-O.V.P.W-O.H.I.W	Production	✓	-	-
		Injection	-	✓	-

From past research work, it is observed that N₂ adsorption on coal is much less compared to CO₂ but the benefit of having N₂ in the system is that it reduces the partial pressure of CH₄ and supports early desorption of it from coal surface into the cleat system which results in

early production and an early revenue. N_2 breakthrough happens in the early stages of flue gas injection compare to CO_2 breakthrough. Till the point of CO_2 breakthrough, sequestration or storage of CO_2 happens by occupying most of the space in coal bed methane reservoir and after breakthrough the percentage of CO_2 in the produced gas increases at high rate. There is no point in injecting the flue gas after CO_2 breakthrough as there will be less sequestration of CO_2 and less methane gas produced which is not cost and time effective. To see the production life of coal bed methane reservoir, 100 years of production period is set for seven enhanced recovery base models (model 5 to model 11) to compare the breakthrough of CO_2 in all cases and judge whether the reservoir is potential enough to produce for above 50 years or not.

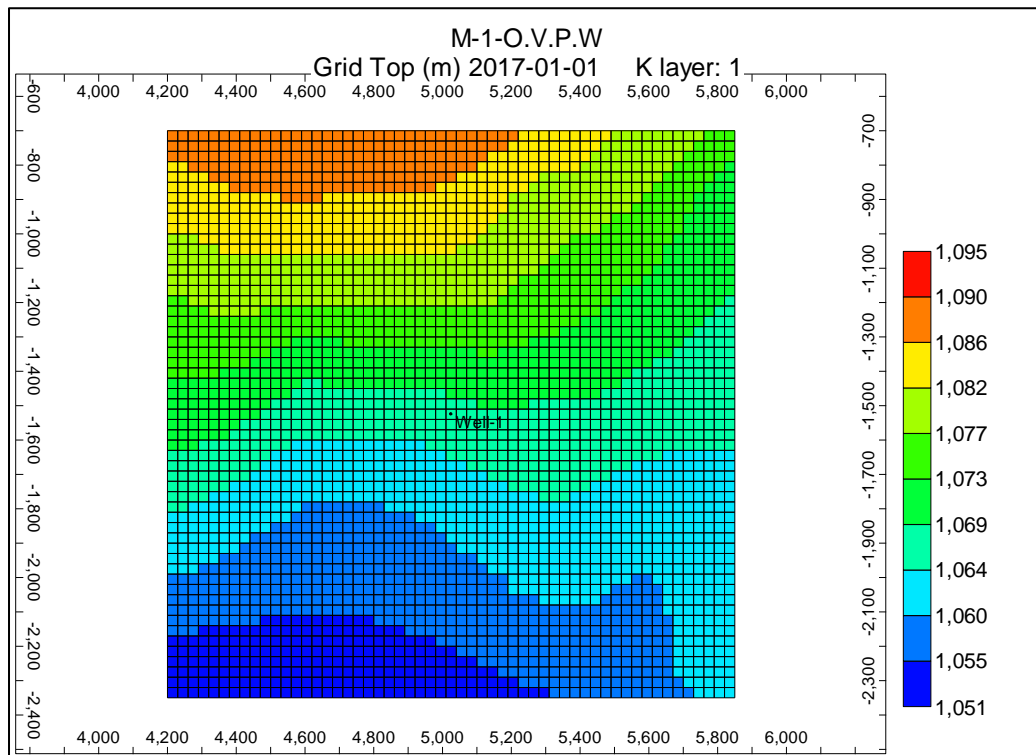


Figure 4.1. Top view of Model 1 – O.V.P.W. (vertical production well)

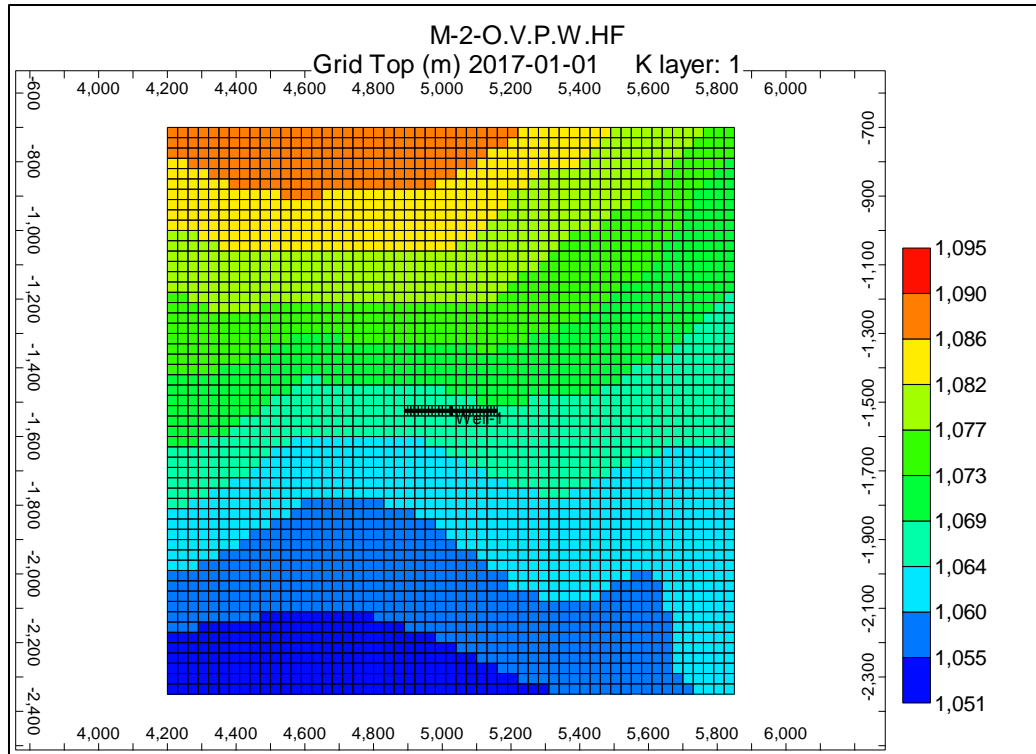


Figure 4.2. Top view of Model 2 – O.V.P.W.HF. (Vertical production well with Hydraulic fracturing)

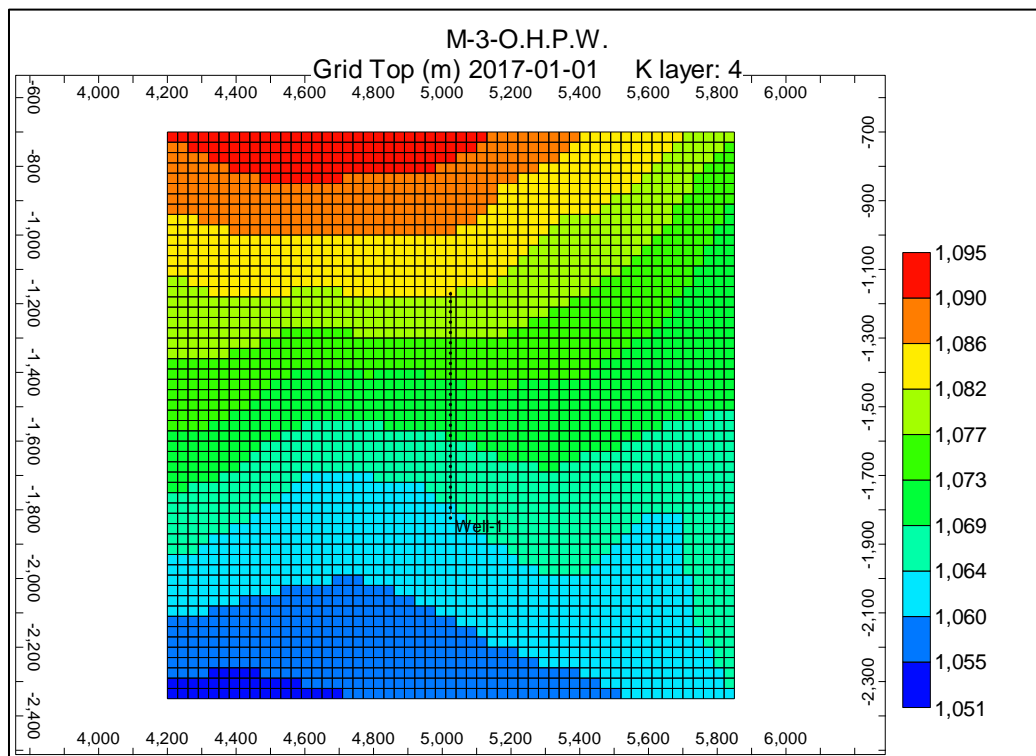


Figure 4.3. Top view of Model 3 – O.H.P.W. (Horizontal production well)

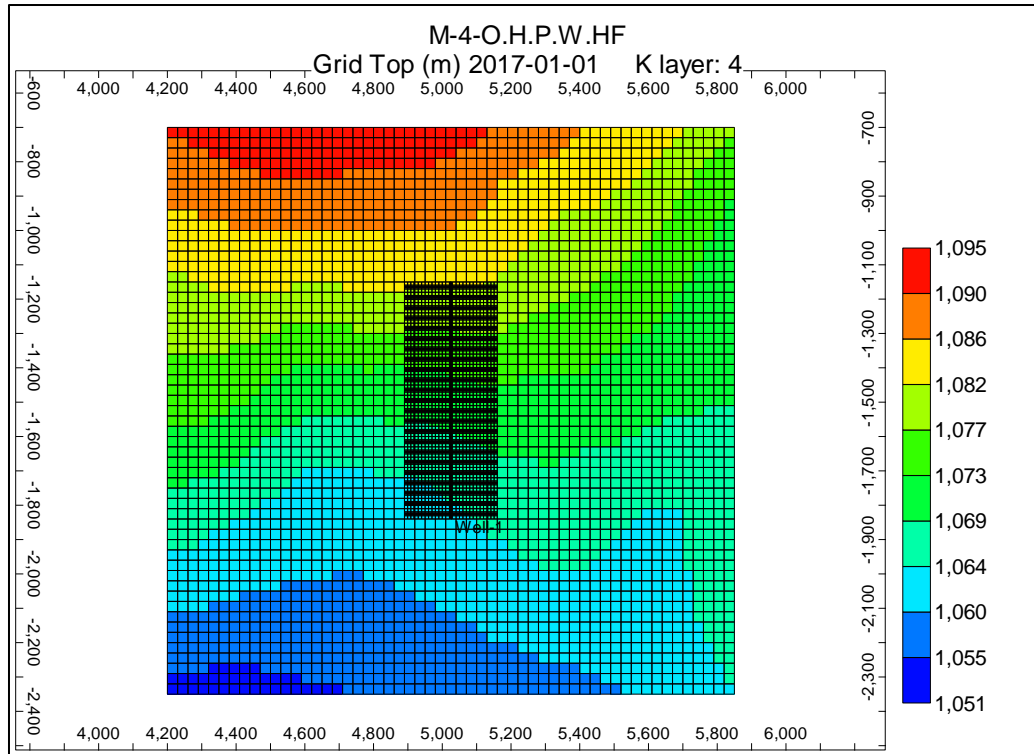


Figure 4.4. Top view of Model 4 – O.H.P.W.HF. (Horizontal production well with Hydraulic fracturing)

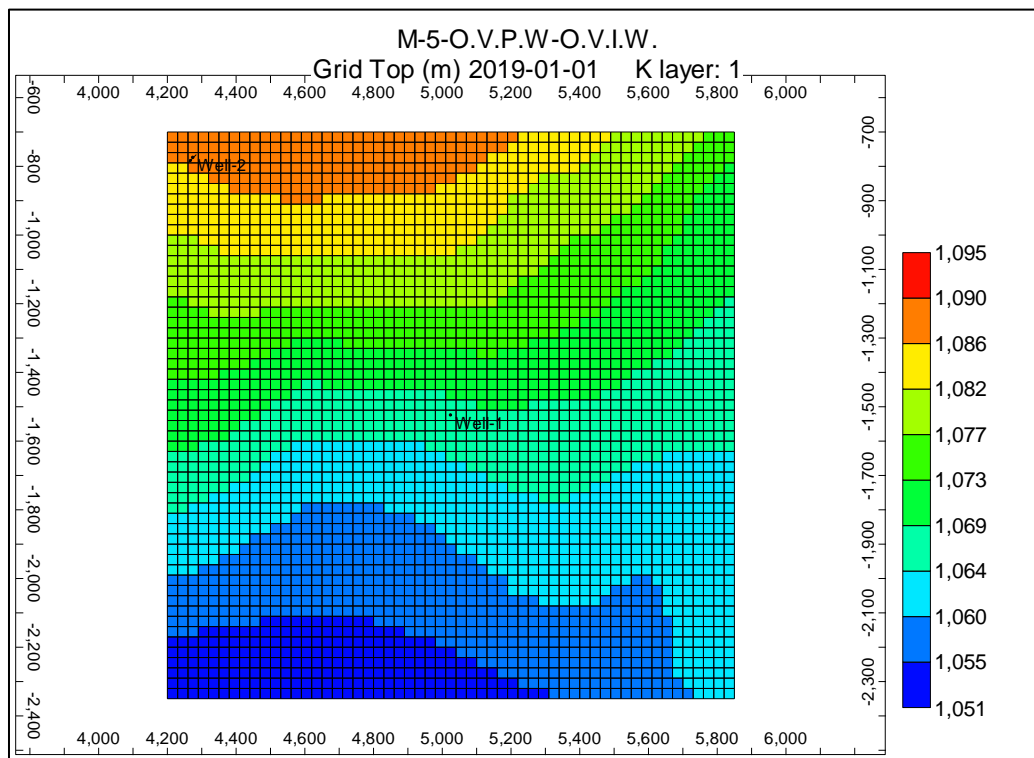


Figure 4.5. Top view of Model 5 – O.V.P.W-O.V.I.W. (Vertical production and injection well)

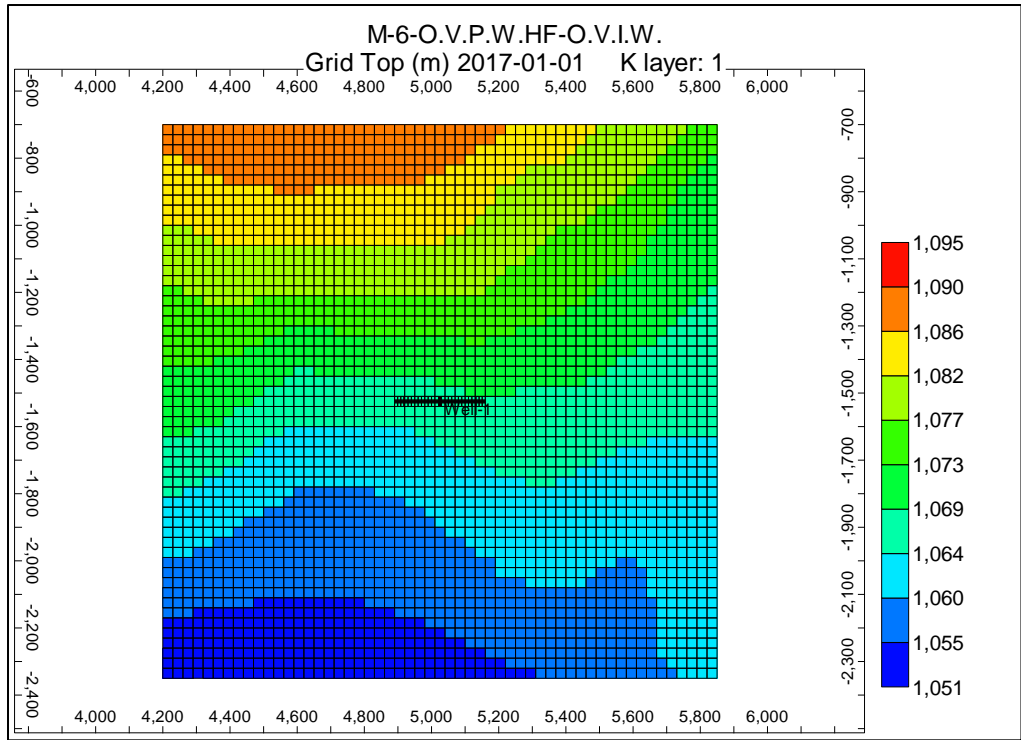


Figure 4.6. Top view of Model 6 – O.V.P.W.HF – O.V.I.W. (Vertical production well with hydraulic fracturing and vertical injection well)

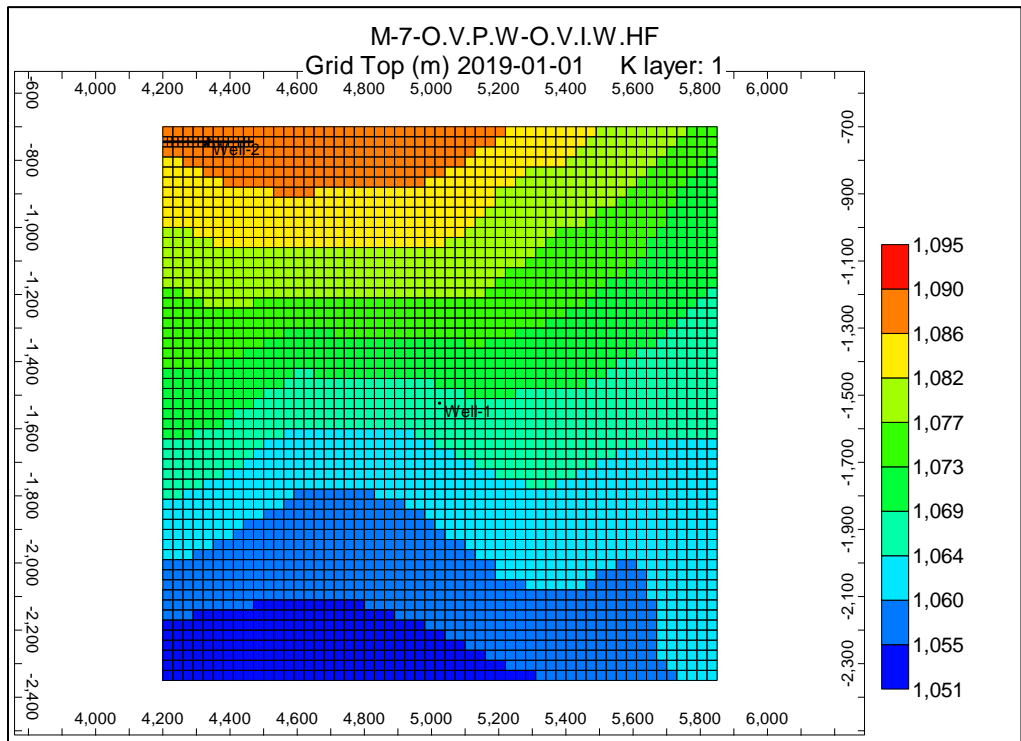


Figure 4.7. Top view of Model 7 – O.V.P.W. – O.V.I.W.HF. (Vertical production well and vertical injection well with hydraulic fracturing)

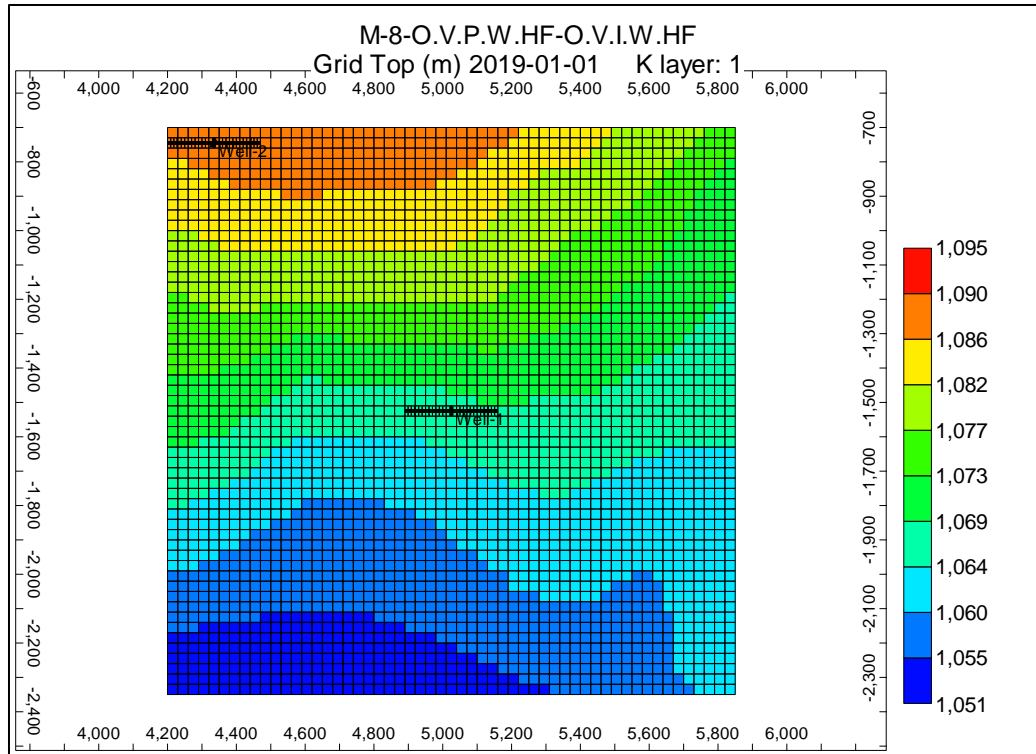


Figure 4.8. Top view of Model 8 – O.V.P.W.HF. – O.V.I.W.HF. (Vertical production and injection well both with hydraulic fracturing)

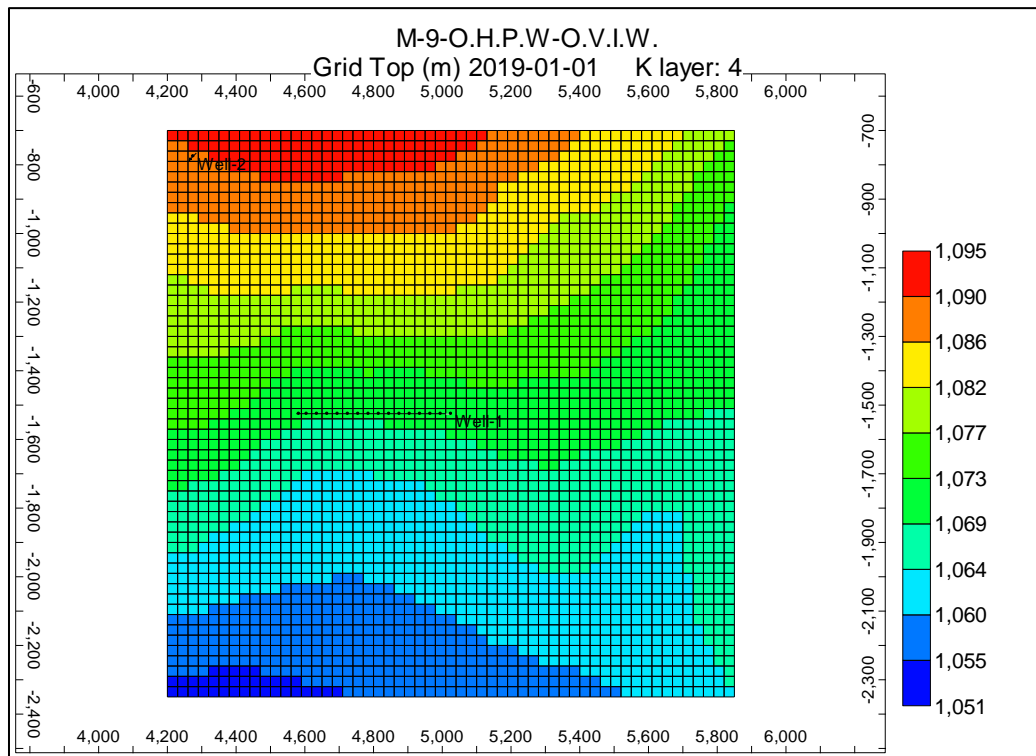


Figure 4.9. Top view of Model 9 – O.H.P.W. – O.V.I.W. (Horizontal production and injection well)

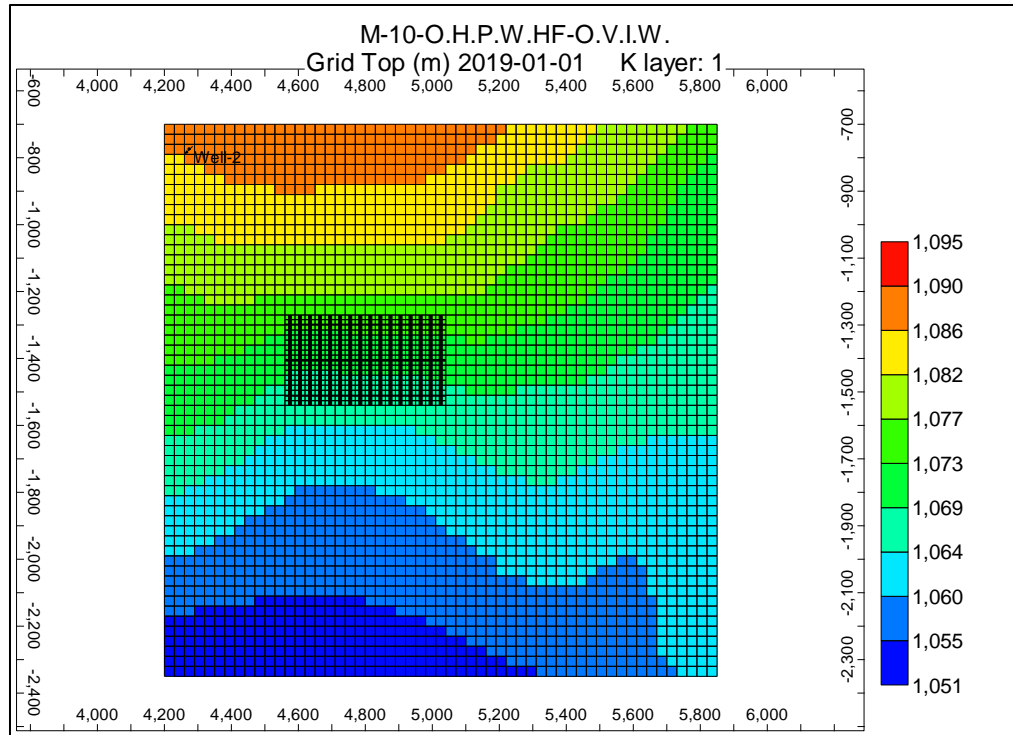


Figure 4.10. Top view of Model 10 – O.H.P.W.HF – O.V.I.W. (Horizontal production well with hydraulic fracturing and vertical injection well)

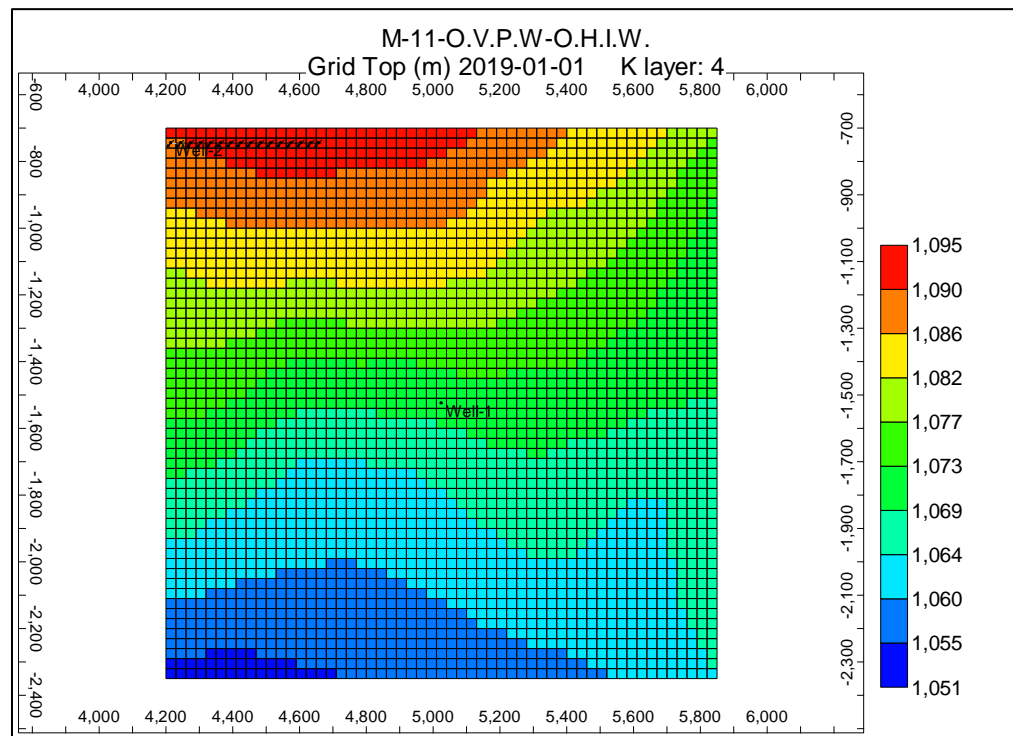


Figure 4.11. Top view of Model 11 – O.V.P.W. – O.H.I.W. (Vertical production well and horizontal injection well)

4.1. Matrix Shrinkage and swelling effects in the model:

Detailed explanation on the effects of matrix shrinkage and swelling is given in previous chapters. To see how these effects are impacting in our model, base model 1 which is simply a primary depletion model (M-1-O.V.P. W) is considered. The rock mechanical parameters given in **Table 4.2** are taken as inputs.

Table 4.2. Rock compaction data used in matrix shrinkage and swelling modelling for primary depletion

Parameter	value
P_i (Fracture), kPa	12000
P_i (Matrix), kPa	10500
C_f , (1/ kPa)	$2e^{-5}$
ϵ_L	0.0085
Φ_i (fraction)	0.005
P_L , kPa	4826.33
K/M	0.56
γ	0.25
E, kPa	$9.997e^6$

The porosity and permeability changes that tabulated in the **Table 4.3** are produced by substituting the rock mechanics parameters in the equations **3.7** to **3.10**. The graph trend in **Figure 4.12** shows that the rock compaction data that are considered for CBM modelling are valid and showing the exact trend in change in permeability that is expected. The CBM

reservoir in this model is under saturated, i.e., the fracture pressure is higher compared to the matrix pressure which making the gas to completely adsorbed on coal surface. The initial pressure in the fractures is 12000 kPa and as the pressure depletes during primary production, the pressure in the fractures drops and the permeability in fractures is reducing due to overburden compression.

Table 4.3. Changes in porosity and permeability calculated by P and M model

P, kPa	ϕ/ϕ_i	K/K _i	P, kPa	ϕ/ϕ_i	K/K _i
1000	1.191	1.419	11000	0.976	0.953
2000	1.116	1.246	12000	0.982	0.965
3000	1.065	1.134	13000	0.990	0.981
4000	1.0297	1.060	14000	1.000	1.001
5000	1.005	1.010	15000	1.011	1.023
6000	0.988	0.977	16000	1.024	1.049
7000	0.978	0.957	17000	1.038	1.078
8000	0.972	0.946	18000	1.053	1.110
9000	0.971	0.942	19000	1.069	1.144
10000	0.972	0.945	20000	1.086	1.181

The equilibrium pressure in the matrix at initial gas content is 10500 kPa and since the difference in initial fracture and matrix pressure is less, the permeability reduction doesn't continue for long time.

As the pressure in the fractures goes below the desorption pressure (between 8000 – 8500 kPa), the matrix blocks shrink inward because of gas desorption and resulting in increasing fracture permeability. An interesting fact that emerges from here is that the rate of change in permeability increases as the fracture pressure (drawdown) decreases. The reason behind this fact is that as the fracture pressure reduces, higher amount of CH₄ is pulled from coal surface into cleat system and higher desorption makes the matrix to shrink inward at a greater rate which creates increase in permeability in less time.

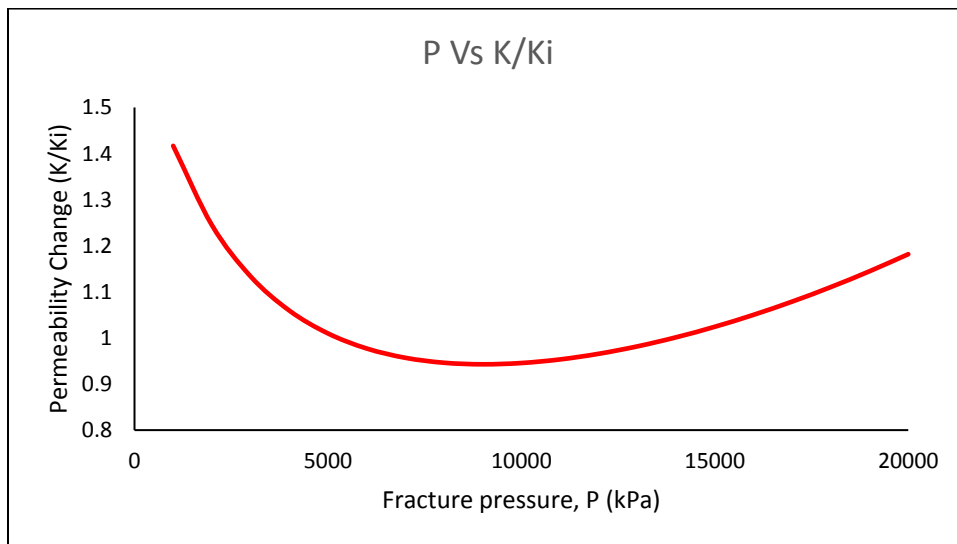


Figure 4.12. Change in Permeability w.r.t. fracture pressure

The same rock mechanic parameters are considered in all eleven base cases. **Figures** from **4.13 to 4.23** show the comparison of cumulative gas recoveries with and without considering the P and M model parameters in the simulation models. These output gas recovery graphs clearly indicate that the consideration of rock mechanic properties is very important in CBM reservoir modelling. In models from 1 to 4, since there is only primary

production, the matrix shrinkage effects are very dominant resulting in increasing permeability. In models from 5 to 11, flue gas is injected into the system because of which matrix swelling effects come into picture and the difference in magnitude of matrix swelling and shrinkage decides whether the fracture permeability increase or decrease. Except the model 11, in all other model permeability of fractures increasing steadily due to which cumulative gas recoveries are always higher compared to the models without P and M parameters which indicating that matrix is shrinking highly compared to swelling due to flue gas (CO₂ and N₂) adsorption. In model 11, till the year 5, gas recovery is little high indicating that matrix shrinkage effects are dominant and after year 5, the gas recovery is reduced indicating the presence of dominant matrix swelling due to high CO₂ and N₂ adsorption which is clearly justified because the injection well is horizontal in model 11 and adsorption per unit time per well is high compared to gas production per unit time per well from vertical production well and due to high CO₂ adsorption, drawdown pressure is not sufficient for CH₄ to desorb from the coal surface.

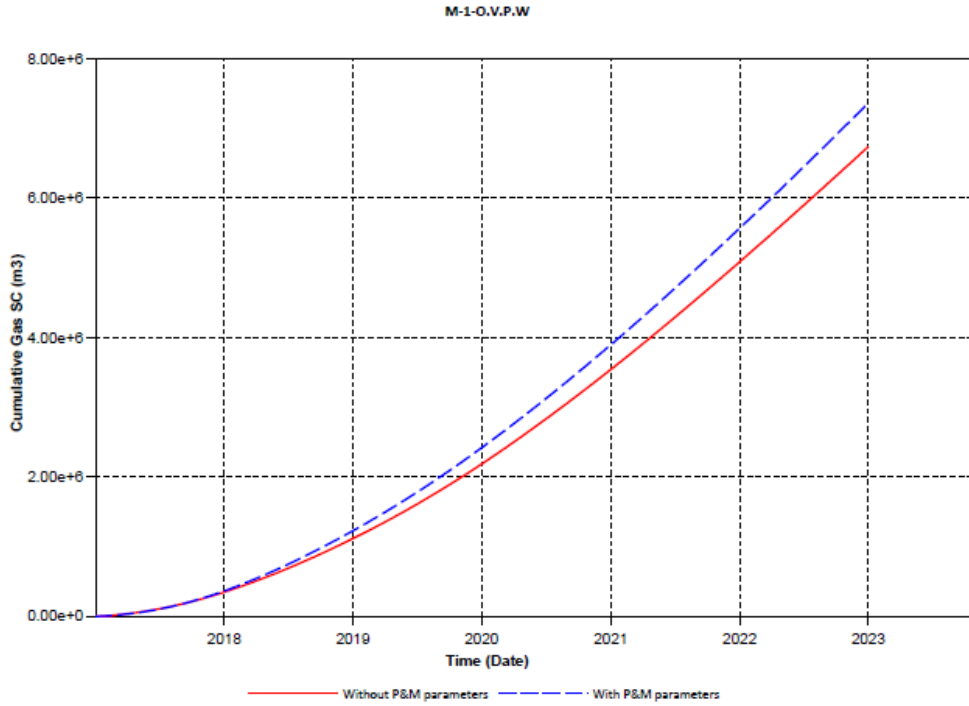


Figure 4.13. Comparison of gas recovery with and without P and M parameters in Model 1

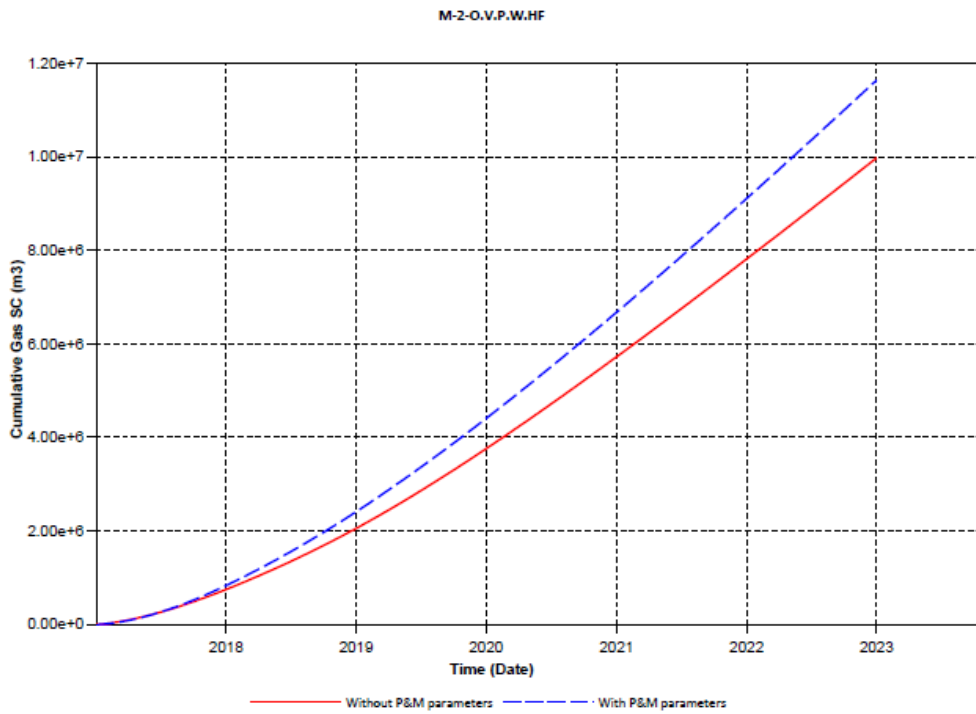


Figure 4.14. Comparison of gas recovery with and without P and M parameters in Model 2

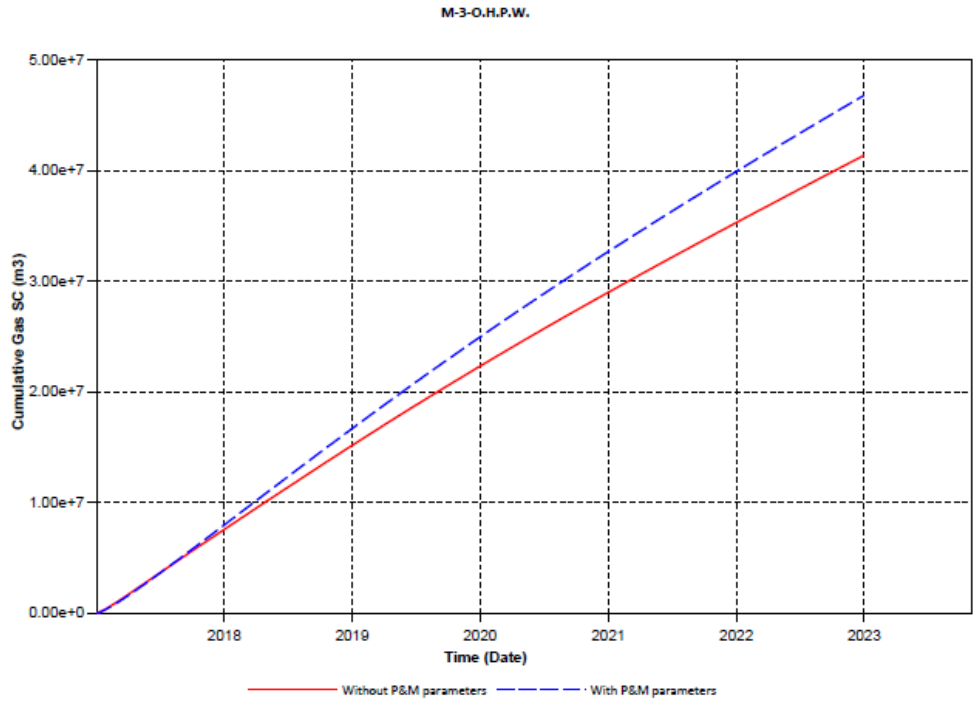


Figure 4.15. Comparison of gas recovery with and without P and M parameters in Model 3

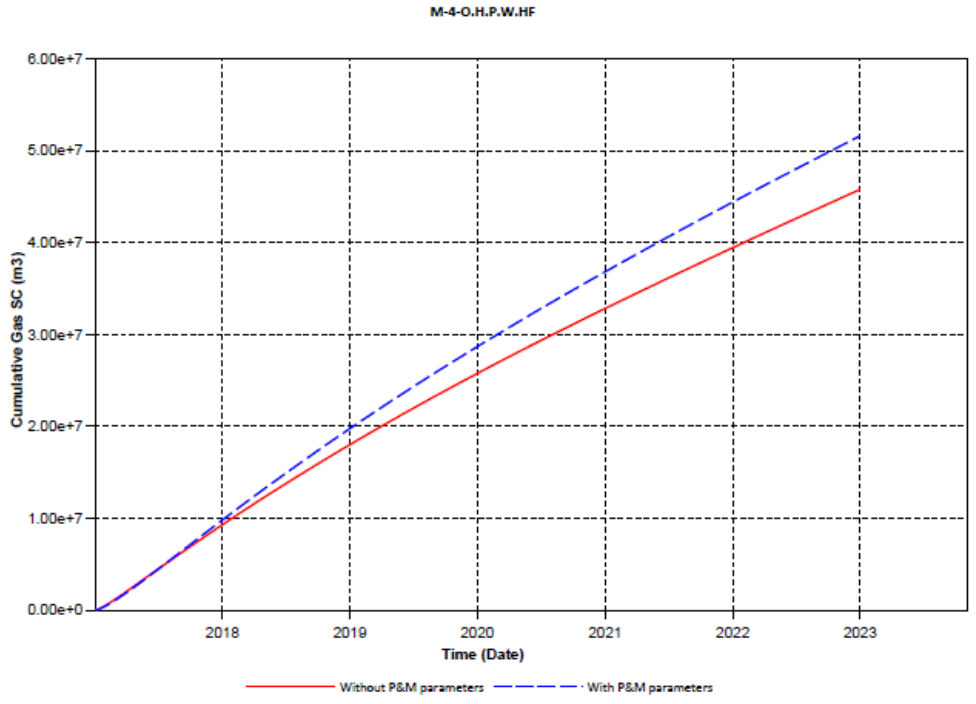


Figure 4.16. Comparison of gas recovery with and without P and M parameters in Model 4

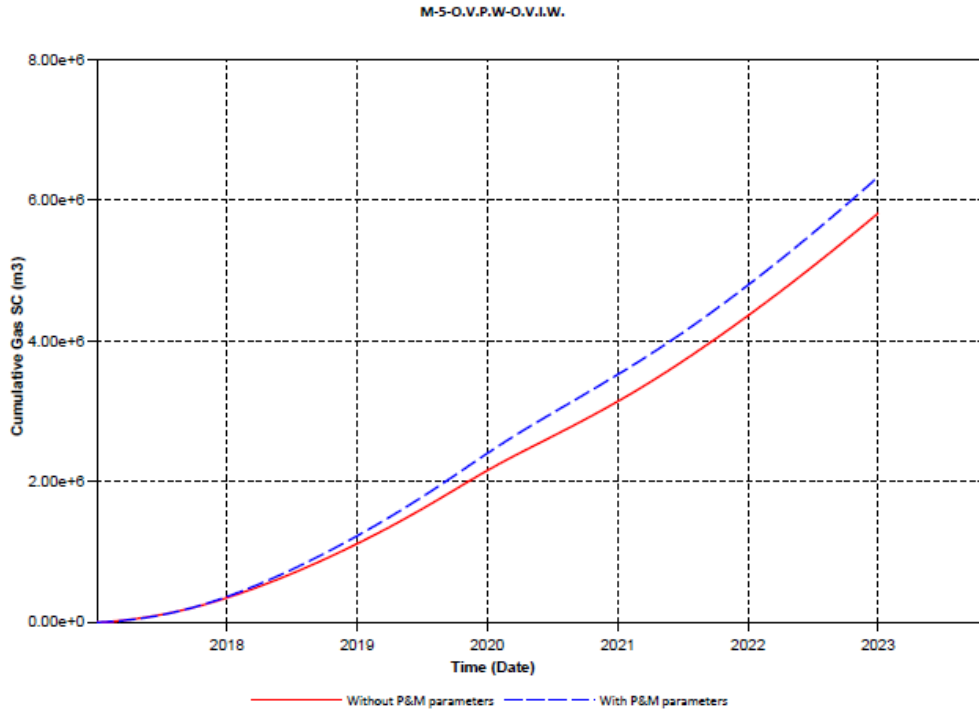


Figure 4.17. Comparison of gas recovery with and without P and M parameters in Model 5

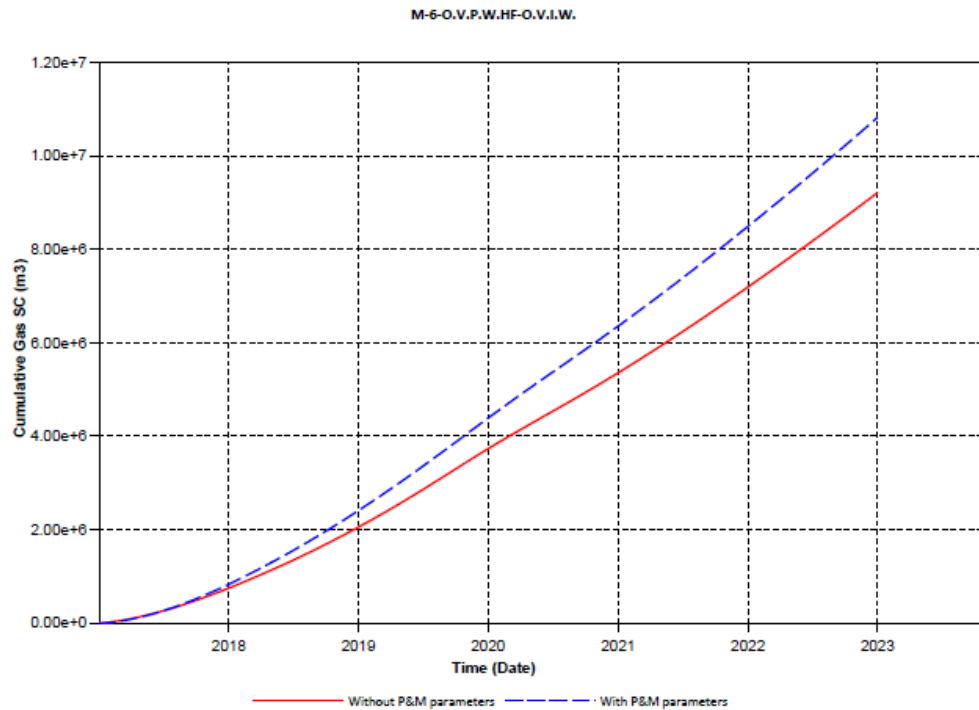


Figure 4.18. Comparison of gas recovery with and without P and M parameters in Model 6

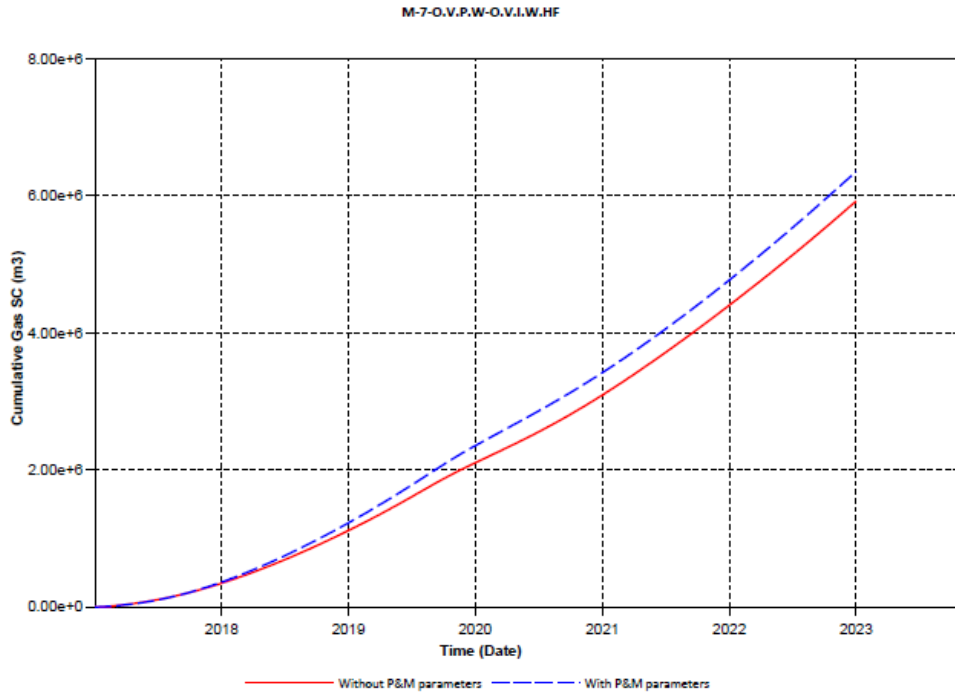


Figure 4.19. Comparison of gas recovery with and without P and M parameters in Model 7

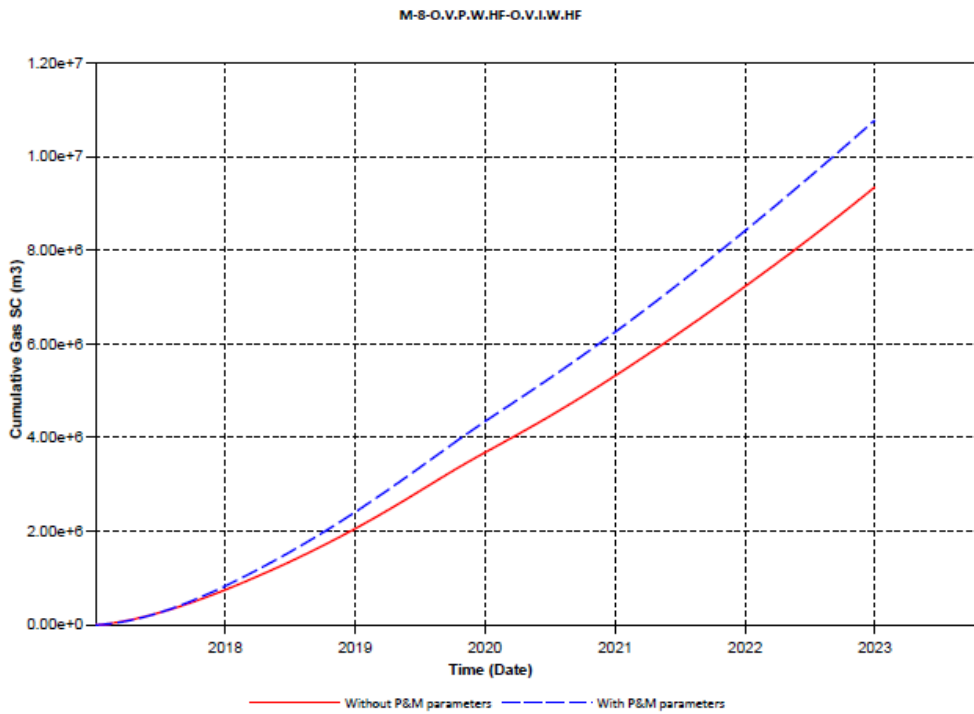


Figure 4.20. Comparison of gas recovery with and without P and M parameters in Model 8

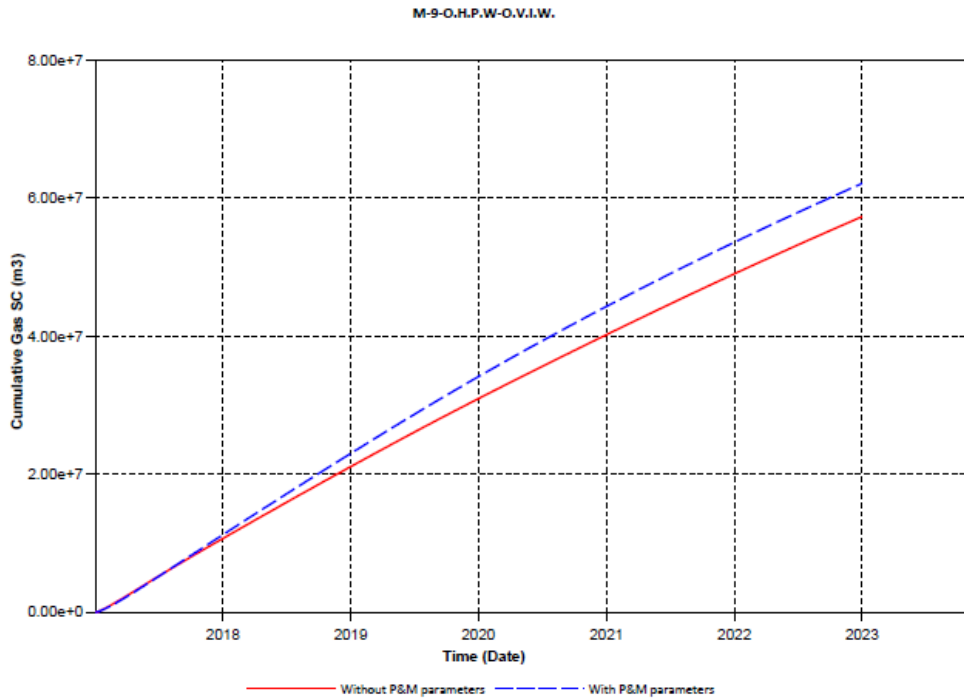


Figure 4.21. Comparison of gas recovery with and without P and M parameters in Model 9

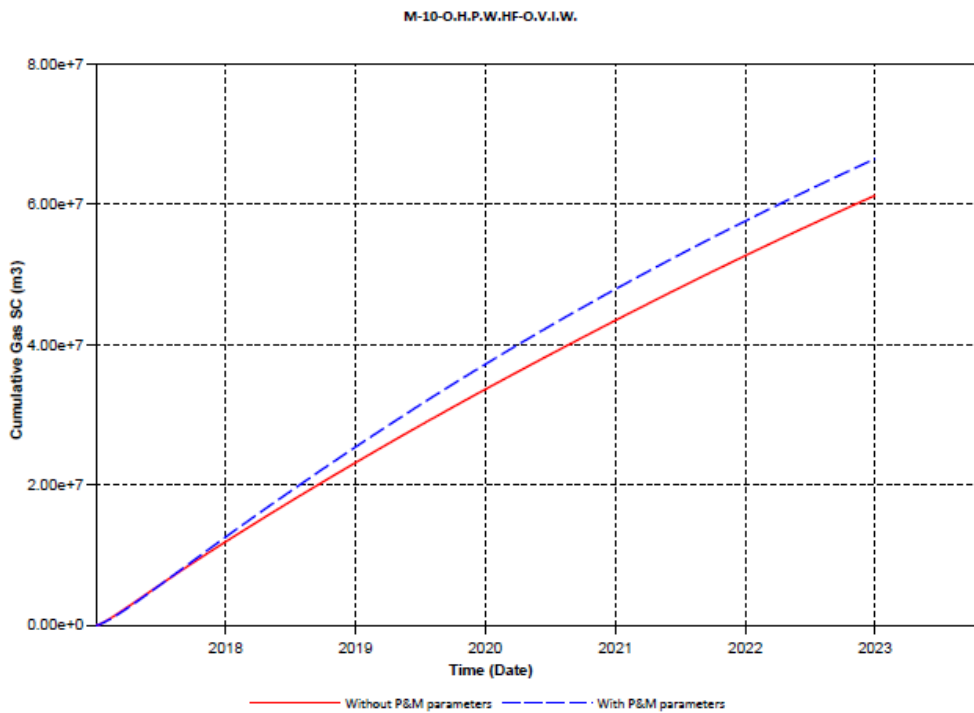


Figure 4.22. Comparison of gas recovery with and without P and M parameters in Model 10

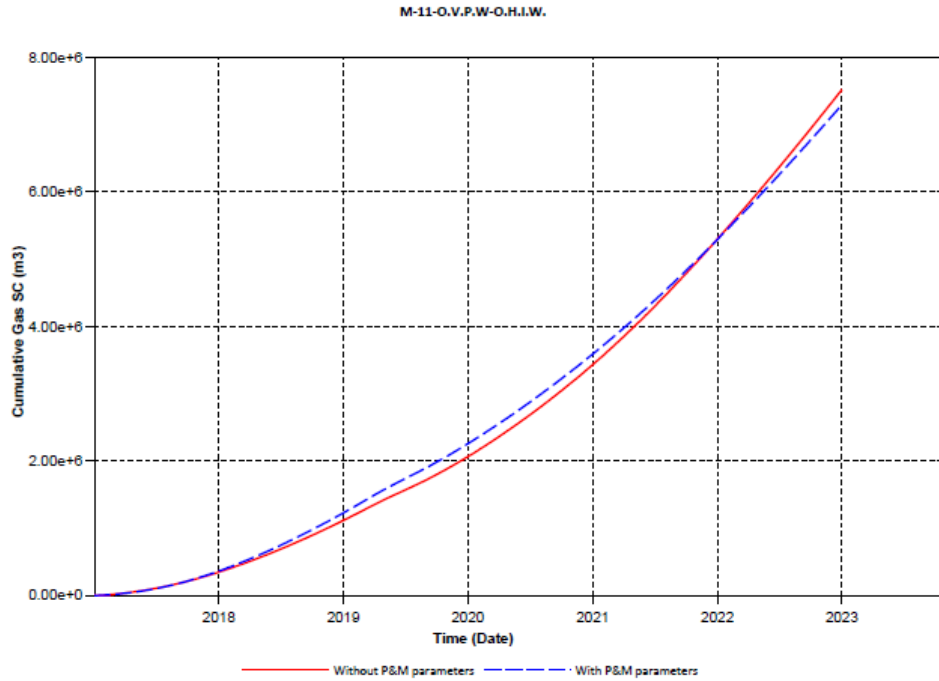


Figure 4.23. Comparison of gas recovery with and without P and M parameters in Model 11

4.2. CO₂ Breakthrough:

The most significant feature about CBM resources is that they are the potential resources for natural gas production and at the same time can be used as geological sinks for greenhouse gas storage by adsorption mechanism where Enhanced Coal Bed Methane Recovery by flue gas (CO₂ and N₂) injection comes into picture. As explained in previous chapters, the CO₂ molecule replaces the CH₄ molecule on coal surface at 2:1 ratio, N₂ reduces the partial pressure of CH₄ which enhances desorption and it has less affinity towards coal due to which early breakthrough of N₂ takes place.

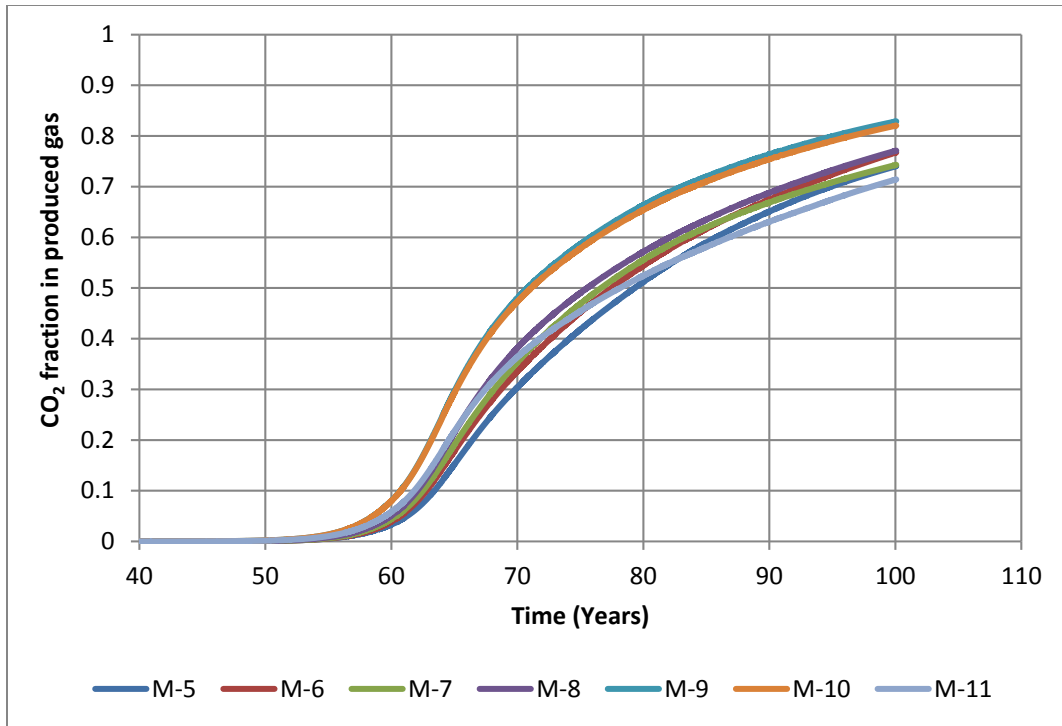


Figure 4.24. CO₂ fraction in produced gas of model 5 to model 11

CO₂ breakthrough occurs when it reaches the maximum adsorption capacity of the coal and sometimes due to presence of hydraulic fractures. Like in water flooding EOR methods, water injection is stopped after certain period of water breakthrough in production well because the fraction of injected fluid in producing fluid increases rapidly and sweep efficiency of injected fluid reduces. In case of CBM reservoirs, the same reasons will justify along with the less chances of greenhouse gas storage. Therefore, it is important to forecast the production life of a CBM reservoir by forecasting the CO₂ breakthrough in ECBM recovery by flue gas injection.

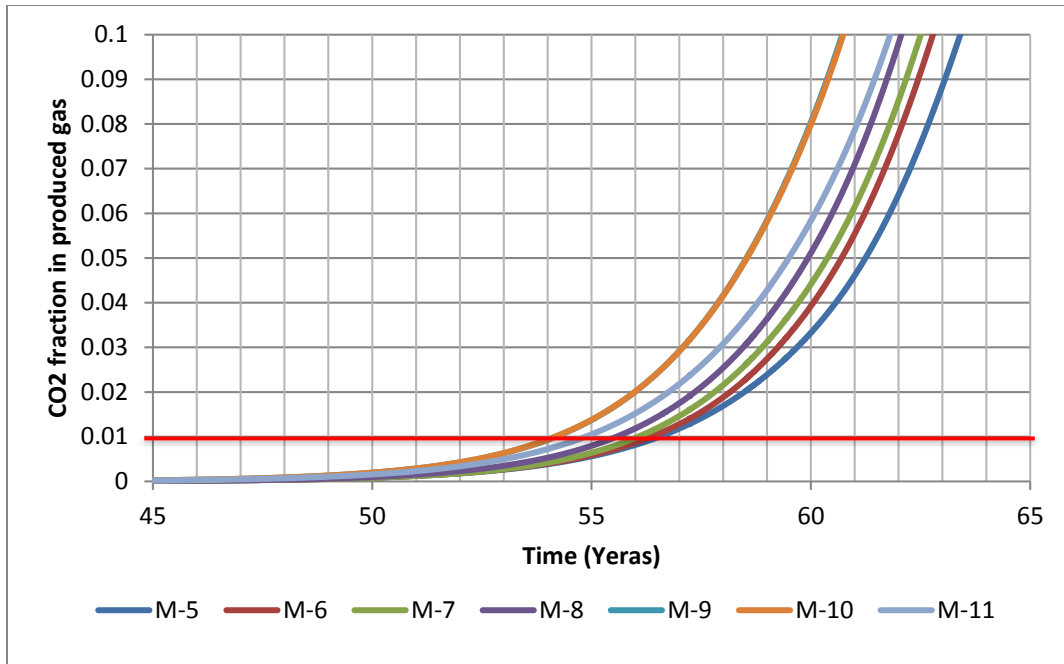


Figure 4.25. Breakthrough time of model 5 to model 11 determined at 5% of CO₂ in produced gas

Breakthrough time can be determined based on ratio of produced gas components. In this simulation modelling, ratio of amount of CO₂ in the produced gas to the total produced gas (CH₄, CO₂ and N₂) is used to determine the CO₂ breakthrough time. **Figure 4.24** illustrates the fraction of CO₂ in the produced gas. It shows that after breakthrough the fraction of CO₂ in produced gas is increasing very rapidly, which indicates the necessity to stop the flue gas injection shortly after breakthrough to not to make the production less economic. Based on TransCanada pipeline gas quality specifications, a 1 % of CO₂ composition in the produced gas is considered as breakthrough point and the breakthrough time for models from 5 to 11 determined out from **Figure 4.25** and are summarized in **Table 4.4**.

It is observed that in all models the breakthrough time is around 55 years i.e. this CBM reservoir which mostly resembles Mannville coal zone has potential to produce for long

time as shown in **Figure 4.26** and the capacity is large enough to store all the CO₂ that injected in 55 years of production period. In all the base cases, the parameters are same except for the type of wells drilled and stimulations included. The CO₂ adsorbed area in 20, 40, 60 years of production is shown for the models from 5 to 11 in **Figures 4.27 to 4.33** which indicating that the CO₂ adsorption, CO₂ breakthrough and CH₄ production doesn't only depends upon reservoir aspects but also on well drilling methods, pattern size because in models 5 to 11 all the reservoir and operational parameters are same except for the well drilling methods.

Model 5 to 8 are all having vertical injection and production wells, and model 9 to 11 are combination of horizontal and vertical wells. When the CO₂ adsorption trends of these models compared, model 9 to 11 having early breakthrough of CO₂ than model from 5 to 8. Among models 5 to 8, model 7,8 having early breakthrough and in model 9 to 11, model 10 having early breakthrough. The reason behind this argument is that the horizontal wells and hydraulic fractures create high drawdown in production well compared to vertical wells in the primary production period due to their high aerial extent which enhances the permeability of the CBM reservoir and the injected gas has sufficient pave for flow through the reservoir.

By closely observing the adsorption patterns of model 5 to 11, an interesting fact emerges is that model with horizontal injection well (M - 11) is only having highest CO₂ adsorption because with constant injection rate and bottom hole pressure, high amount of flue gas is injected per unit time by horizontal well compared to vertical well and vertical production

wells create less drawdown due to which the flue gas front moves very slowly and its resident time increases during which CO₂ molecules tries to occupy maximum space on coal surface.

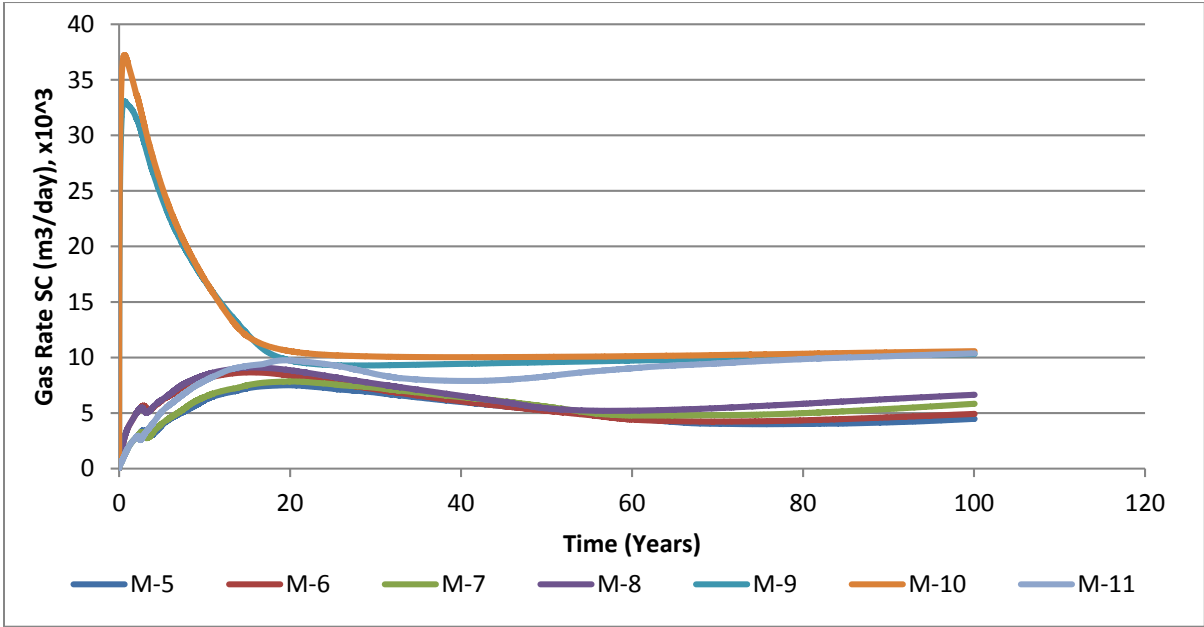


Figure 4.26. Forecast of gas rates for models from 5 to 11

Table 4.4. Breakthrough times and adsorbed CO₂ amount of model 5 to model 11

Model Name	Breakthrough time (Years)	CO ₂ adsorbed (10 ⁶ kg)
M-5-O.V.P. W-O.V.I. W	56.51	249.53
M-6-O.V.P.W. HF-O.V.I. W	56.34	270.66
M-7-O.V.P. W-O.V.I.W. HF	56.05	295.22
M-8-O. V.P. W. HF-O.V.I.W. HF	55.56	321.79
M-9-O.H.P. W-O.V.I. W	54.16	246.03
M-10-O.H.P.W. HF-O.V.I. W	54.14	230.92
M-11-O.V.P. W-O.H. IW	54.86	399.98

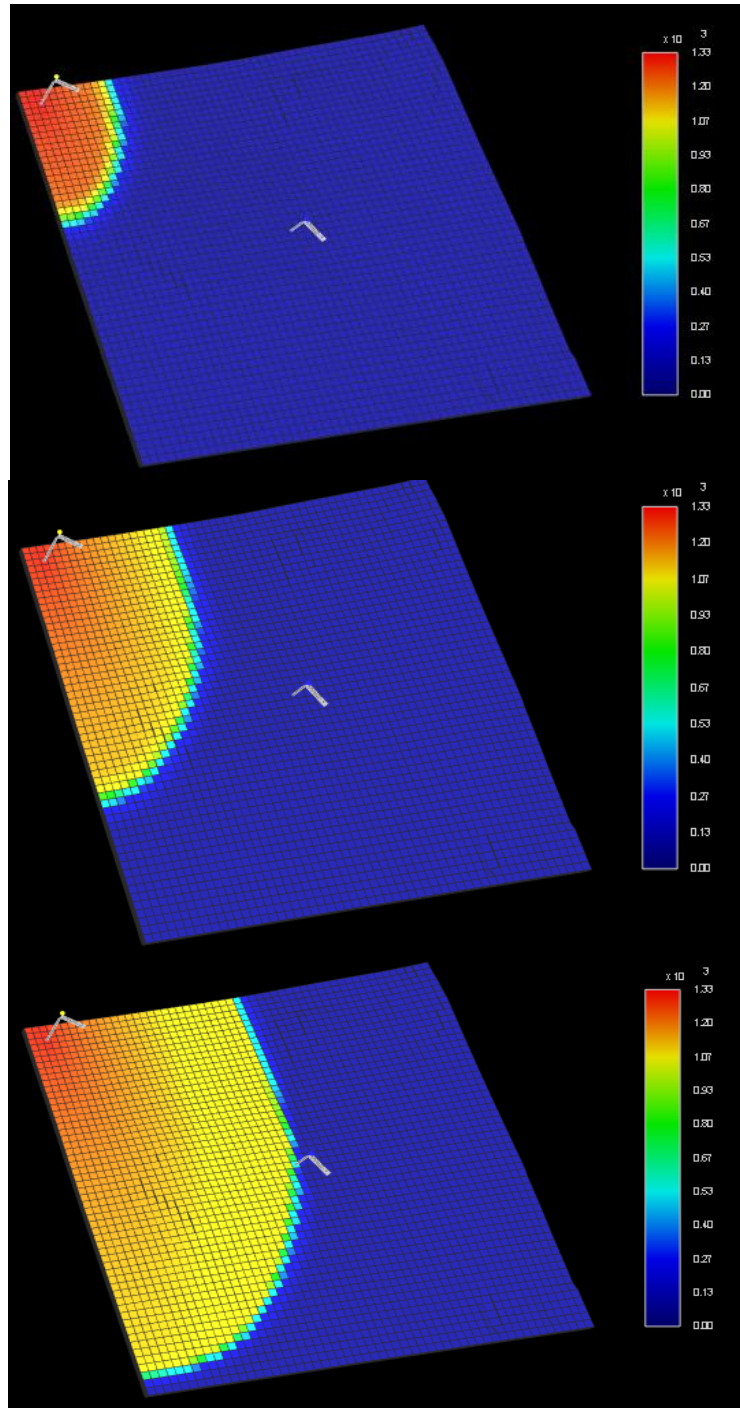


Figure 4.27. CO₂ adsorption in Model 5 in 20, 40 and 60 years of flue gas injection

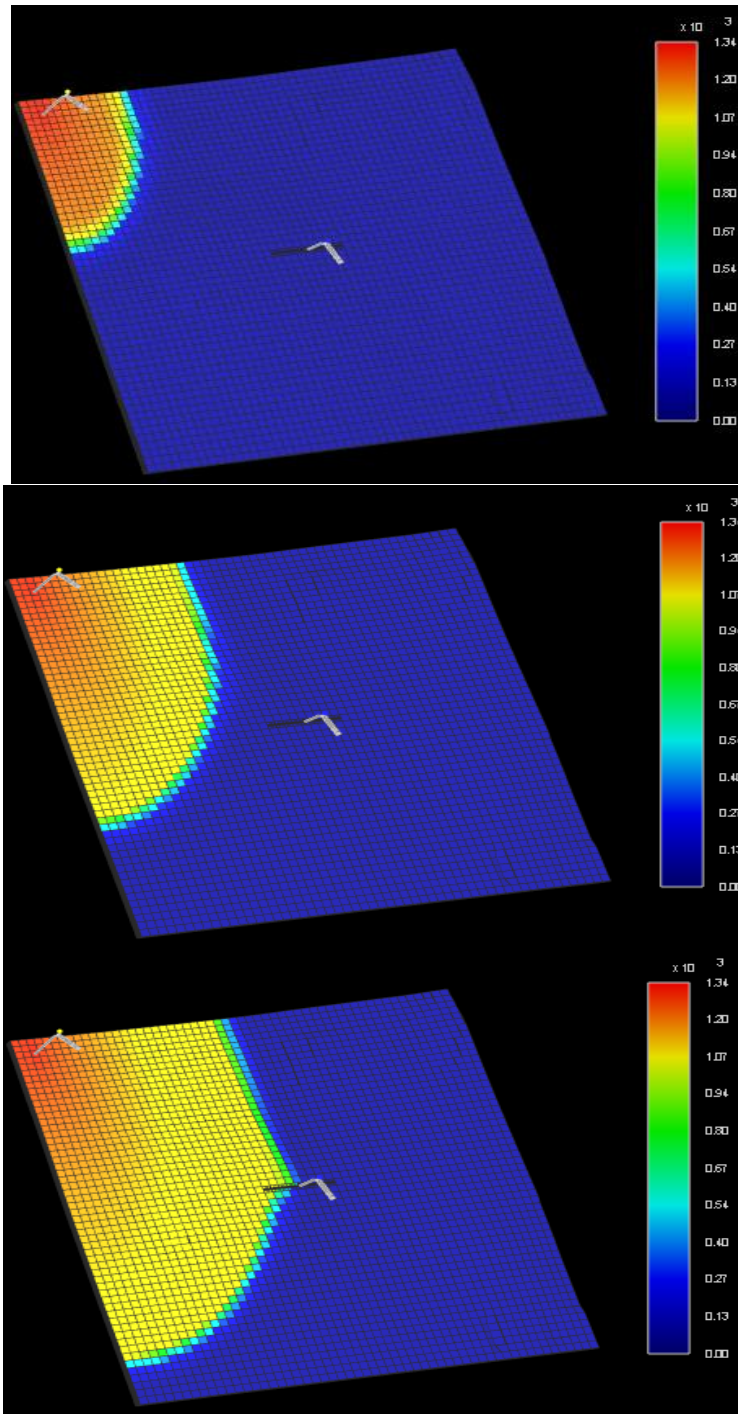


Figure 4.28. CO₂ adsorption in Model 6 in 20, 40 and 60 years of flue gas injection

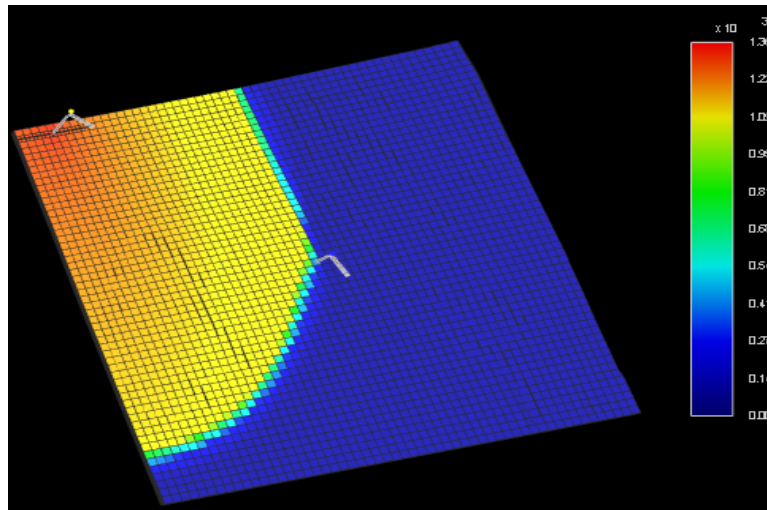
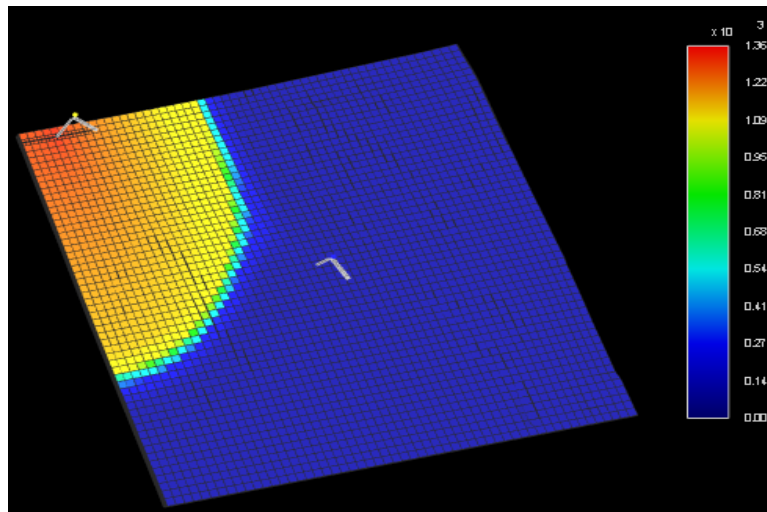
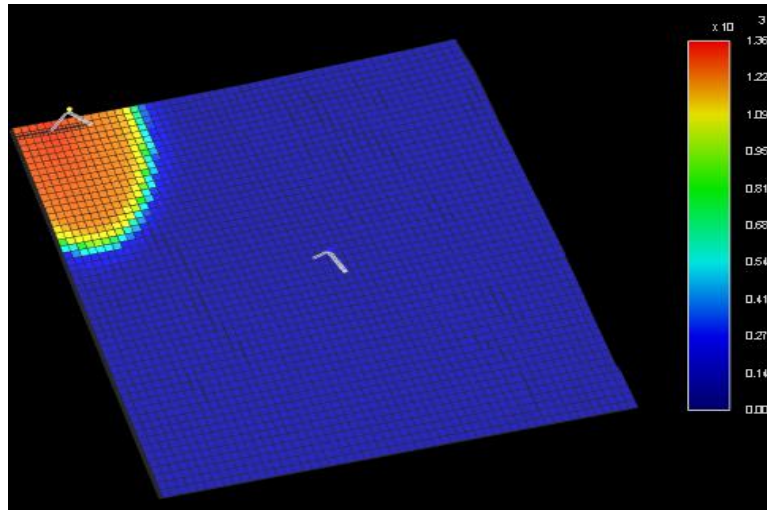


Figure 4.29. CO₂ adsorption in Model 7 in 20, 40 and 60 years of flue gas injection

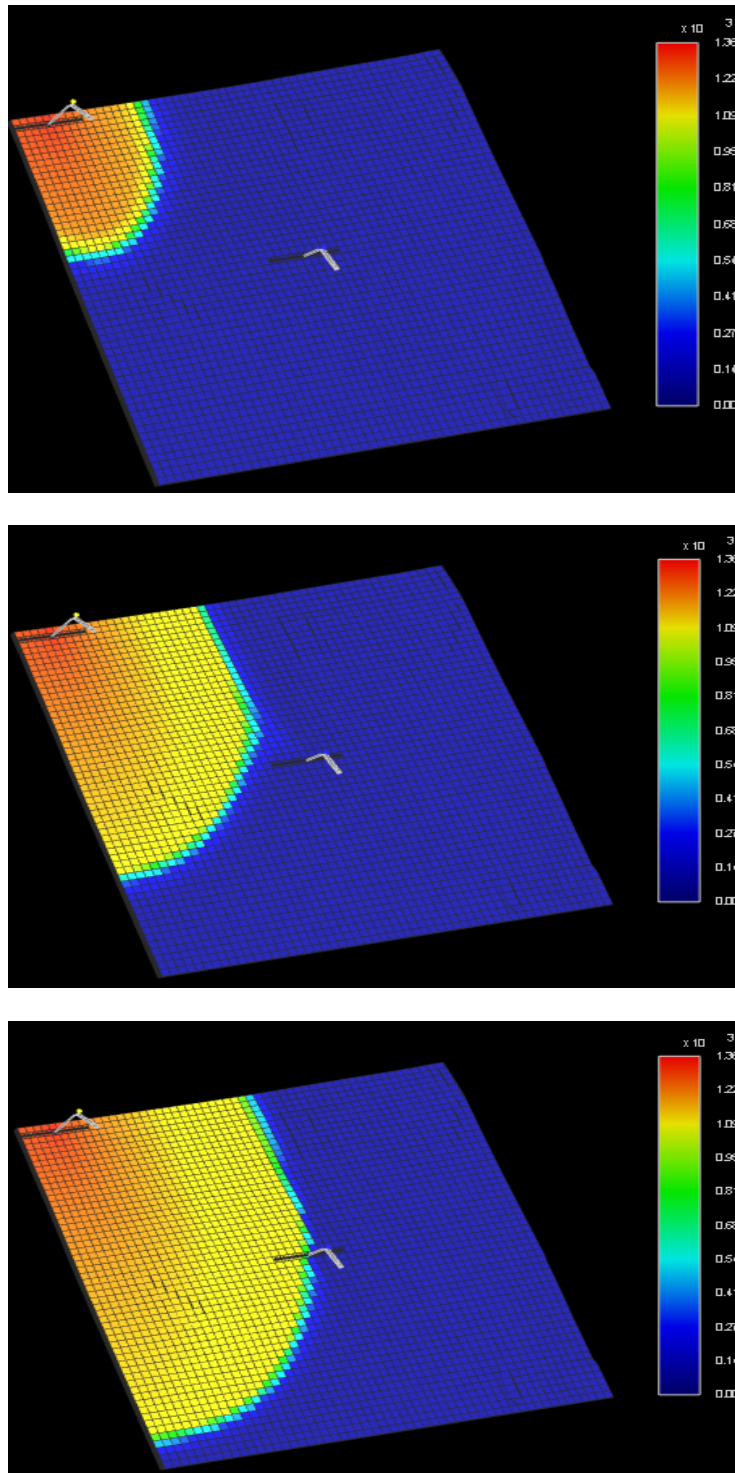


Figure 4.30. CO₂ adsorption in Model 8 in 20, 40 and 60 years of flue gas injection

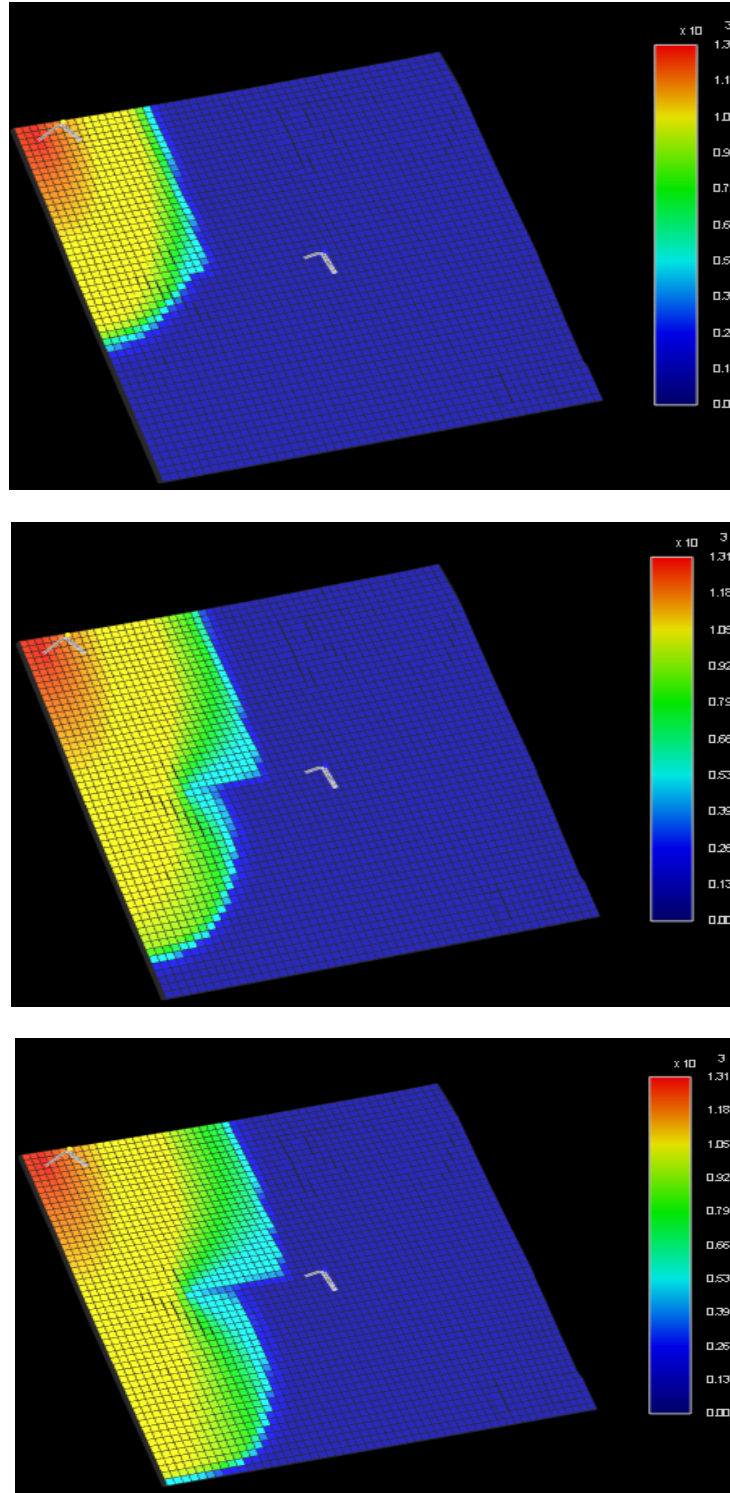


Figure 4.31. CO₂ adsorption in Model 9 in 20, 40 and 60 years of flue gas injection

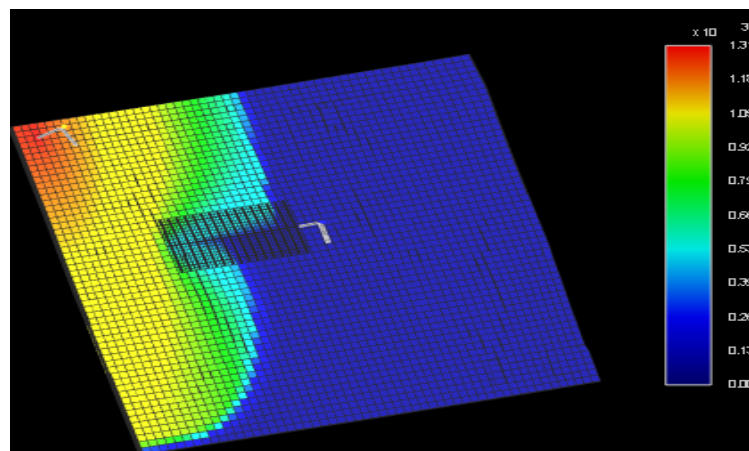
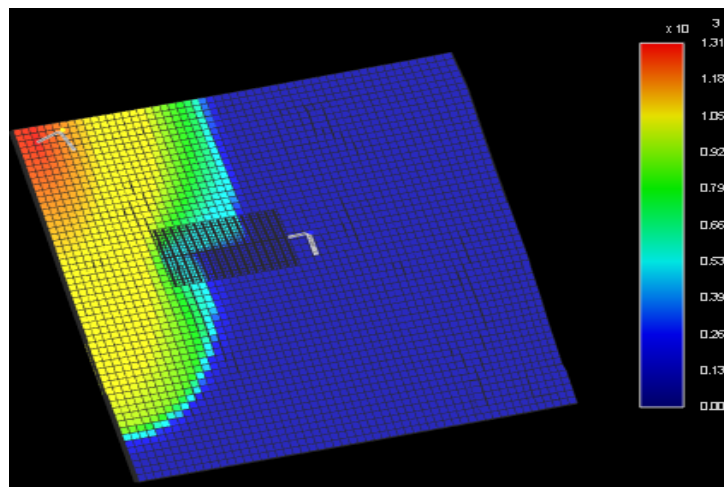
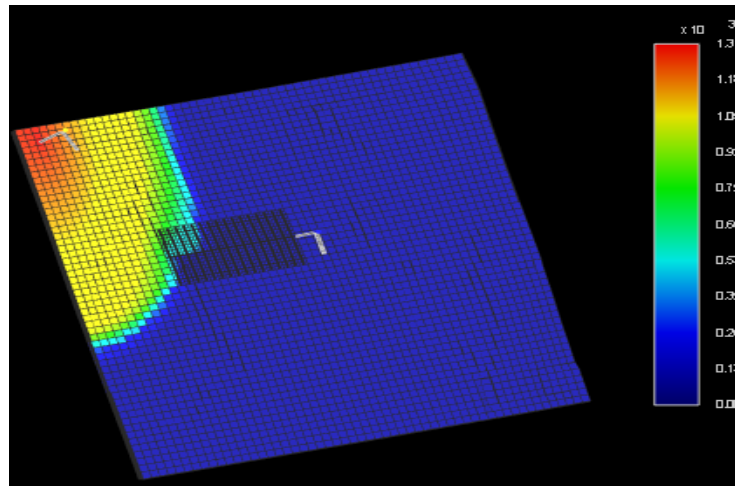


Figure 4.32. CO₂ adsorption in Model 10 in 20, 40 and 60 years of flue gas injection

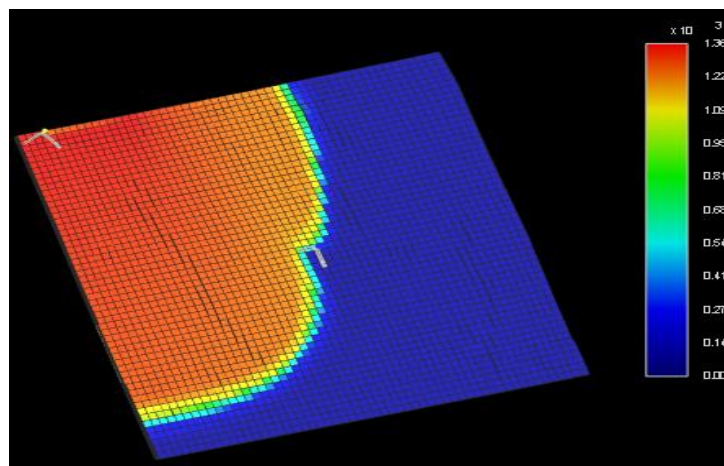
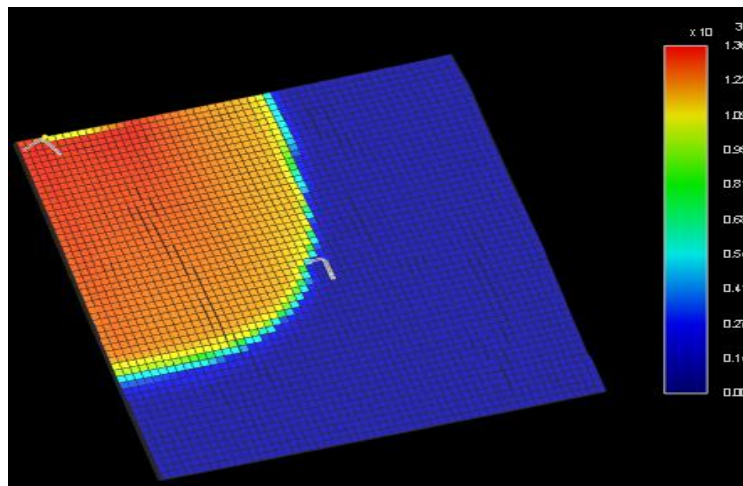
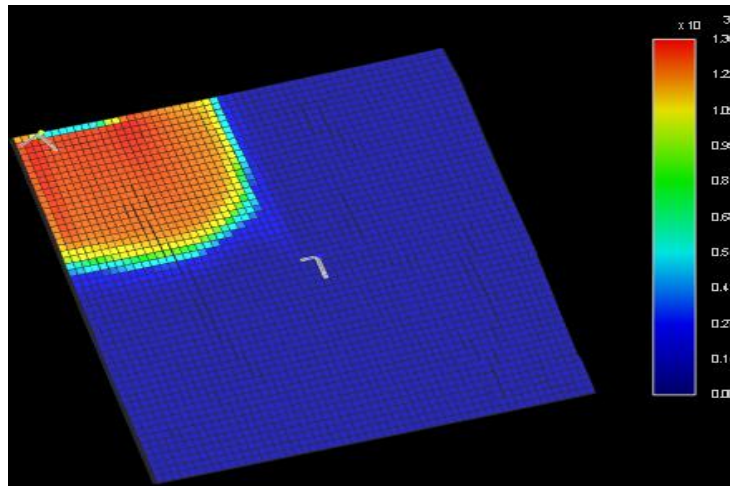


Figure 4.33. CO₂ adsorption in Model 11 in 20, 40 and 60 years of flue gas injection

4.3. Sensitivity Analysis and Optimization:

All the eleven base models are not the best models when cumulative gas recoveries from reservoir are considered. For further analysis, screening of base models (with P and M parameters) is done depending upon the maximum cumulative gas recoveries and CO₂ gas adsorption. **Figure 4.34** and **4.35** illustrates the cumulative gas recoveries of models from 1 to 11 and amount of CO₂ adsorbed on coal surface in models 5 to 11 respectively. It has been observed from both the figures that model 10 with horizontal production well having hydraulic fractures and vertical injection well is giving maximum cumulative gas recovery of 6.65×10^7 m³ and 5.95×10^8 gmole of CO₂ adsorption on coal surface.

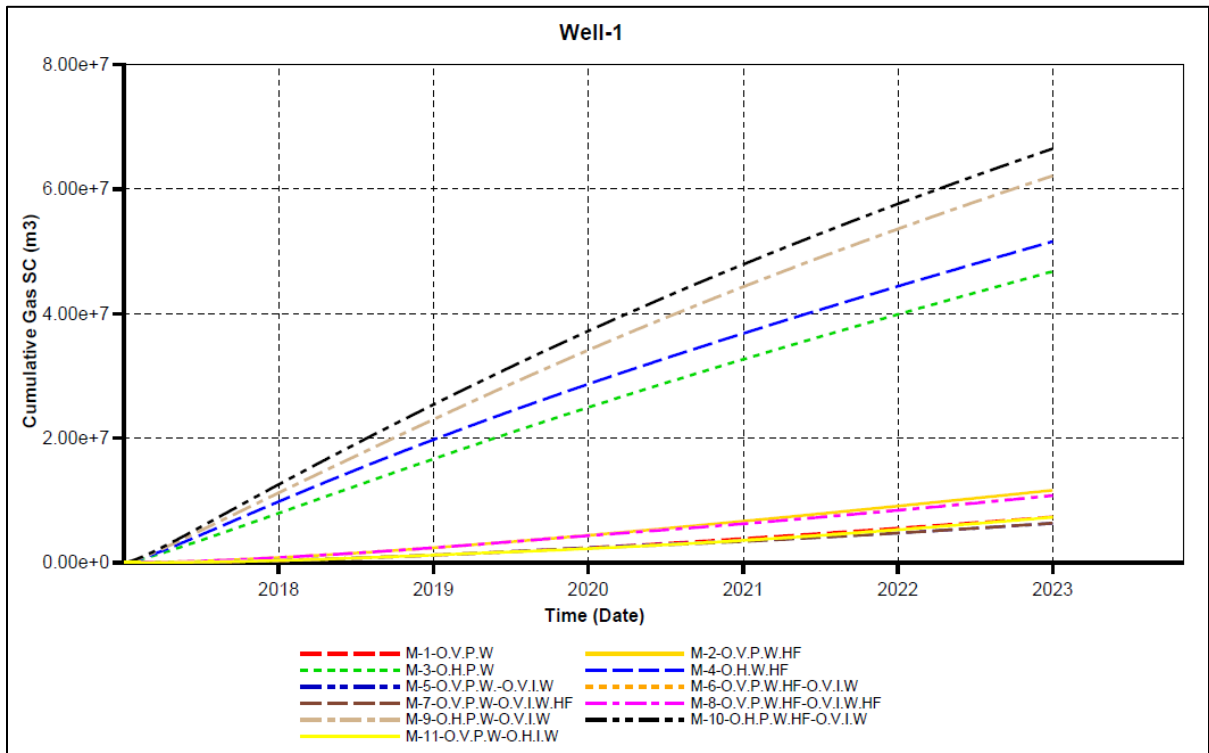


Figure 4.34. Cumulative Gas Recovery of models from 1 to 11

Exclusively comparison of the gas recoveries of model 9 and model 11 concludes that horizontal well drilling and well stimulations in injection well is having no significance when maximum gas recoveries are expected from CBM reservoir and horizontal production well give higher gas recoveries but in case of CO₂ gas adsorption horizontal injection wells are significant due to the high aerial extension. Therefore, by this initial analysis, keeping maximum cumulative gas recovery as primary objective model 10 is considered for further analysis.

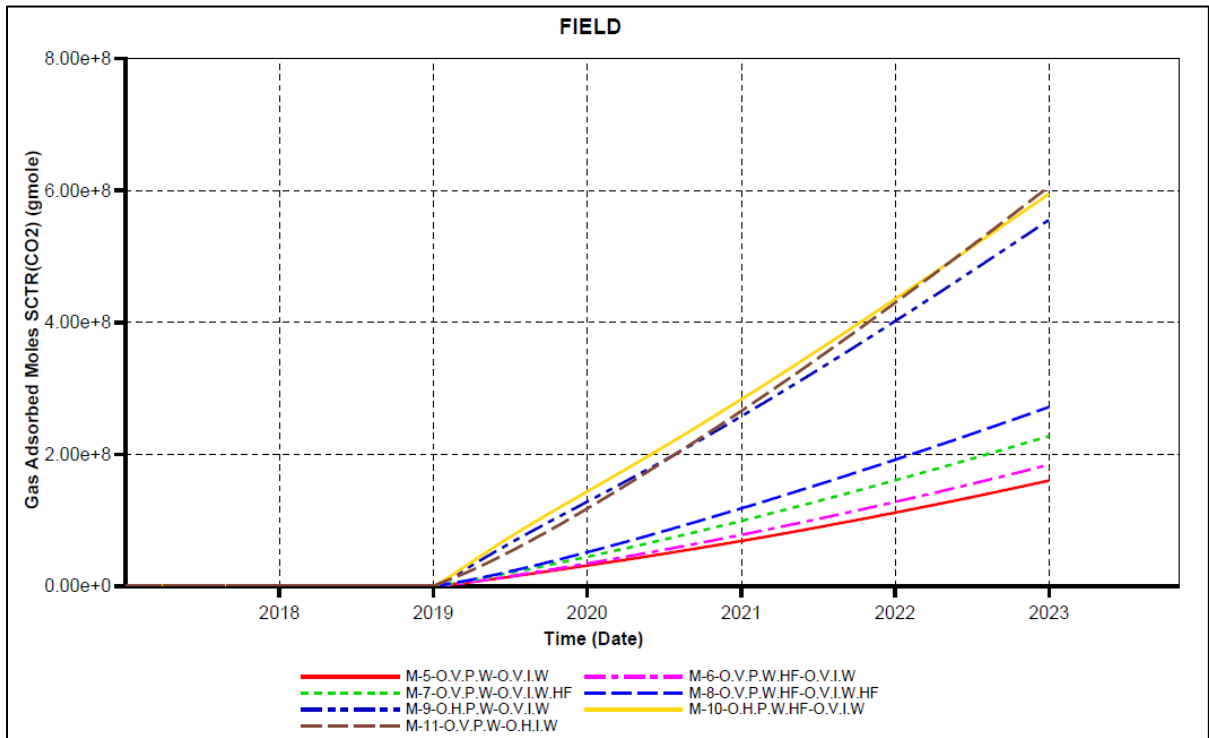


Figure 4.35. Amount of CO₂ gas adsorption in models from 5 to 11

In the base model all the parameters are observed from the published papers and with better judgment to resemble the coal zones in Mannville coal formation. But these parameters are less reliable, and it is not yet known that which of these parameters are highly influential or sensitive towards production from CBM reservoir. Twelve parameters which mainly comprise of rock mechanical properties; hydraulic fracturing and operating parameters with a range of values as given in table 3.7 to 3.9 are considered for conducting further analysis. These ranges of values are taken to submit number of jobs with different combinations of these twelve parametric values to run in CMG's CMOST software and Cumulative gas recovery and CO₂ gas adsorption are considered as main objective function to check their sensitivity towards these parameters i.e. "if some parameter is increased or decreased by certain amount, how much will these objective functions increase or decrease?". Initially response surface methodology is used to conduct sensitivity analysis in which multiple parameters are adjusted together to analyze results by fitting a response surface or a polynomial equation to results. These polynomial equations are the combination of linear, quadratic and interaction terms as **shown in equations 4.1 to 4.3** and the model type is automatically chosen by the simulator or can be changed manually.

Linear Model:

$$y = a_0 + a_1x_1 + a_2x_2 + \dots + a_kx_k \quad (4.1)$$

Linear + Quadratic Model:

$$y = a_0 + \sum_{j=1}^k a_j x_j + \sum_{j=1}^k a_{jj} x_j^2 \quad (4.2)$$

Linear + Quadratic + Interaction:

$$y = a_0 + \sum_{j=1}^k a_j x_j + \sum_{j=1}^k a_{jj} x_j^2 + \sum_{i < j} \sum_{j=2}^k a_{ij} x_i x_j \quad (4.3)$$

Nearly 40 simulation jobs are run using this method, but these experiments are not sufficient to get the reliable model; therefore, further analysis is conducted using particle swarm optimization technique to improve the gas recoveries and CO₂ adsorption. Around 120 simulation jobs are run and the obtained tornado plot, Morris and Sobol analysis charts are discussed in the following pages. The most reliable solutions for cumulative gas recovery and CO₂ gas adsorption are 1.03e⁸ m³ and 9.20e⁸ gmole respectively.

Figure 4.36 and 4.37 represent the tornado plots for cumulative gas recovery and CO₂ gas adsorption respectively. These plots provide quantitative information like which parameter is highly influencing the objective function. The parameters on the top of plot are highly influential and the influence reduces as going down the plot. This influence may be positive or negative.

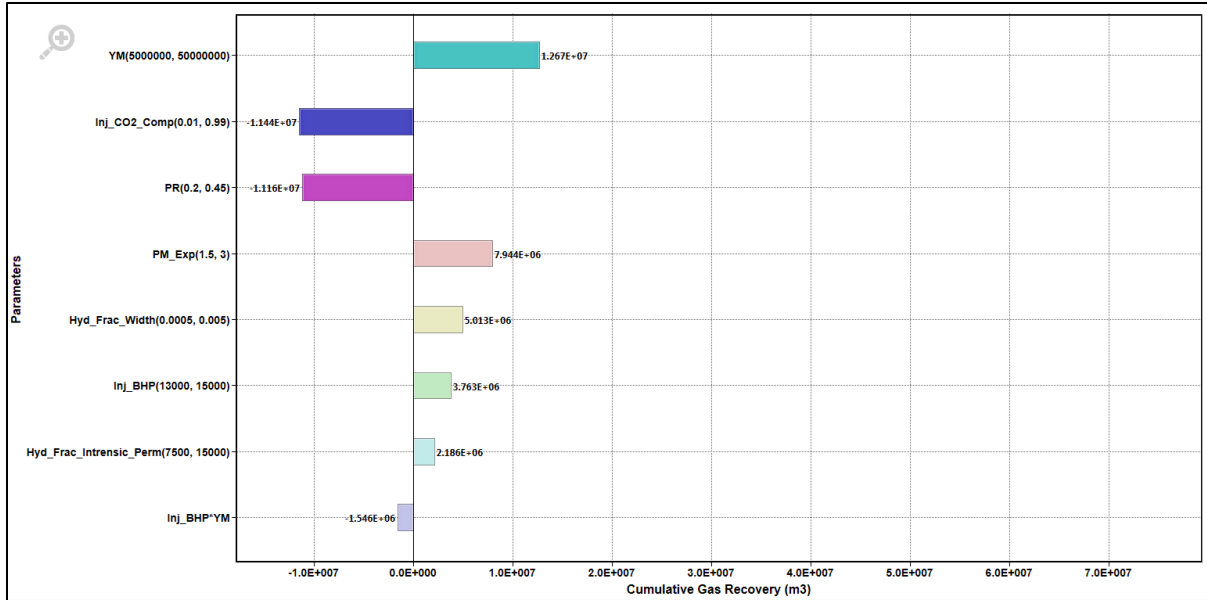


Figure 4.36. Sensitivity of parameters towards Cumulative gas recovery by Tornado plot

From **Figure 4.36**, it is observed that cumulative gas recovery is more sensitive towards P and M rock mechanical properties and least sensitive towards hydraulic fracture parameters. Firstly, Young's modulus of rock is affecting in positive trend i.e., as the Young's modulus value is increased from $5e^6$ kPa to $5e^7$ kPa, the cumulative gas recovery is increased by $1.26e^7$ m³. Secondly, Poisson's ratio is having negative effect on cumulative gas recoveries i.e., as the property value increased from 0.2 to 0.45; the gas recovery is reduced by $1.116e^7$ m³.

As it is known that Young's modulus and Poisson's ratio are used in equations from **3.7** to **3.9** for calculating change in fracture permeability and the above results concluding that as the young's modulus value is increased the matrix shrinkage is very dominant which enhances the fracture permeability and as Poisson's ratio is increased matrix swelling is

dominant which counter acting each other's effect, but the difference of their effects is a positive value indicating increased gas recovery.

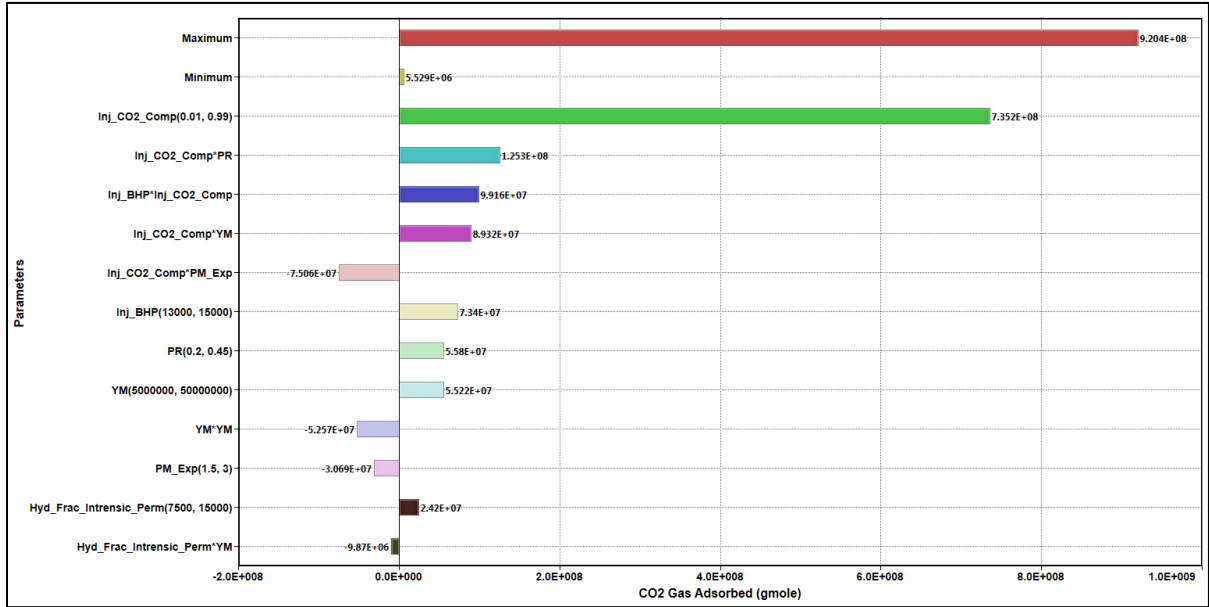


Figure 4.37. Sensitivity of parameters towards CO₂ gas adsorption by Tornado plot

Injecting flue gas composition is the second influential parameter having negative effect on gas recovery which is explained by the reason that as the flue gas is injected, CO₂ is adsorbed on coal surface and the local pressure is increased in the matrix due to which desorption of methane molecules into fractures will be slow effecting gas recoveries.

Figure 4.37, showing that CO₂ gas adsorption is highly influenced by operating parameters mainly CO₂ gas composition in injecting flue gas i.e., as CO₂ composition in the flue gas is increased from 0.01 to 0.99, CO₂ gas adsorption on coal is increased by 7.352e⁸ gmole and it is also showing that the interaction of parameters is highly affecting rather than the individual parameters. The results from both figures conclude that CO₂ composition in the

injecting flue gas is having counter-effect on cumulative gas recovery and CO₂ gas adsorption.

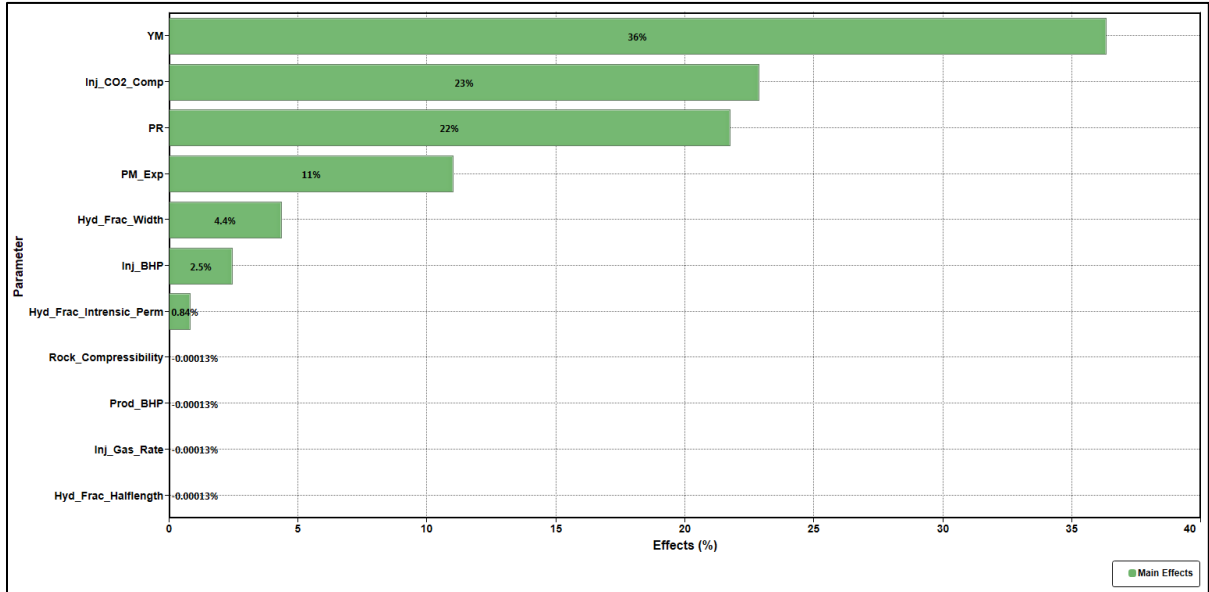


Figure 4.38. Sobolj Result Analysis for Cumulative Gas Recovery

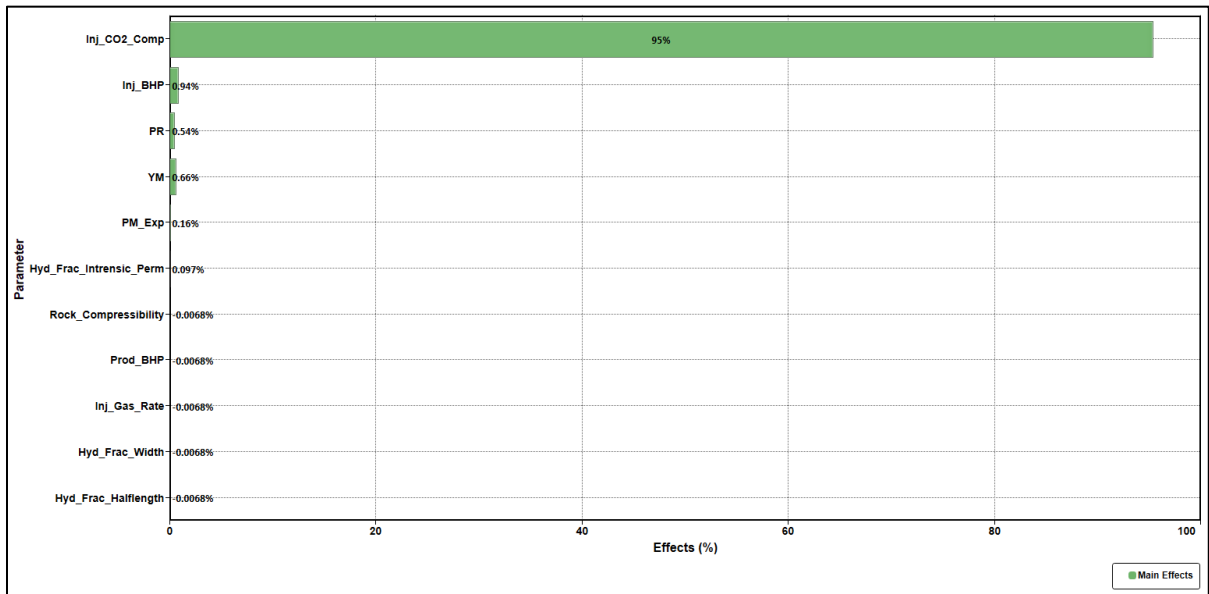


Figure 4.39. Sobolj Result Analysis for CO₂ Gas Adsorption

Sobol analysis charts for cumulative gas recovery and CO₂ gas adsorption are shown in **Figures 4.38** and **4.39** respectively. Sobol analysis charts represent the qualitative effects which provide information of percentage impact of each parameter on objective functions. From these figures it is observed that young's modulus and CO₂ composition in flue gas have their highest effect of 36% and 95% on cumulative gas production and CO₂ gas adsorption respectively.

4.4. Uncertainty Assessment:

In Oil and Gas industry, the decisions are made based on probability distribution. Even though the optimization studies in the previous section gives highest reliable values for gas recovery and CO₂ adsorption, probability of getting this results in real field operation is unknown and it might be less or high. Therefore, uncertainty assessment is must to get the complete probability distribution of objective functions. To do so, Monte Carlo simulation method is used in which all the parameters are normally distributed in their ranges. The experiments in previous optimization studies are again used in this assessment to obtain the reliable distribution of objective functions.

Around 130 simulations run to get the results as shown in **Figures 4.40** and **4.41** which represents probability distribution of cumulative gas recovery and CO₂ gas adsorbed with respect to probability density and cumulative probability respectively. The vertical bold lines across the distribution are namely P10, P50 and P90 (cumulative distributions) which defines the estimations of objective functions. These terms have different explanation in oil and gas sector. As it is said before, it can never be sure exactly how much gas is available for

production in the CBM reserves. However, having a good estimation is very effective in decision making process to obtain a high economic recovery. In doing so, a low, best, and high estimation of objective function are provided using probability distribution.

P10 – There should be at least a 10% probability that the quantities recovered will equal or exceed the highest estimate. This is the possible case and highest figure i.e., 10 % of the calculated estimates will be equal or exceed P10.

P50 - There should be at least a 50% probability that the quantities recovered will equal or exceed the highest estimate. This is more likely to occur because it is closer to median.

P90 - There should be at least a 90% probability that the quantities recovered will equal or exceed the highest estimate. This is kind of a proved case and lowest figure i.e., 90% of the calculated estimates will be equal and or exceed P90 estimate.

In this thesis, among these three percentiles, P50 is chosen for further analysis because of following reasons;

- P50 is closer to the mean which is highest, the mean will incorporate both the higher and lower estimations of objective functions which will smooth the differences when added together,
- P10 is over-optimistic, P90 is more conservative estimate which could potentially produce less gas and both provide confusing future trends.

Table 4.5 provides the values of individual parameters that have been used in Monte Carlo simulation to get Cumulative gas recovery and CO₂ gas adsorption values at P50 and these are mostly reliable and occurring results.

Table 4.5. Individual parameters to obtain objective function values at P50

Property	For Cumulative Gas Recovery of 8.02e⁷ m³	For CO₂ gas adsorption of 3.77e⁸ gmole
Hydraulic fracturing parameters		
Half length, m	201.81231	162.25849
Width, m	0.001566	0.003683156
Intrinsic permeability, mD	11555.706	13648.827
Operating parameters		
Injection well BHP, kPa	13434.02	14150.71
Injection gas rate, m ³ /day	15328.58	15135.41
Injection CO ₂ composition	0.425836	0.447112
Production well BHP, kPa	244.8811	239.7525
P and M Rock mechanical parameters		
Rock compressibility, kPa ⁻¹	5.13E-05	6.99E-05
Young's modulus, kPa	2.66E+07	3.19E+07
Poisson's ratio	0.350838	0.379353
P and M Exponent	2.477791	2.36426

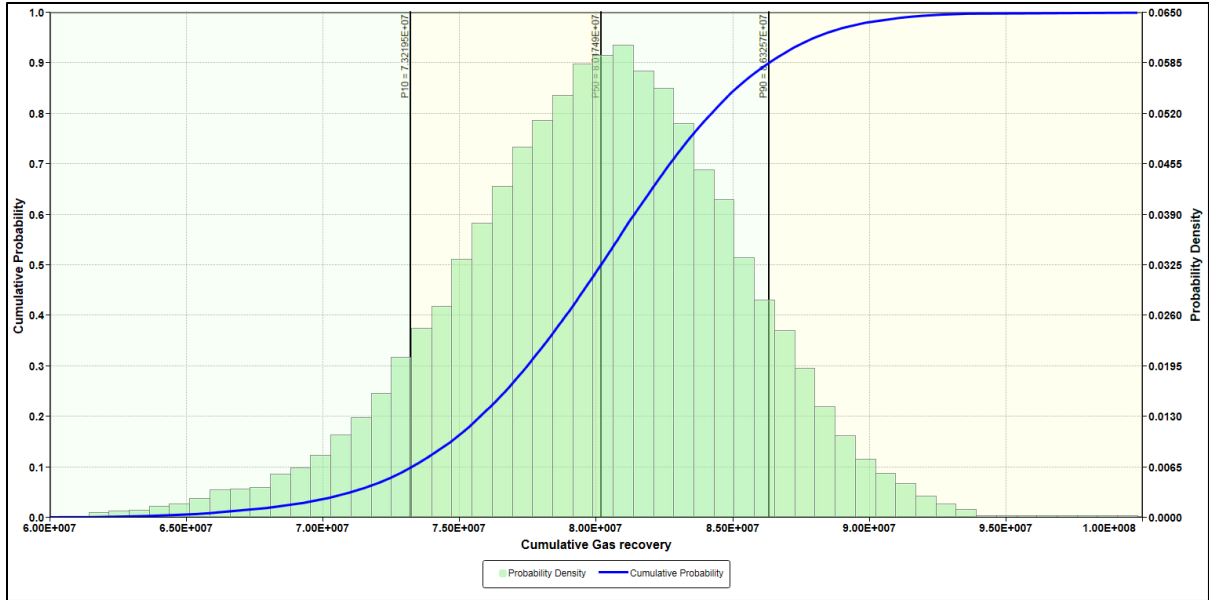


Figure 4.40. Probability distribution of Cumulative Gas Recovery

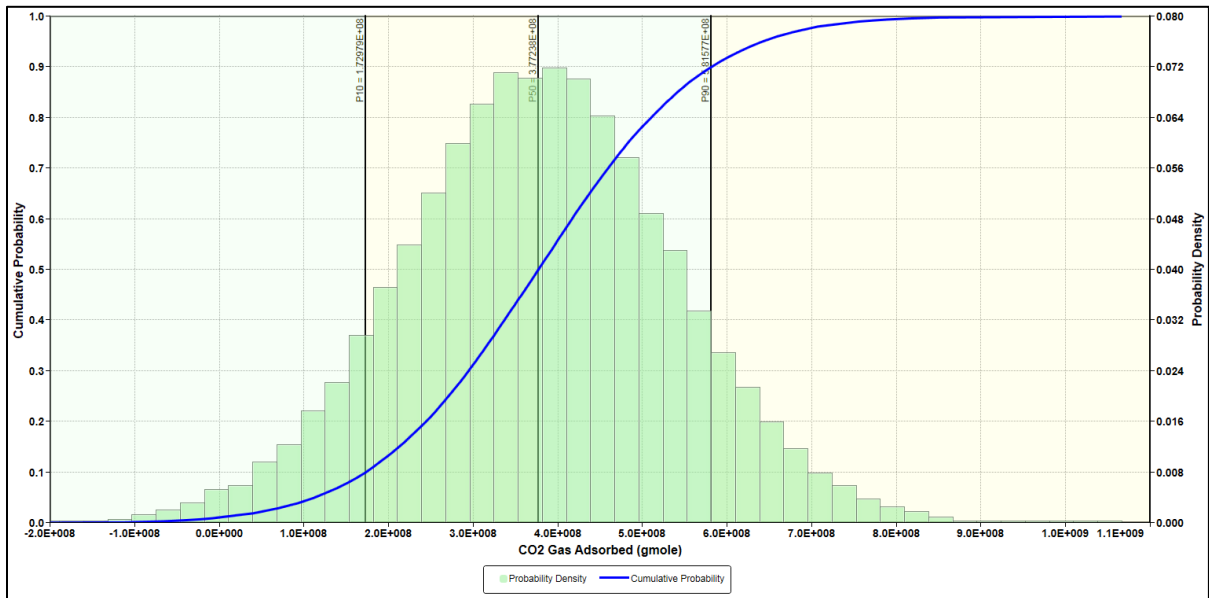


Figure 4.41. Probability distribution of CO₂ gas adsorption

Apart from this, in previous sensitivity analysis, a clarification is obtained on to which parameters objective functions are sensitive towards. The main objective of this analysis is

to find flue gas compositions that results in effective gas recovery and CO₂ gas adsorption. In doing so, two base models with the parametric values given in **Table 4.5** are created for cumulative gas recovery and CO₂ gas adsorption and only operating parameters are taken as variables to conduct further analysis.

Around 60 simulations are run for both the cases and results shows that injecting flue gas composition is the high influential parameter relative to other operating parameters and having > 95% effect, but this effect is positive for CO₂ gas adsorption and negative for Cumulative gas recovery. This statement can be explained using the equation **3.11** which is the extended P and M model equation. Flue gas composition is an operating parameter before it is injected into the CBM reservoir but after injecting into reservoir, the interaction of the gas components with coal is very important to be considered. When the equation is observed, porosity changes are highly dependent on rock mechanical properties and composition of each gas component present in the CBM reservoir. Therefore, all rock mechanical parameters are kept constant and the only variable on which permeability changes depend is the composition of gas component and there is no other operating parameter is appearing in the equation which explains its high impact on objective functions.

The final results of flue gas compositions that giving effective and highest cumulative gas recovery and CO₂ gas adsorption are given in **Figures 4.42 and 4.43** and as expected the values are counteracting each other i.e., cumulative gas recovery requires less fraction of CO₂ and high fraction of N₂ and CO₂ gas adsorption requires more fraction of CO₂ and less

fraction of N₂. High density of reliable and effective CO₂ composition values for gas recovery and CO₂ sequestration are observed to be in between 0.0 – 0.3 and 0.4-0.8 respectively.

The reason behind these trends is that for high gas recovery high permeability is required and high N₂ composition in the flue gas reduces the partial pressure of CH₄ and enhances the desorption process rapidly due to which matrix shrinkage effects are dominant compared to swelling effects due to CO₂ adsorption which resulting in increase in permeability. When CO₂ composition is high in flue gas, the front moves very slowly due to high affinity of CO₂ towards coal and occupies maximum coal surface area. During this process, the rate of increase in permeability decreases due to dominant swelling effects. These results summarize that when the cumulative gas recoveries are desired low CO₂ composition is effective and when CO₂ sequestration is desired high (>0.4) CO₂ composition is effective.

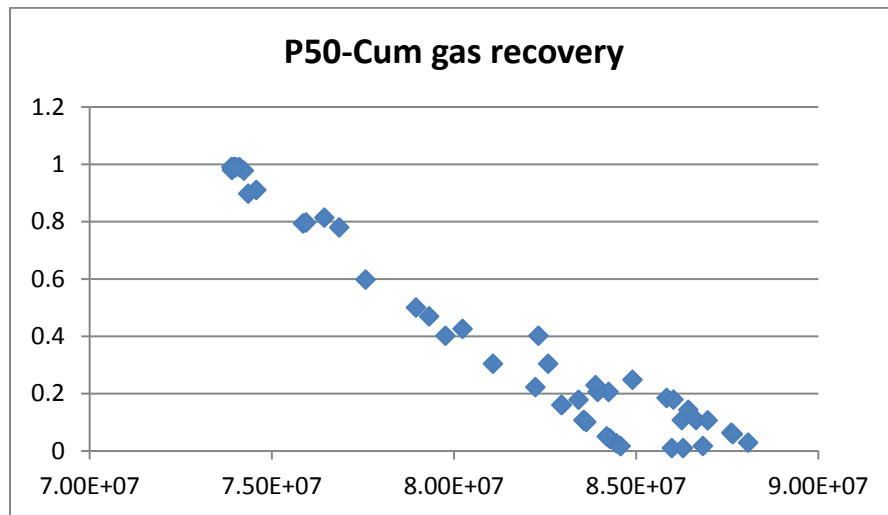


Figure 4.42. Cumulative gas recovery vs CO₂ gas composition in flue gas

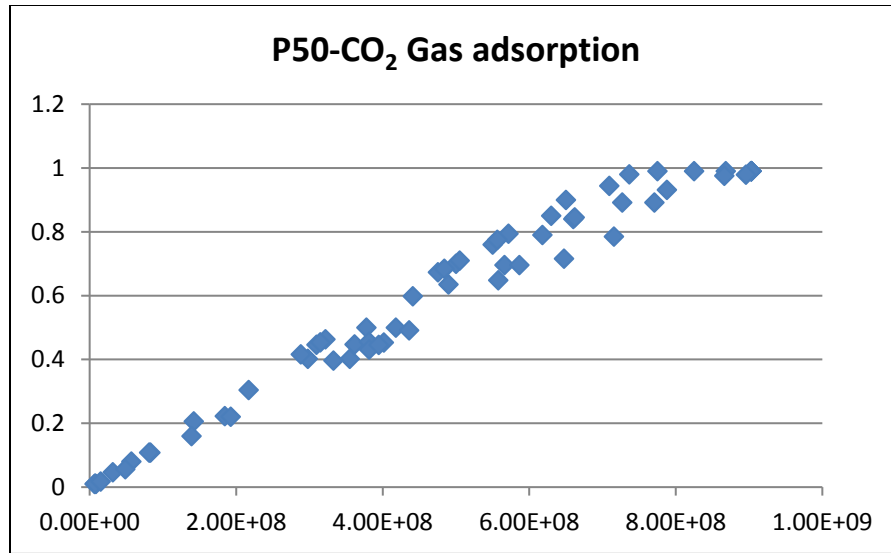


Figure 4.43. CO₂ gas adsorption vs CO₂ gas composition in flue gas

Chapter 5 : Conclusions and Recommendations

The sensitivity analysis and optimization were done to simulate ECBMR by flue gas injection and find the dominant factors that influence the gas recovery and subsequent CO₂ sequestration. Based on the findings of the sensitivity analysis, the following conclusions are summarized along with recommendations to achieve effective and reliable outputs from Canadian CBM resources.

1. The unminable coal has distinct behavior towards the fluids in the system. Coal properties are one of the essential criteria to accurately simulate the enhanced gas productions and CO₂ sequestration. Among the coal properties, matrix shrinkage and swelling are hard to express and easy to be ignored. However, the results proved that the simultaneous adsorption and desorption of gas components on coal surface changes the permeability of the fracture system.
2. The swelling and shrinkage effects result in positive or negative effects on efficiency of gas production depending on which effect is more dominant. When swelling effects are dominant due to flue gas injection, gas production declines and when shrinkage effects are dominant due to high CH₄ desorption, gas production enhances.
3. When the composition of CO₂ in the injecting flue gas is high compared to N₂, coal swelling is dominant due to high affinity of CO₂ towards coal which enhances CO₂ sequestration and declines gas production. When the composition of N₂ in the injecting flue gas is high compared to CO₂, coal shrinkage effects are dominant because N₂

reduces the partial pressure of CH₄ and promotes early desorption which enhances the gas production.

4. Apart from coal properties, well drilling and stimulation methods are impactful on enhanced gas recoveries. It has been observed from the results that, under five spot pattern flue gas injections, having horizontal and hydraulic fractured production well is testified as the best strategy for early and enhanced gas production and having horizontal injection wells as the best strategy for the greenhouse gas storage.
5. CO₂ breakthrough time for enhanced gas recovery models (from model 5 to model 11) shows that the CBM reserves under the taken operating conditions have potential to store 60 years of CO₂ injection.
6. Enhanced production methods applied to injection well could considerably decrease the requirement of high injection pressure caused by coal matrix swelling due to CO₂ adsorption. Moreover, stimulating injection well could increase the amount of CO₂ sequestration.
7. Enhanced production methods applied to production well could shorten the time to reach breakthrough, which indicates less production time. At the same time, it substantially increases CH₄ recovery compared with un-stimulated vertical production well.
8. The sensitivity analysis showed that the enhanced gas recovery and CO₂ gas adsorption are more sensitive towards Palmer and Mansoori rock mechanical parameters relative to operating and hydraulic fracture parameters.

9. Young's modulus of rock and poisson's ratio which create matrix shrinkage and swelling effects are highly influential among all rock mechanical parameters and CO₂ composition in injection flue gas is negatively affecting the gas production and positively affecting CO₂ gas adsorption among all other operating parameters.
10. In case of CO₂ gas adsorption, flue gas composition having CO₂ composition in the range of 0.4-0.8 are giving the most probable and effective CO₂ sequestration.
11. In case of cumulative gas recovery, flue gas composition having CO₂ composition in the range of 0-0.2 are giving the most probable and effective gas recoveries.
12. It concludes that the CO₂ sequestration and gas recovery counteracts each other i.e., if we want high gas production, CO₂ sequestration is possible but high capacity of storage is not possible and vice versa.

Recommendations for future work:

1. The complete work is simulation based and even though sensitivity analysis, optimization and uncertainty assessment are conducted, it is very hard to say whether the same results can be obtained when applied in real field. Therefore, modification of the models based on production data from CBM reservoirs with history matching and lab work will justify the accuracy and reliability of this simulation work.
2. The enhanced methane gas recovery by flue gas injection save the surface separation cost of pure CO₂ capturing but at the same time separation units are required to separate N₂ from produced gas to improve the quality of gas to pipeline specification. If the separation of N₂ cost is lesser than the flue gas injection cost, the project is more economical. Therefore, economic evaluation with details can be done to judge the commercial value of CO₂ sequestration and ECBM recovery.
3. It is not well known whether the gas components instantaneously adsorb or desorb from coal surface. A proper understanding of the desorption timing of gas components may contribute to the enhanced recoveries and CO₂ sequestration.
4. Multilateral horizontal wells can be added as new alternative drilling method for enhancing coal bed methane recovery.

REFERENCES

1. Arri L. E., Yee D., Morgan W. D., and Jeanson M. W., "Modeling Coalbed Methane Production with Binary Gas Sorption", SPE 24363, 1992, PP: 459-472.
2. BP Statistical Review of World Energy 2004, 2005, 2006, 2007, 2011, 2012, 2013, 2014, 2015, 2016 and 2017.
3. Available at British Petroleum website: <http://www.bp.com/>
4. Brunauer S., Emmett P. H., and Teller E., "Adsorption of Gases in Multi-Molecular Layers", Journal of the American chemical society, Vol: 60, 1938, pp: 309-319.
5. Busch A., Gensterblum Y., and Krooss B. M., "Methane and CO₂ Sorption and Desorption Measurements on Dry Argonne Premium Coals: Pure Components and Mixtures", International Journal of Coal Geology, Vol: 55, 2003, pp: 205-224.
6. Bustin M., "Research Activities on CO₂, H₂S and SO₂ Sequestration at UBC", Coal Sequestration I Forum, Houston, 2002.
7. Coal Bed Methane resource information. Available at: <http://www.albertacanada.com/>
8. Cervik J., "Behavior of Coal-Gas Reservoirs", Bureau of Mines Technical Progress, Report 10, U.S. Department of Interior, 1969.
9. Curt M.W, Duane H. S., Kenneth L.J., Angela L.G., Sinisha A.J., Robert B.L., Stephen B.D., Ekrem O., Badie I.M., and Karl T.S., "Sequestration of Carbon Dioxide in Coal with Enhanced Coalbed Methane Recovery- A Review", Energy and Fuels – An American Chemical Society Journal, Vol. - 19.3, 2005, pp: 659-724.
10. Dai Z., Viswanathan H., Middleton R., Pan F., Ampomah W., Yang C., Jia W., Xiao T., Lee S.Y., McPherson B. and Balch R., "CO₂ Accounting and Risk Analysis for CO₂ Sequestration at Enhanced Oil Recovery Sites", Environmental science and technology, Vol: 50(14), 2016, pp:7546-7554.
11. Deisman N., Gentzis T., and Chalaturnyk R. J., "Unconventional Geomechanical Testing on Coal for Coalbed Reservoir Well Design: The Alberta Foothills and Plains", International Journal of Coal Geology, Vol: 75, 2008, pp: 15-26.

12. Durucan S., Mustafa A., and Shia J. Q., "Matrix Shrinkage and Swelling Characteristics of European Coals", *Energy Procedia*, Vol: 1, 2009, pp: 3055-3062.
13. Gentzis T., "Subsurface Sequestration of Carbon Dioxide – An Overview from an Alberta (Canada) Perspective", *International Journal of Coal Geology*, Vol: 43, 2000, pp: 287-305.
14. Gentzis T., and Bolen D., "The Use of Numerical Simulation in Predicting Coalbed Methane Producibility from the Gates Coals, Alberta Inner Foothills, Canada: Comparison with Mannville Coal CBM Production in the Alberta Syncline", *International Journal of Coal Geology*, Vol: 74, 2008, pp: 215-236.
15. Gentzis T., "Stability analysis of a horizontal coalbed methane well in the Rocky Mountain Front Ranges of southeast British Columbia, Canada", *International Journal of Coal Geology*, Vol: 77, 2009, pp: 328-337.
16. Goodarzi F., Gentzis T., Cheung F. K., and Defarge F., L., "Coalbed Methane Producibility from the Mannville Coals in Alberta, Canada: A comparison of Two Areas", *International Journal of Coal Geology*, Vol: 74, 2008, pp: 237-249.
17. Greaves K. H., Owen L. B., and McLennan J. D., "Multi-Component Gas Adsorption-Desorption Behavior of Coal", *International Coalbed Methane Symposium*, Tuscaloosa, AL, 1993.
18. Gunter W. D., Gentzis T., Rottenfusser B.A. and Richardson R.J.H., "Deep Coalbed Methane in Alberta, Canada- A Fuel Resource with the Potential of Zero Greenhouse Gas Emissions", *Energy Conversion and Management*, vol. 38, 1997, pp: S217-S222.
19. Godec M., Koperna G. and Gale J., "CO₂-ECBM: A Review of its Status and Global Potential", *Advanced Resources International*, Arlington, USA, 2014, pp: 5858-5869.
20. Gu F., "Thesis: Reservoir and Geomechanical Coupled Simulation of CO₂ Sequestration and Enhanced Coalbed Methane Recovery", *University of Alberta*, 2009.
21. Harpalani S., and Zhao X., "An Investigation of the Effect of Gas Desorption on Coal Permeability", *University of Alabama*, Tuscaloosa, AL, April 17-20, 1989; pp 57-64.

22. Harpalani S. and Schraufnagel R. A., "Shrinkage of Coal Matrix with Release of Gas and its Impact on Permeability of Coal", *Fuel*, Vol: 69, 1990, pp: 551-556.
23. Harpalani S., Chen G., "Estimation of Changes in Fracture Porosity of Coal with Gas Emission", *Fuel* (74), 1995, pp: 1491–1498.
24. Harpalani S., Prusty B. K., and Dutta P., "Methane/CO₂ Sorption Modeling for Coalbed Methane Production and CO₂ Sequestration", *Energy and Fuels*, Vol: 20, 2006, pp: 1591-1599.
25. House N.J., Faulder D.D., Olson G.L., Fanchi J.R., "Simulation study of CO₂ Sequestration in a North Sea Formation", SPE 81202, Exploration and Production Environmental Conference, San Antonio, Texas, U.S.A., 2003.
26. International Union of Pure and Applied Chemistry (IUPAC) Manual of Symbols and Terminology for Physio Chemical Quantities and Units; Butterworth: London, U.K., 1972.
27. Jikich S.A., Smith D.H., Sams W.N. and Bromhal G.S., "Enhanced Gas Recovery (EGR) with Carbon Dioxide Sequestration: A simulation study of Effects of Injection Strategy and Operational Parameters", SPE 84813, SPE Eastern Regional, Pittsburgh, Pennsylvania, U.S.A., 2003.
28. Lai K. S., Pao W. K. S. and Iskandar B. S., "Assessment of Different Matrix-Fracture Shape Factor in Double Porosity Medium", *Journal of Applied Sciences*, Vol: 13, 2013, pp: 308-314.
29. Langmuir I., "The Adsorption of Gases on Plane Surfaces of Glass, Mica and Platinum", *Journal of the American chemical society*, Vol: 40, 1918, pp: 1361-1403.
30. Law B. E. and Curtis J.B., "Introduction to Unconventional Petroleum Systems", *AAPG Bulletin*, Vol: 86, 2002, pp: 1851-1852.
31. Levine J. R., "Model Study of the Influence of Matrix Shrinkage on Absolute Permeability of Coal Bed Reservoirs", *Geological Society, London*, Vol: 109, 1996, pp: 197-212.
32. Lim K. T. and Aziz K., "Matrix-fracture transfer shape factors for dual porosity simulators", Stanford University, Depart of Petroleum Engineering, 1994.

33. Liu X., and Nie B., "Fractal Characteristics of Coal Samples Utilizing Image Analysis and Gas Adsorption", *Fuel*, Vol: 182, 2016, pp: 314-322.
34. Mastalerz M., Gluskoter H., and Rupp J., "Carbon Dioxide and Methane Sorption in High Volatile Bituminous Coals from Indiana, USA", *International Journal of Coal Geology*, Vol: 60, 2004, pp: 43-55.
35. Mitra A., and Harpalani S., "Modeling Incremental Swelling of Coal Matrix with CO₂ Injection in Coalbed Methane Reservoirs", SPE 111184, 2007.
36. Moore T. A., "Coalbed Methane: A Review", *International Journal of Coal Geology*, Vol: 101, 2012, pp: 36-81.
37. Oldenburg C.M. and Benson S.M., "CO₂ Injection for Enhanced Gas Production and Carbon Sequestration", SPE 74367, SPE International Petroleum Conference, Exhibition in Mexico, Mexico, 2002.
38. Palmer I., and Mansoori J., "How Permeability Depends on Stress and Pore Pressure in Coalbeds: A New Model", SPE-52607, 1998.
39. Pan Z., and Connell L. D., "Modelling Permeability for Coal Reservoirs: A Review of Analytical Models and Testing Data", *International Journal of Coal Geology*, Vol: 92, 2012, pp: 1-44.
40. Pekot L.J, and Reeves S.R., "Modeling Coal Matrix Shrinkage and Differential Swelling with CO₂ Injection for Enhanced Coalbed Methane Recovery and Carbon Sequestration Applications", Topical Report, Advanced Resources International, US Department of Energy, Contract No.: DE-FC26-00NT40924, 2002.
41. Production potential of Alberta's CBM resources, Earth Science Report, 2003. Available at website: <http://ags.aer.ca/reports/reports.htm>
42. Rahul S., and Sarma H.K., "Thesis: An Investigation of Carbon Sequestration/ECBM Potential in Australian Coals: A Simulation study for Sydney Coal Basin", University of Adelaide, 2006.
43. Reucroft P. J., and Patel H., "Gas- Induced Swelling in Coal", *Fuel*, Vol: 65, 1986, PP: 816-820.

44. Sams W.N., Bromhal G.S., Odusote O., Jikich S.A., Ertekin T. and Smith D.H., "Simulating Carbon dioxide Sequestration/ECBM Production in Coal Seams: Effects of Coal Properties and Operational Parameters", SPE 78691, SPE Eastern Regional Meeting, Lexington, Kentucky, 2002.
45. Saulsberry J. L., Schafer P.S., and Schraufnagel R.A., "A Guide to Coalbed Methane Reservoir Engineering", Gas Research Institute, 1996.
46. Sawyer W. K., Paul G. W., and Schraufnagel R. A., "Development and Application of a 3-D Coalbed Simulator", Annual technical meeting. Petroleum Society of CIM/SPE, pp: CIM/SPE 90-119, 1990.
47. Scott A.R., "Composition and Origin of Coalbed Gases from Selected Basins in the United States", Proceedings of the International Coalbed Methane Symposium, Tuscaloosa, Alabama, 1993, pp: 207-222.
48. Seidle J. P., Jeansonne M. W., and Erickson D. J., "Application of Matchstick Geometry to Stress Dependent Permeability in Coals", SPE Rocky Mountain regional meeting, SPE 24361, 1992, pp: 433-444.
49. Seidle J. P., and Huitt L. G., "Experimental Measurement of Coal Matrix Shrinkage due to Gas Desorption and Implications for Cleat Permeability Increases", SPE International Meeting on Petroleum Engineering, Beijing, China, November 14-17, SPE 30010, 1995, pp: 575-582.
50. Seidle J. P., "Fundamentals of Coalbed Methane Reservoir Engineering", Penn Well Books, 2011, pp: 1-5.
51. Shi J.Q., and Durucan S., "Drawdown Induced Changes in Permeability of Coalbeds: A New Interpretation of the Reservoir Response to Primary Recovery", Transport in porous media, Vol: 56, 2004, pp: 1-16.
52. Shi J.Q., and Durucan S., "A Model for Changes in Coalbed Permeability during Primary and Enhanced Methane Recovery", SPE Reservoir Evaluation and Engineering 8(4), 2005, pp: 291-299.

53. Sing K. S. W., Everett D. H., Haul R. A. W., Moscou L., Pierotti R. A., Rouquerol J., and Siemieniewska T., "Reporting Physisorption Data for Gas/Solid Systems with Special Reference to the Determination of Surface Area and Porosity", *Pure and applied chemistry*, Vol: 57, 1985, pp: 603-619.
54. Smith D.H., Sams W.N., Bromhal G.S., Jikich S.A. and Ertekin T., "Simulating Carbon dioxide Sequestration/ECBM Production in Coal Seams: Effects of permeability anisotropies and Other Coal Properties", SPE 84423, SPE Annual Technical Conference, Colorado, U.S.A., 2003.
55. Stefanska G. C., Zarębska K., and Wolszczak J., "Sorption of Pure Components and Mixtures CO₂ and CH₄ on Hard Coals", *Gospodarka Surowcami Mineralnymi*, 24 (4/1), 2008, PP: 123-131.
56. St. George J. D., and Barakat M.A., "The Change in Effective Stress Associated with Shrinkage from Gas Desorption in Coal", *International Journal of coal Geology*, Vol: 45, 2001, pp: 105-113.
57. Thakur P., "Chapter 1: Global Reserves of Coal Bed Methane and Prominent Coal Basins", *Advanced Reservoir and Production Engineering for Coal Bed Methane*, 2017, pp: 1-15.
58. Warren J.E., Root P.J., *Society of Petroleum Engineers Journal*, 1968, pp: 81-88.
59. Wei Z., and Zhang D., "A Fully Coupled Multiphase Multicomponent Flow and Geomechanics Model for Enhanced Coalbed Methane Recovery and CO₂ Storage", *SPE Journal*, Vol: 18, 2013, pp: 448-467.
60. Wo S. and Liang J.T., "Simulation Assessment of N₂/CO₂ Contact Volume in Coal and its Impact on Outcrop Seepage in N₂/CO₂ Injection for Enhanced Coalbed Methane Recovery", SPE 89344, SPE/DOE Fourteenth Symposium on Improved Oil Recovery, Tulsa, Oklahoma, U.S.A., 2004.
61. Yee D., Seidle J. P., and Hanson W. B., "Gas Sorption on Coal and Measurement of Gas Content: Chapter 9", 1993, pp: 203-218.

62. Yi H., Li F., Ning P., Tang X., Peng J., Li Y. and Deng H., "Adsorption separation of CO₂, CH₄, and N₂ on Microwave Activated Carbon", Chemical Engineering Journal 215-216, 2013, pp: 635-642.